UNIVERSITY OF THE AEGEAN

ΕΛΛΗΝΙΚΟ ΑΝΟΙΚΤΟ ΠΑΝΕΠΙΣΤΗΜΙΟ

ARISTOTLE UNIVERSITY OF THESSALONIKI

UNIVERSITY OF BIRMINGHAM

Detectors for Particle and Astroparticle Physics

Ioannis Manthos

(University of Birmingham)

SCHOOL OF APPLIED MATHEMATICAL AND PHYSICAL SCIENCES
NATIONAL TECHNICAL UNIVERSITY OF ATHENS

ioannis.manthos@cern.ch
i.manthos@bham.ac.uk

1/11/2021

Career path

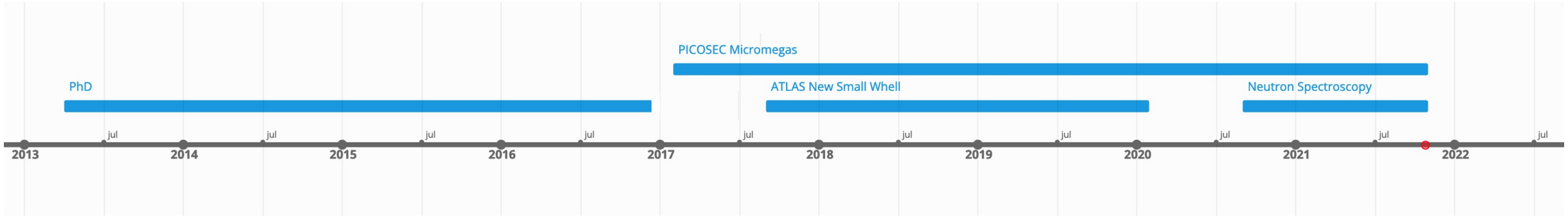

- **Apr. 2013 – Nov. 2016:** Ph.D. - Detection and study of extensive air showers using innovative detectors and algorithms *(University of the Aegean – Hellenic Open University)*
- **Sep. 2017 – Jan. 2020:** ATLAS New Small Wheel, LM2 drift panels construction and QA/QC *(Aristotle University of Thessaloniki)*
- **Feb. 2017 – today:** PICOSEC Micromegas R&D *(Aristotle University of Thessaloniki)*
- **Sep. 2020 – today:** Fast Neutron Spectroscopy with the Spherical Proportional Counter *(University of Birmingham)*

Career path

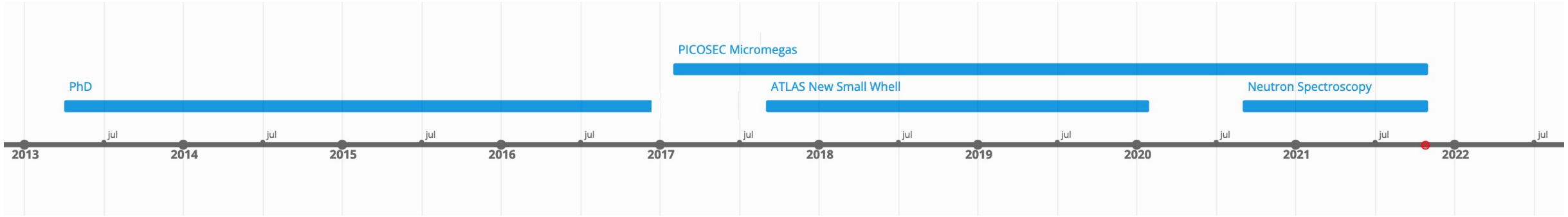

- **Apr. 2013 – Nov. 2016:** Ph.D. - Detection and study of extensive air showers using innovative detectors and algorithms *(University of the Aegean – Hellenic Open University)*
- **Sep. 2017 – Jan. 2020:** ATLAS New Small Wheel, LM2 drift panels construction and QA/QC *(Aristotle University of Thessaloniki)*
- **Feb. 2017 – today:** PICOSEC Micromegas R&D *(Aristotle University of Thessaloniki)*
- **Sep. 2020 – today:** Fast Neutron Spectroscopy with the Spherical Proportional Counter *(University of Birmingham)*

Ph.D. thesis: Detection and study of extensive air showers using innovative detectors and algorithms – Astroneu array

- Detector development for Extensive Air Showers (EAS) based on plastic scintillator counters and RF antennas
- Novel signal processing and data analysis techniques for EAS detection and reconstruction
- Instrumentation and methods for under-water neutrino telescopy: Sea-top calibration and EAS-veto facility
- Operation and evaluation of ASTRONEU performance (a pilot, hybrid EAS detection array)

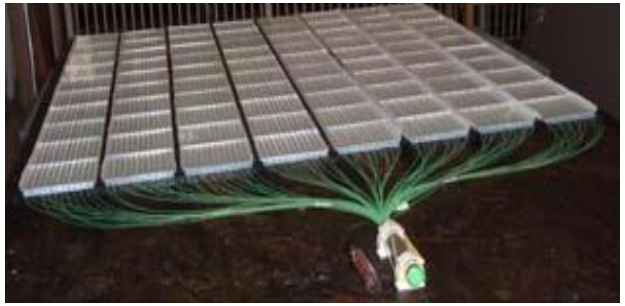

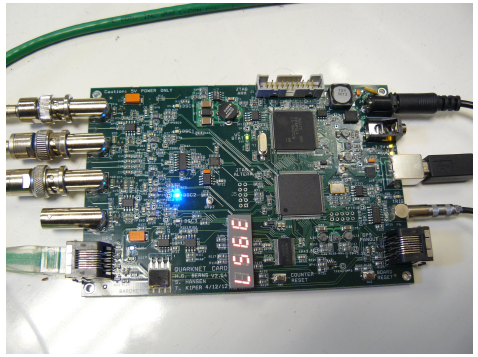

Astroneu array

Scintillation detectors calibration

Development of simulation tools for the detail description of the detector response
Calibration studies using Corsika and real data

Calibration of:

- PMT (single p.e. response, gain curve, dark current)
- Scintillation detectors (MIP response, homogeneity)
- DAQ unit Quarknet (baseline, accurate calibration)
- **Detection station (3 scintillators)**

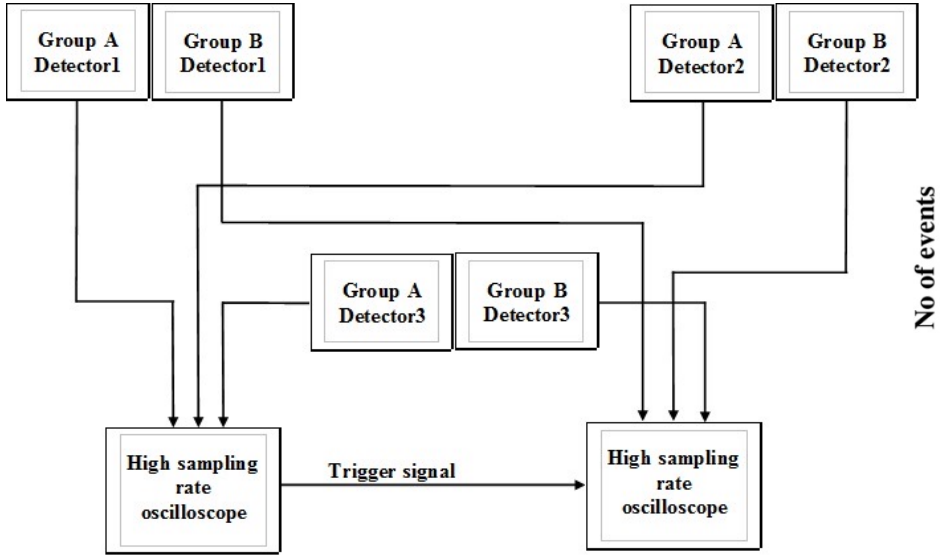

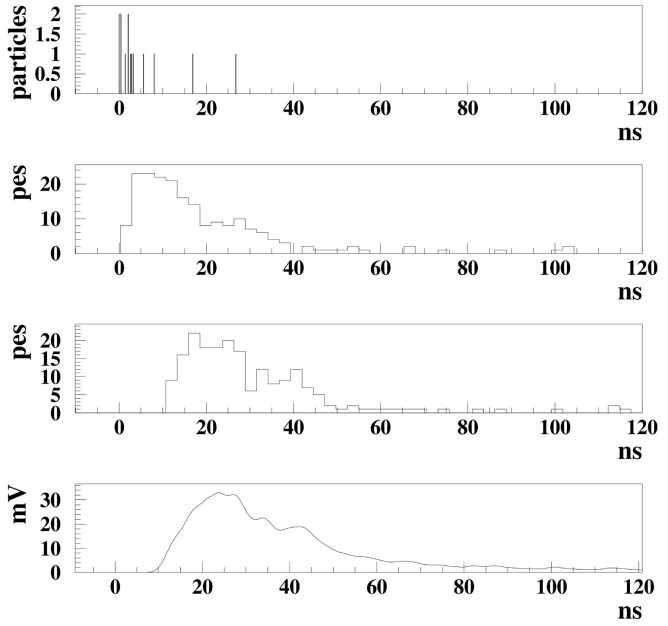

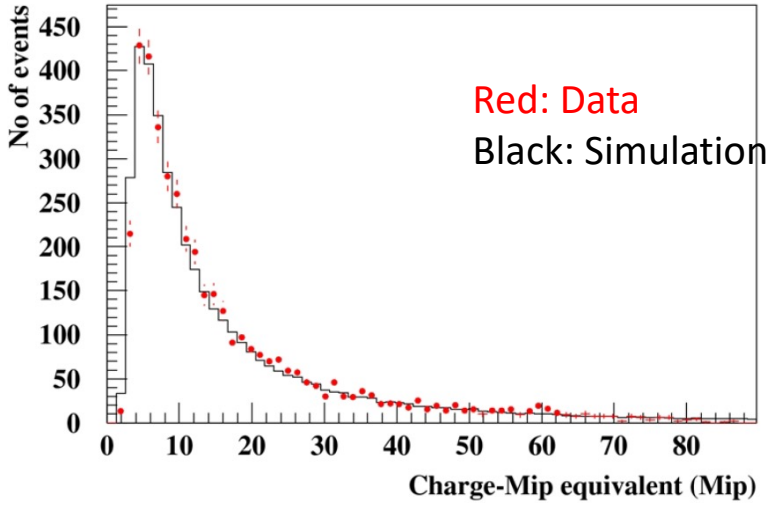

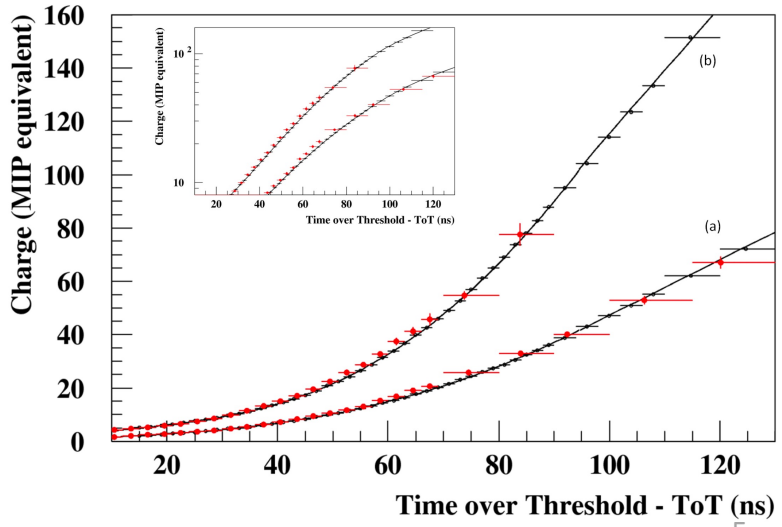

T. Avgitas et al 2020 JINST15 T03003

Astroneu array

Scintillation detectors calibration

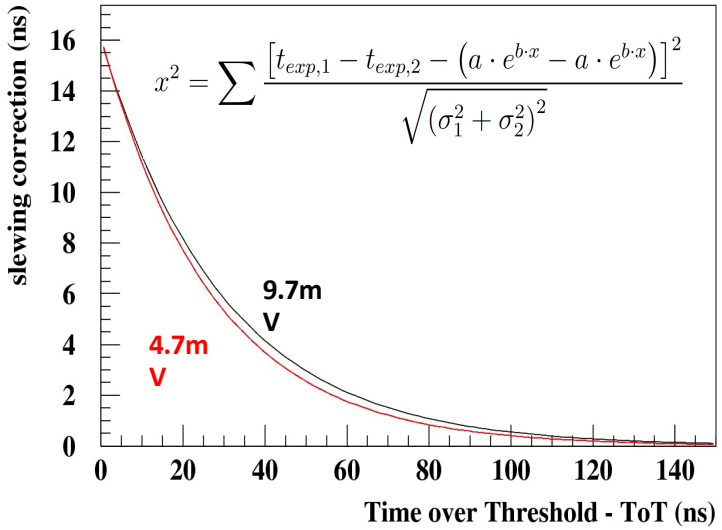

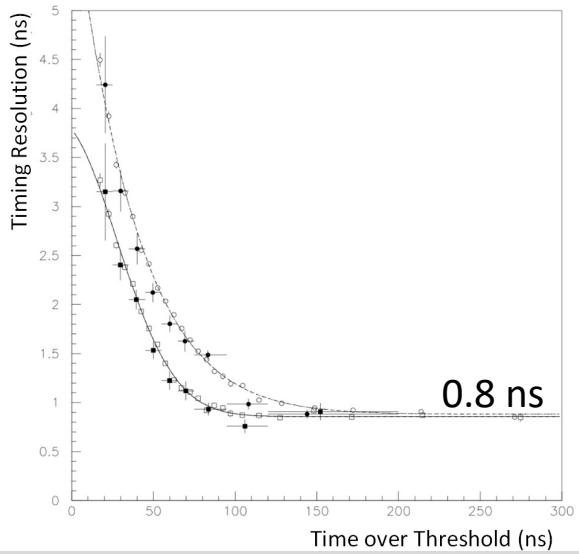

S. Tzamarias et al. Instruments and Experimental Techniques, 2021, Vol. 64, No. 1, pp. 127–140. © Pleiades Publishing Ltd. Springer.

Event reconstruction with triangulation

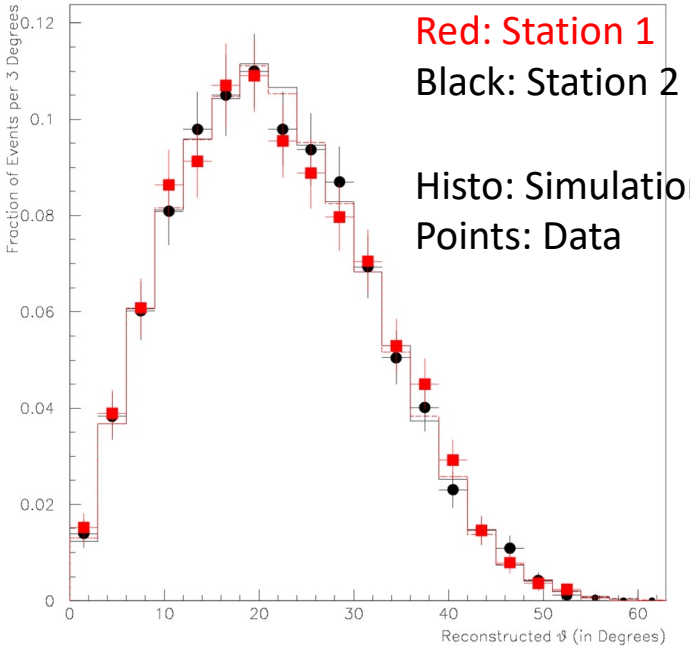

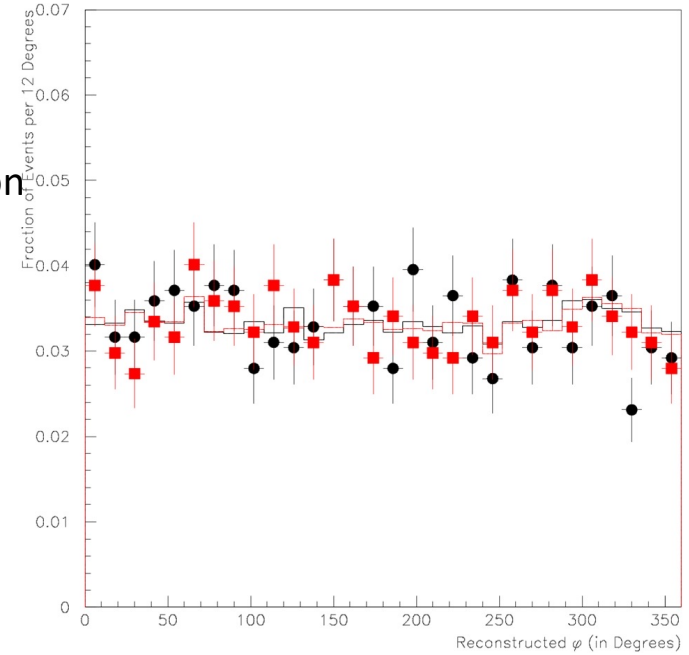

Astroneu array

Feb.2014 – Mar.2016 : 609.001 confirmed EAS detected

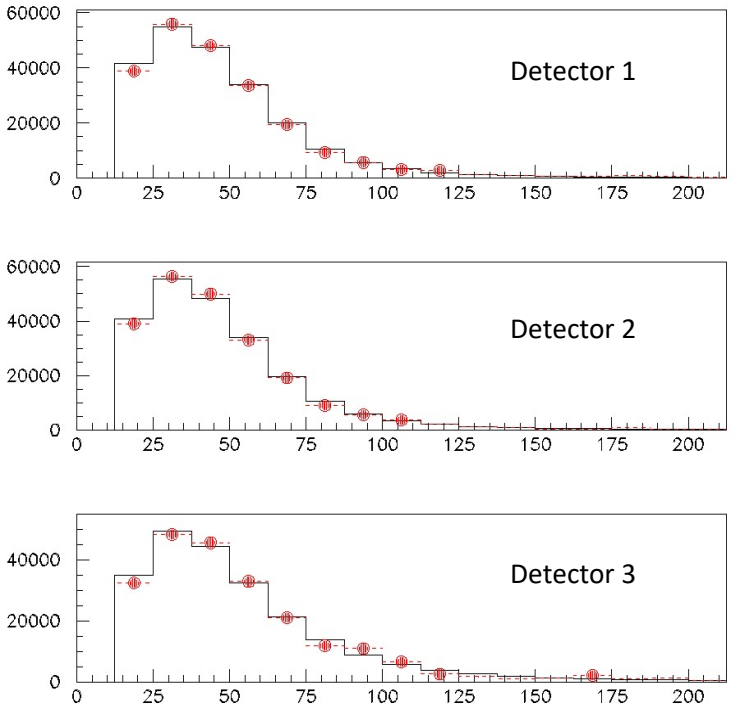

Time over Threshold (ns)

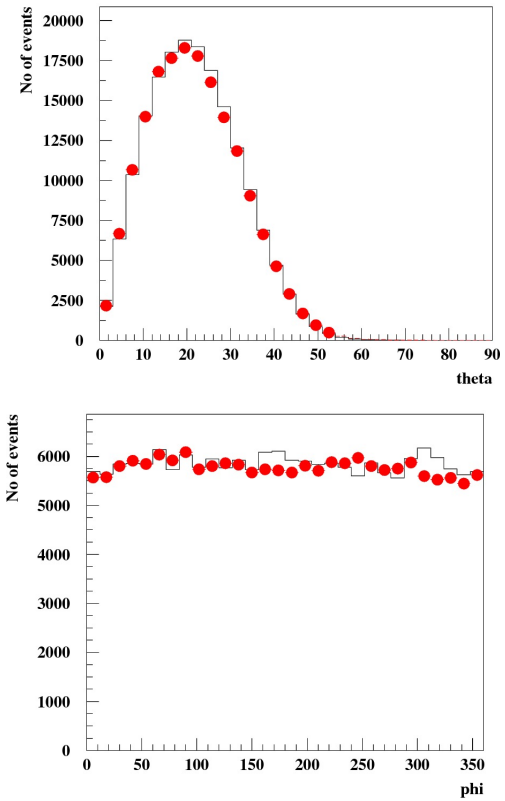

Red: Data

Black: Simulation

Angular resolution studies using simulation

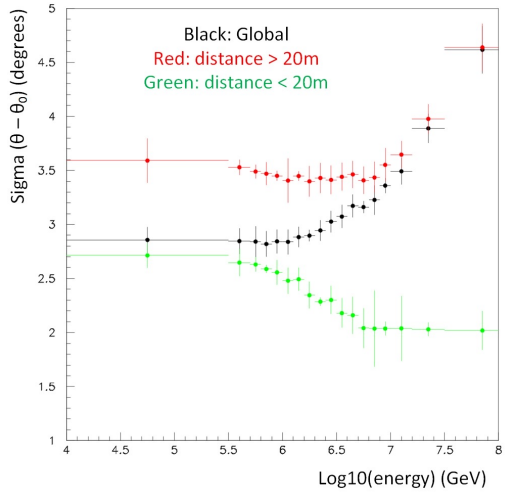

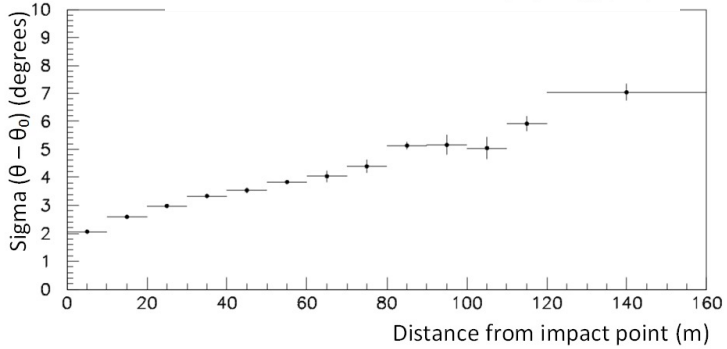

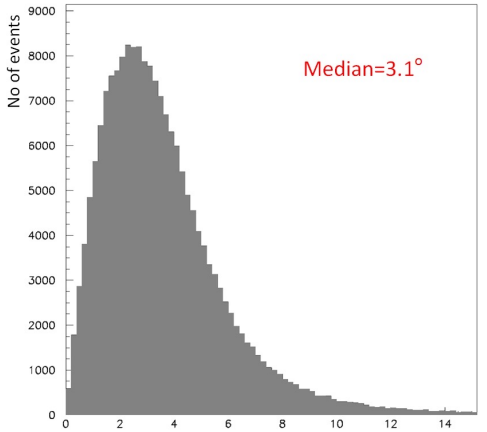

Astroneu array

Coincident events between station 1 and 2

A. Leisos et al. New Astronomy, Vol 82 2021, 101448

- Using GPS times
- Station 1 and 2 distance: 164m
- Compliance between data (1.389) and simulation (1.385) event number for 9.402 h operation time

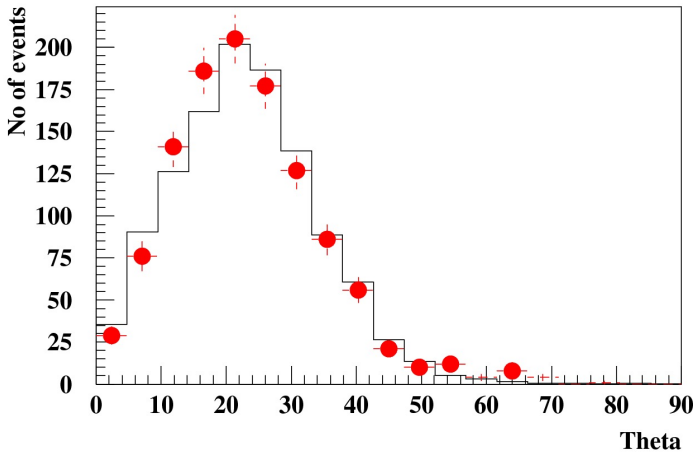

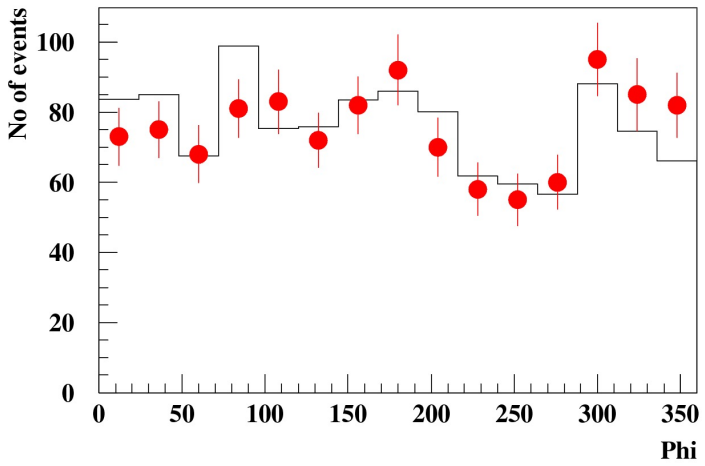

EAS direction reconstruction from 6 detectors, minimizing the following

$$\sum_{i=1}^{5} x^2 = \left(\frac{(t_i^{exp} - t_0^{exp}) - (t_i^{calc} - t_0^{calc})}{\sqrt{t_{err,i}^2 + t_{err,0}^2 + 2 \cdot \left(\frac{10}{\sqrt{12}}\right)^2}} \right)^2$$

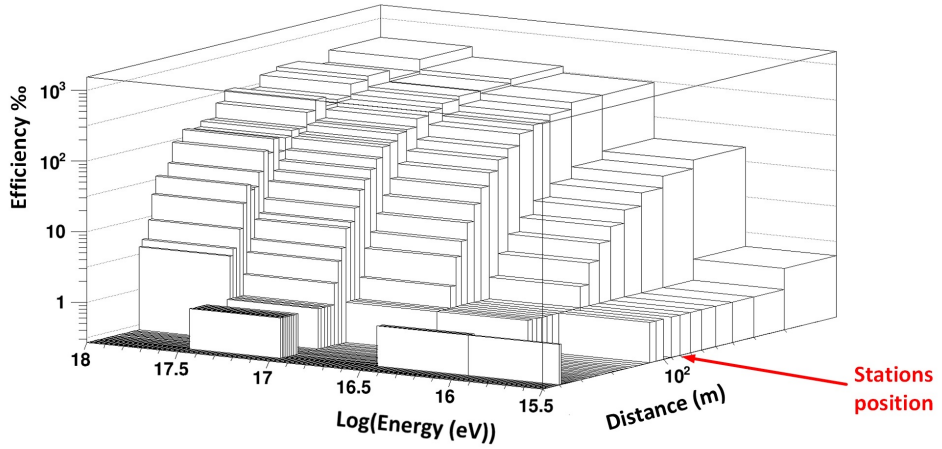

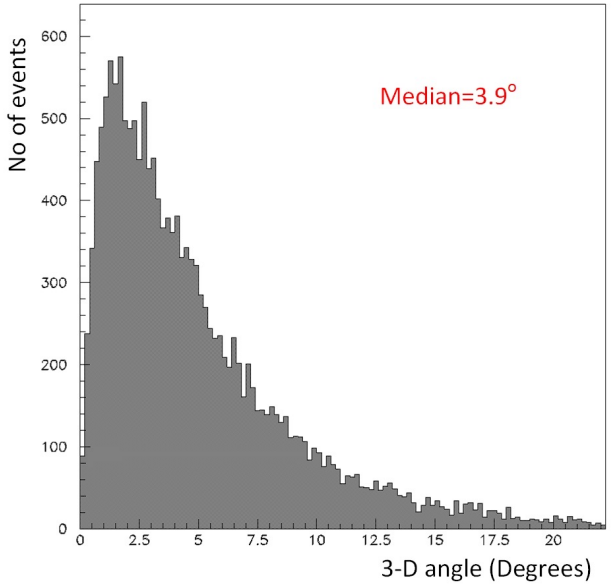

Astroneu array
RF signal detection

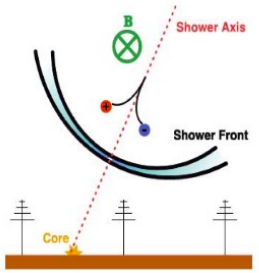

- primary effect: geomagnetic field induces *time-varying* transverse currents

Kahn & Lerche (1967)

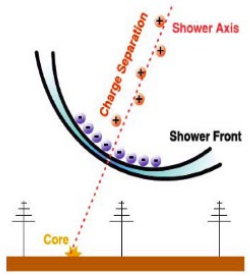

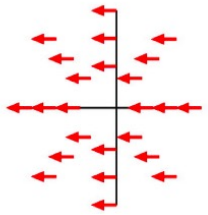

Askaryan (1962,1965)

- secondary effect: *time-varying* net charge excess (Askaryan effect)

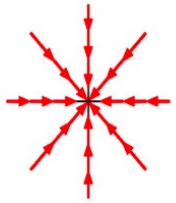

SNR ratio > 5

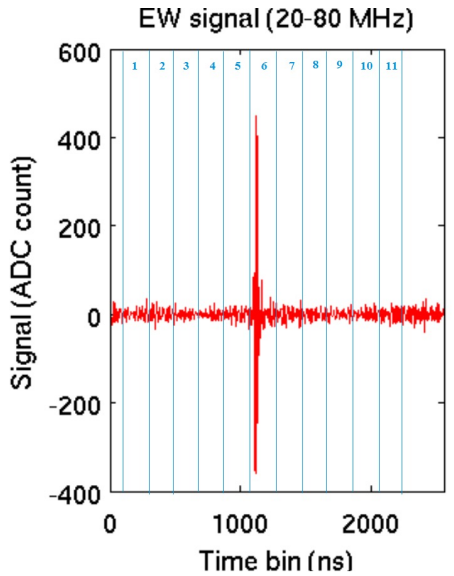

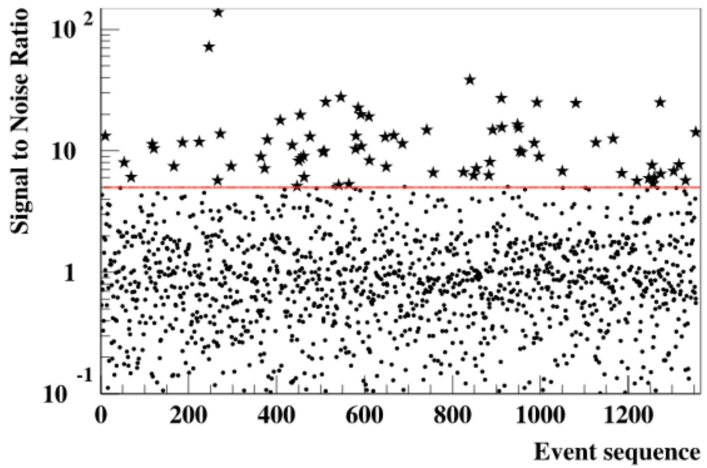

Risetime 10-70% <28ns

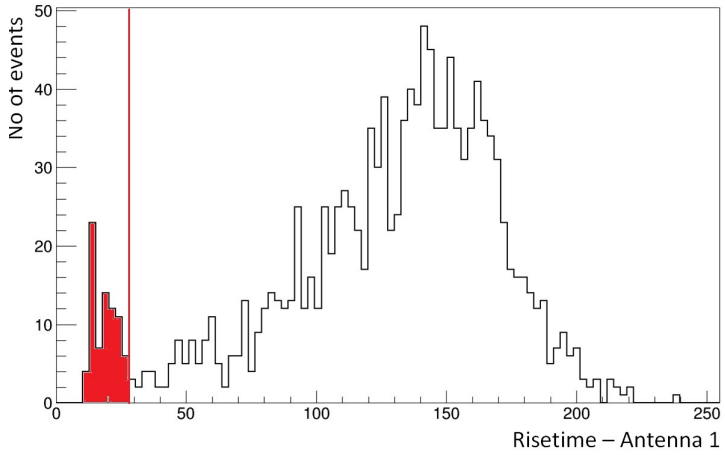

Polarization

$$P = \frac{\sqrt{Q^2 + U^2 + V^2}}{I} > 0.75$$

<u>Criteria for EAS signal:</u>

- Triger from Scintillators
- Signal to Noise Ratio
- Rise time (10-70%) of cumulative signal 128 ns around peak <28ns.
- Polarization (NS vs EW)

I. Manthos et al. New Astronomy, Vol 81 2020, 101443

Career path

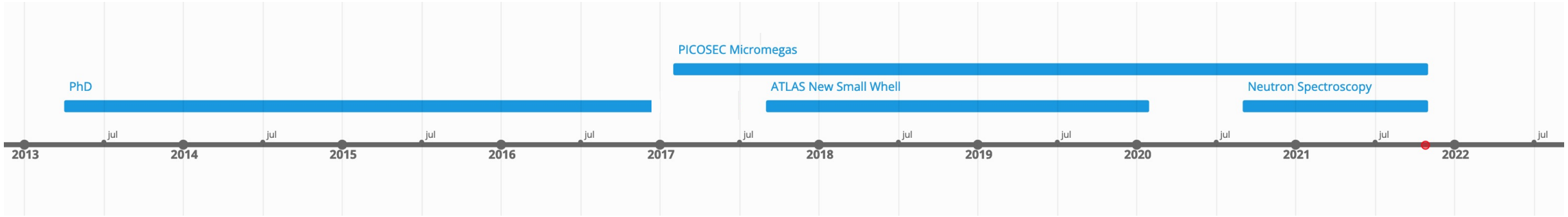

- **Apr. 2013 – Nov. 2016:** Ph.D. - Detection and study of extensive air showers using innovative detectors and algorithms *(University of the Aegean – Hellenic Open University)*
- **Sep. 2017 – Jan. 2020:** ATLAS New Small Wheel, LM2 drift panels construction and QA/QC *(Aristotle University of Thessaloniki)*
- **Feb. 2017 – today:** PICOSEC Micromegas R&D *(Aristotle University of Thessaloniki)*
- **Sep. 2020 – today:** Fast Neutron Spectroscopy with the Spherical Proportional Counter *(University of Birmingham)*

ATLAS NSW: LM2 Drift panel construction and QA/QC

Specifications and Requirements of the NSW

Layout

Compatibility with the existing tracking detectors and endcap alignment system

- Precision coordinate of all chambers parallel to drift tubes of EM and EO stations to within 2 mrad
- coverage: $|\eta| > 1.3$ (minimum size of chambers)
- same segmentation into 16 pie-shaped sectors as the present Small Wheel

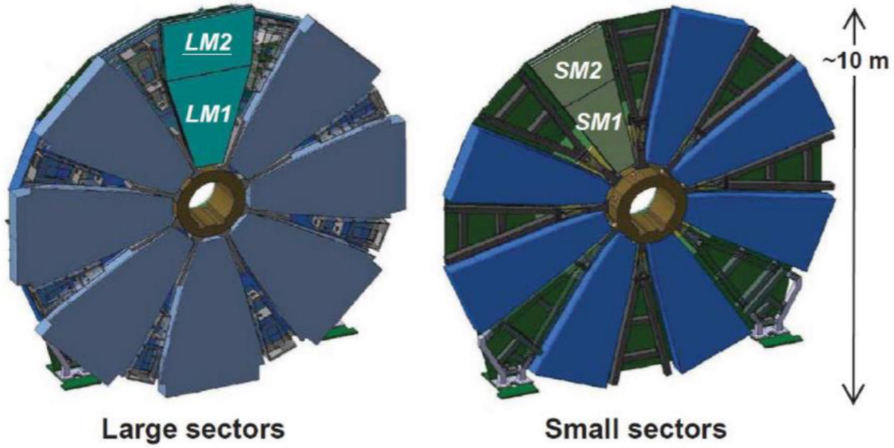

Performance

- Momentum resolution: better than 15% up to p_t= 1 TeV
- Single plane resolution: 100µm, independent from track angle
- Track segment reconstruction: 50 µm
- Track segment efficiency: >= 97% @ p_t> 10 GeV
- Online angular resolution (trig): <= 1 mrad
- Spatial resolution 2nd coordinate: ~cm, from stereo strips or wires
- Hit rate capability: 15 kHz/cm^2 (meeting perform. requ.)
- Accumulated charge without ageing: 1 C/cm^2 (3000 fb^{-1} w/o degradation)

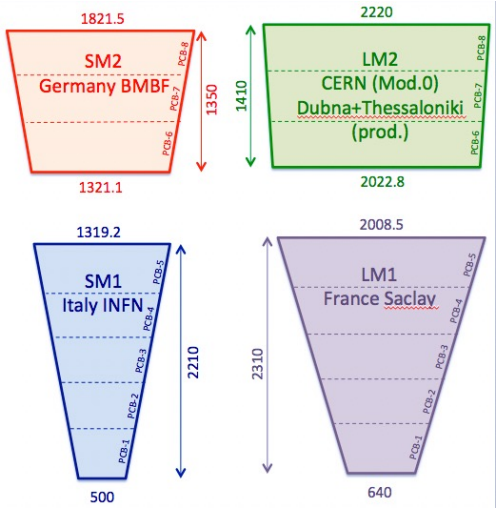

Combination of sTGC (trigger) and MicroMegas (tracking) detector planes

MicroMegas

- Good Spatial resolution < 100 µm
- Good track separation (0.4 mm readout granularity)
- Resistive anode strips → suppress discharge influence on efficiency
- Provide also online segments for trigger

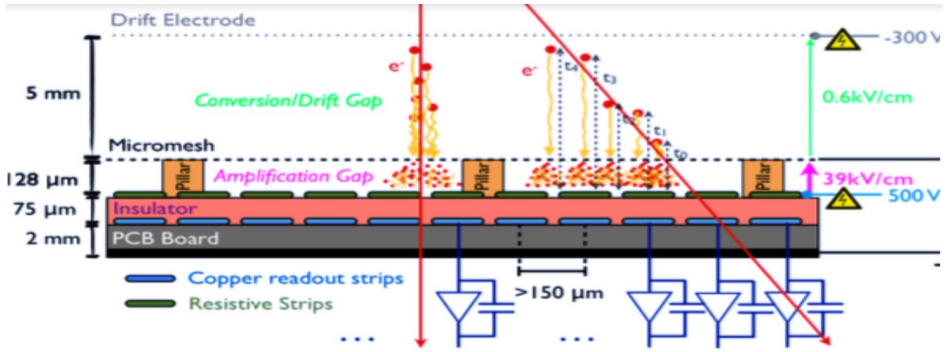

ATLAS NSW: LM2 Drift panel construction and QA/QC

ARISTOTLE UNIVERSITY OF THESSALONIKI

Construction and QA/QC of 105 drift Micromegas panels for ATLAS NSW with strict specifications

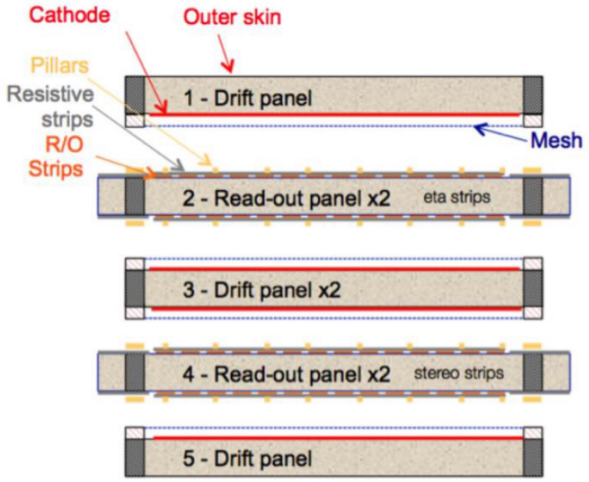

- Thickness and planarity

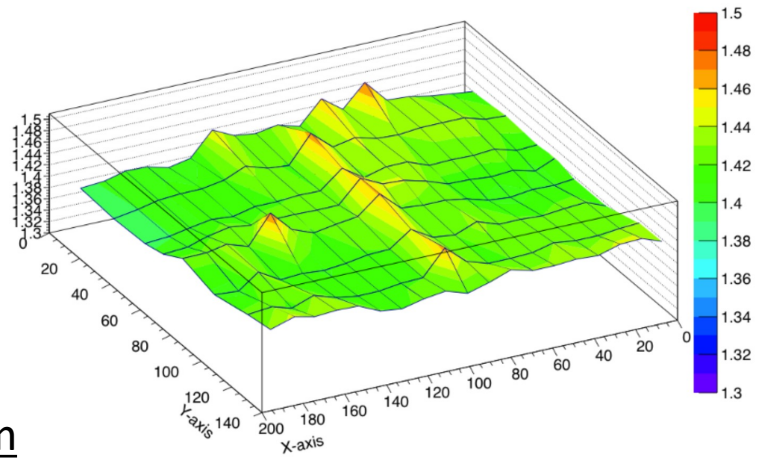

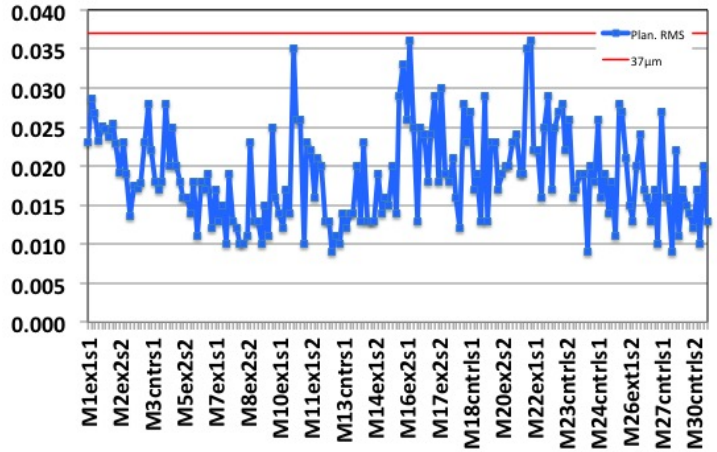

Leading member of the construction team

- Thickness and planarity
- Gas leak measurements
- Mesh installation
- Resistance measurements
- …

I. Manthos et al. The micromegas project for the ATLAS new small wheel AIP Conference Proceedings **2075**, 080010 (2019)

ATLAS NSW: LM2 Drift panel construction and QA/QC

- Gas leak measurements (Pressure drop method)

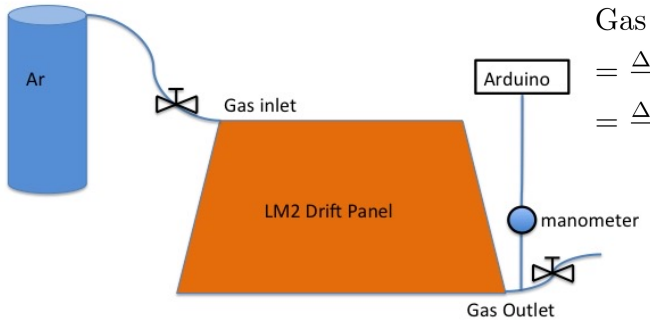

$$\text{Gas leak} = \frac{\Delta p^{atm}}{p_0} + \frac{\Delta p^{over}}{p_0} + \frac{\Delta V}{V_0} + \frac{\Delta T}{T_0}$$
$$= \frac{\Delta p^{atm}}{p_0} + \frac{\Delta p^{over}}{p_0} + k\frac{\Delta p^{over}}{p_0}$$
$$= \frac{\Delta p^{atm}}{p_0} + (k+1)\frac{\Delta p^{over}}{p_0}$$

Pressure drop rate

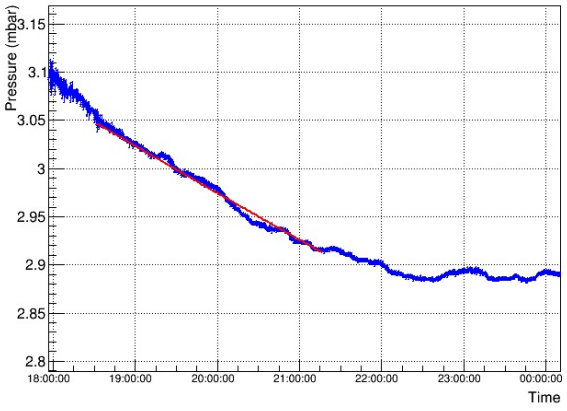

Volume deformation factor (k)

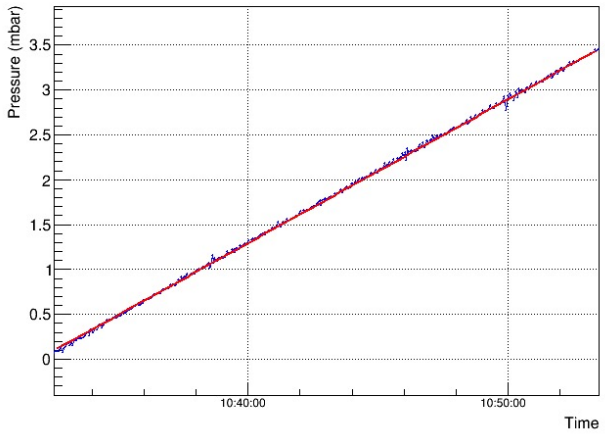

- Mesh installation (140 meshes on 105 panels)

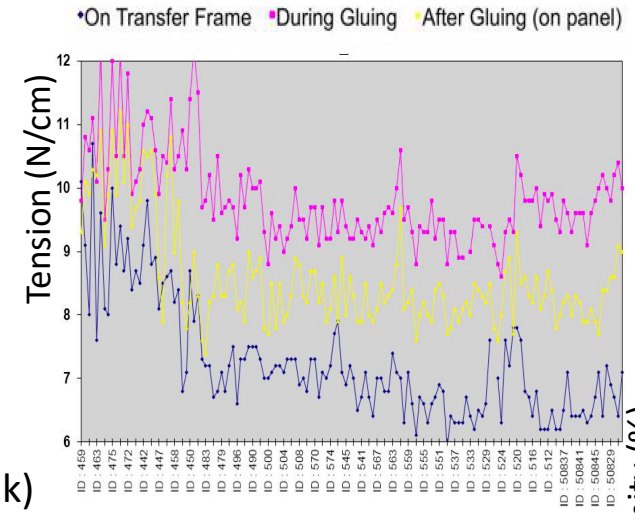

Nominal values
Tension: 7-10 N/cm
Uniformity: <10%

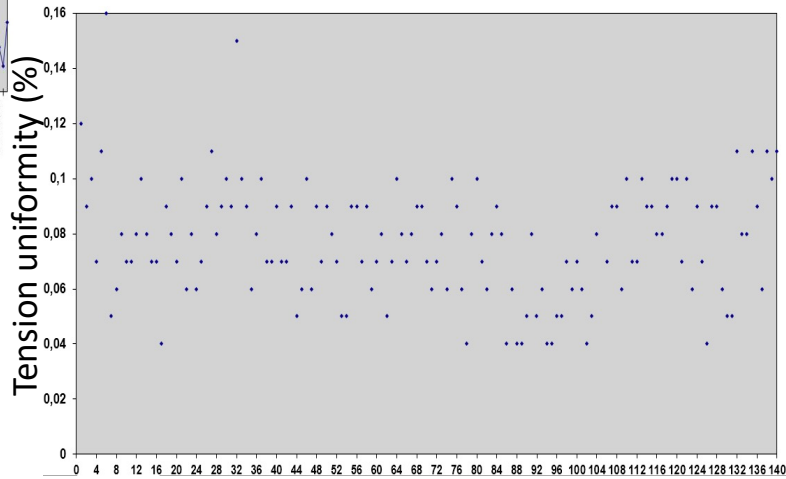

- After construction completion, 2 months visit at CERN / BB5
- Main engagement: FEB installation and noise measurements

Career path

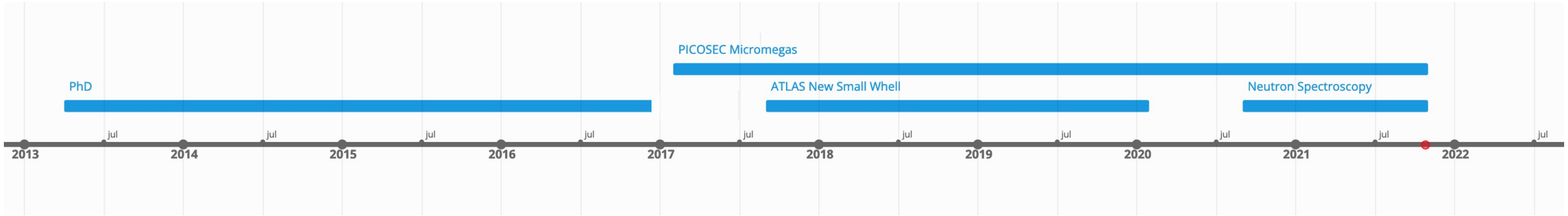

- **Apr. 2013 – Nov. 2016:** Ph.D. - Detection and study of extensive air showers using innovative detectors and algorithms *(University of the Aegean – Hellenic Open University)*
- **Sep. 2017 – Jan. 2020:** ATLAS New Small Wheel, LM2 drift panels construction and QA/QC *(Aristotle University of Thessaloniki)*
- **Feb. 2017 – today:** PICOSEC Micromegas R&D *(Aristotle University of Thessaloniki)*
- **Sep. 2020 – today:** Fast Neutron Spectroscopy with the Spherical Proportional Counter *(University of Birmingham)*

CERN-RD51 PICOSEC Micromegas

ARISTOTLE UNIVERSITY OF THESSALONIKI

R&D for precise timing with the novel PICOSEC Micromegas detector

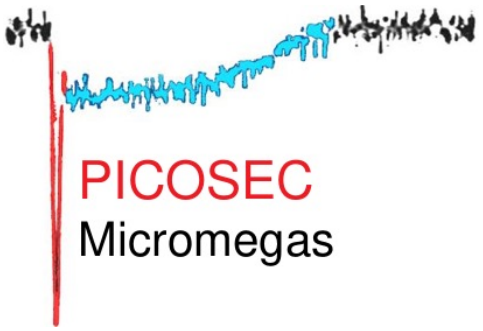

- **High Luminosity LHC:**
  - More than 140 "**pile-up**" proton-proton interactions ("vertices") will happen in the same LHC clock, in close space (Gaussian +- 45mm). 3D tracking of charged particles is not enough to associate them to the correct vertex . Including precise timing **(20-30 ps)** offers an extra dimension of separation.

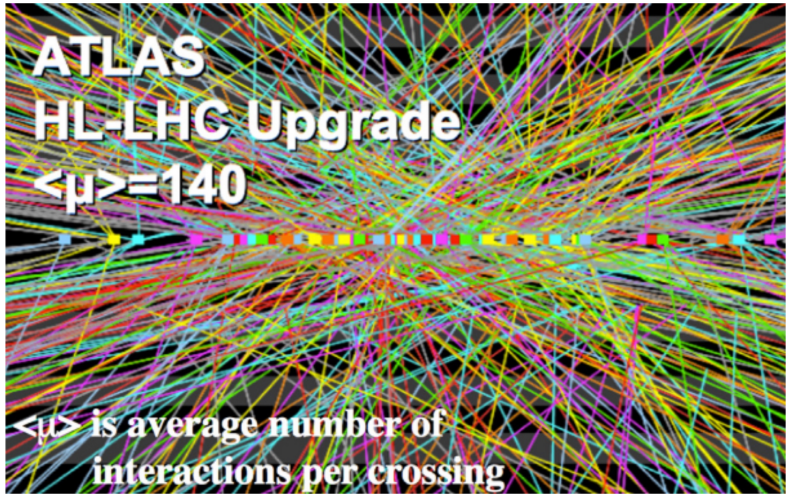

- Precise **Time-of-Flight (ToF)** measurements for Particle Identification (PID) at level of **≈20 ps/MIP** can offer Pion/Kaon and Kaon/Proton separation for a wide momentum range

- **Tagged neutrino beam** (time and flavour of tagging) for event-by-event decay measurements (ENUBET)

CERN-RD51 PICOSEC Micromegas

Detector concept

- **Classic Micromegas**
  Giomataris Y. et al., NIMA 376(1996) 29

- Multiple electrons produced at different points along particle's path in the ~3-6mm drift region → Time jitter order: **few ns**

MicroMegas

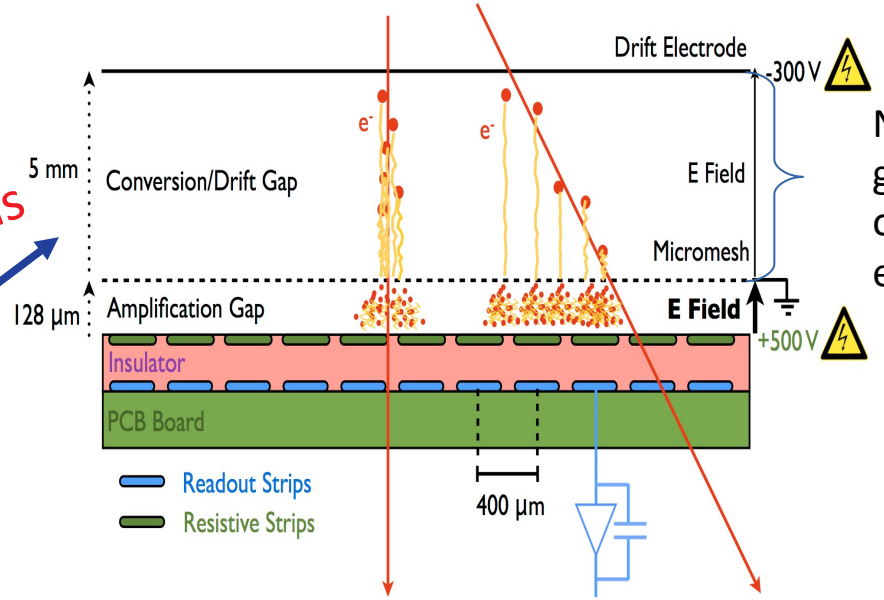

Needed to get enough original electrons

- **Micromegas + Cherenkov radiator + photocathode** → synchronous photo-electrons enter Micromegas

- **Small drift gap** & high field → avalanches start as early as possible with minimal time jitter → Timing resolution a **few tens of ps**

PICOSEC-MicroMegas

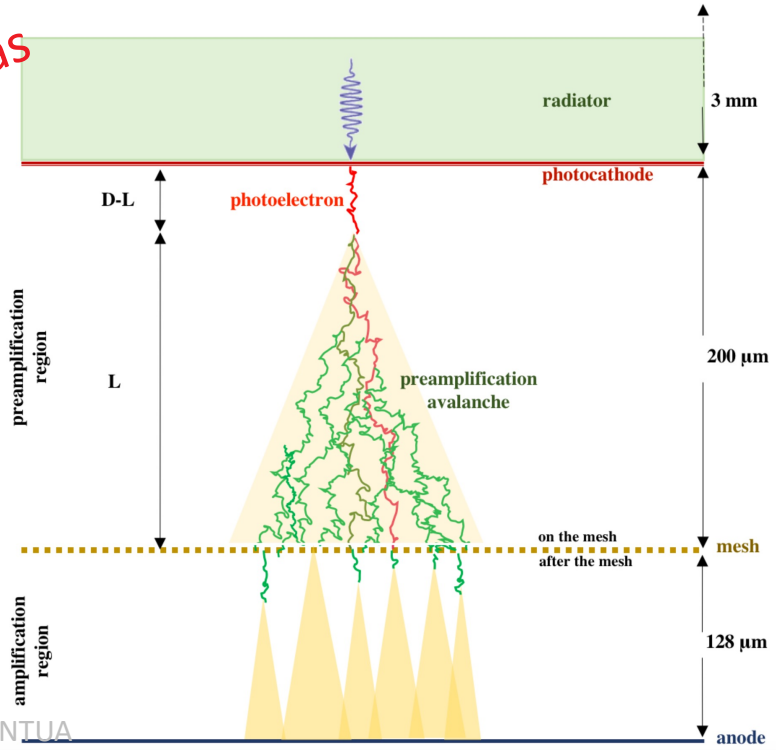

1st prototype

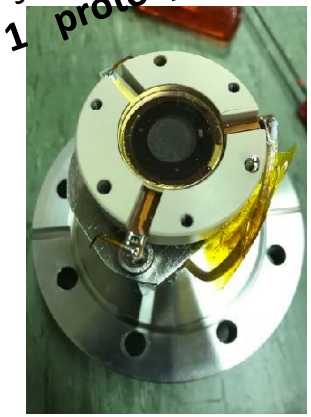

CERN-RD51 PICOSEC Micromegas

ARISTOTLE UNIVERSITY OF THESSALONIKI

R&D for precise timing with the novel PICOSEC Micromegas detector

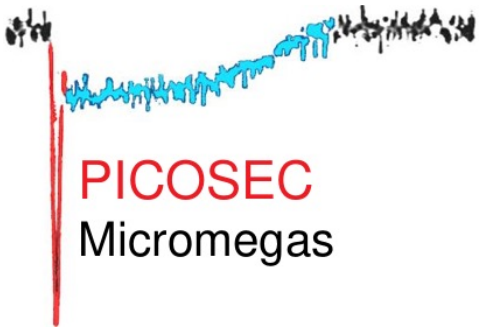

Most significant contributions at PICOSEC detector R&D

- Operation and evaluation of the performance of PICOSEC Micromegas detector
- Development of PICOSEC signal analysis method and demonstration of MIP timing with 24 ps accuracy.
- Simulation and modelling of the detector response
- Development of method to estimate the number of photoelectrons per MIP
- Timing performance of multipad PICOSEC detector, including corrections to restore detector's uniformity due to non-uniformity of the drift gap thickness
- Study of alternative timing methods, aiming to Front-end electronics DAQ

CERN-RD51 PICOSEC Micromegas

Signal analysis method

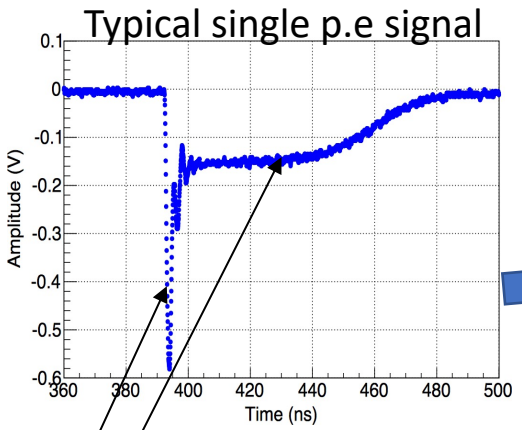

Signal inverted

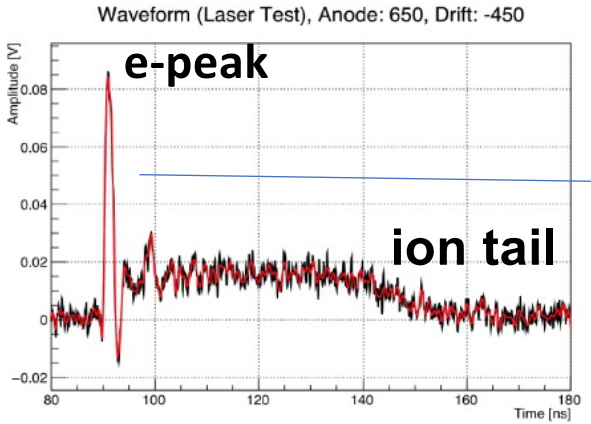

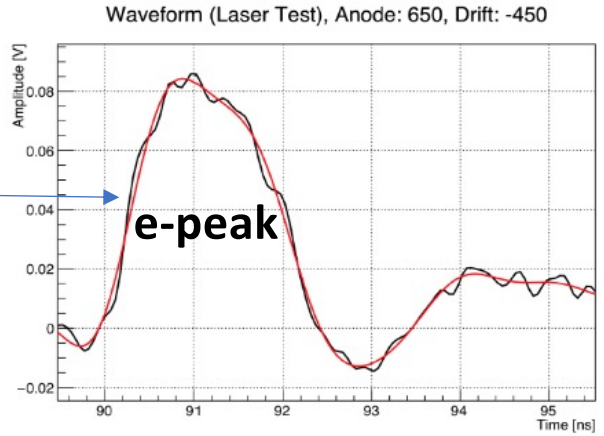

Two-component signal:

* **Electron peak** (“*e-peak*”) → fast (~0.5ns)
* **Ion tail** → slow (~100ns)

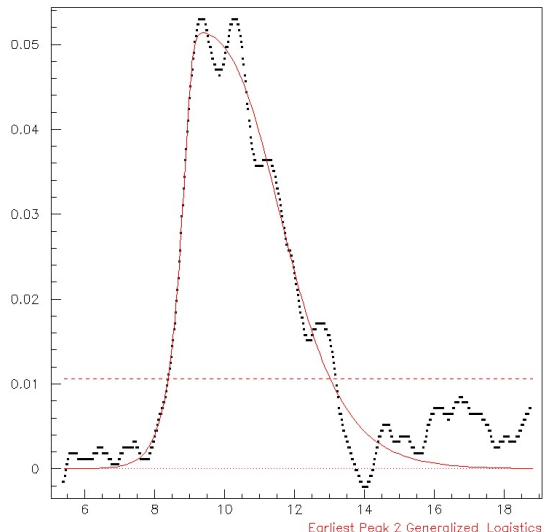

Fit with the difference of two logistic functions

$$f(t;p_0,p_1,p_2,p_3,p_4,p_5,p_6) = \frac{p_0}{\left(1+e^{-(t-p_1)p_2}\right)^{p_3}} - \frac{p_0}{\left(1+e^{-(t-p_4)p_5}\right)^{p_6}}$$

- ✓ Define the start and the end of the e-peak
- ✓ Define Signal Arrival Time
- ✓ Estimate the charge
- ✓ Neutralize noise effects

CERN-RD51 PICOSEC Micromegas

Signal analysis method - Response to single p.e

→ Time the signal arrival with **Constant Fraction Discrimination (CFD)** on the fitted noise-subtracted e-peak
CFD @ 20% of the e-peak amplitude

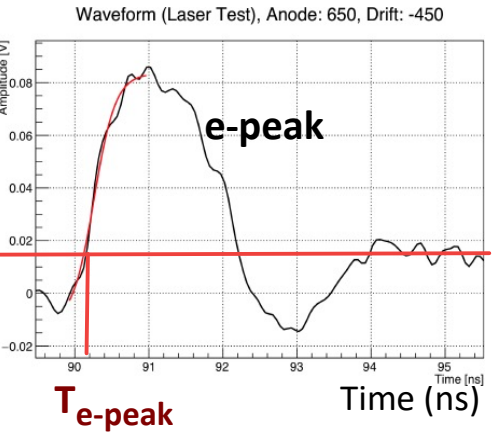

$T_{e\text{-}peak}$ = Signal Arrival Time (SAT)

SAT of a sample of events = $<T_{e\text{-}peak}>$

Time Resolution = RMS[$T_{e\text{-}peak}$]

- t_0 reference: fast photodiode (~10 ps resolution)
- Detector response at different field settings Timing resolution **76.0 ± 0.4 ps** achieved @ drift/anode: -425V / +450 V
- improves strongly with higher drift field, less with anode field

Time Resolution depends mostly on e-peak charge

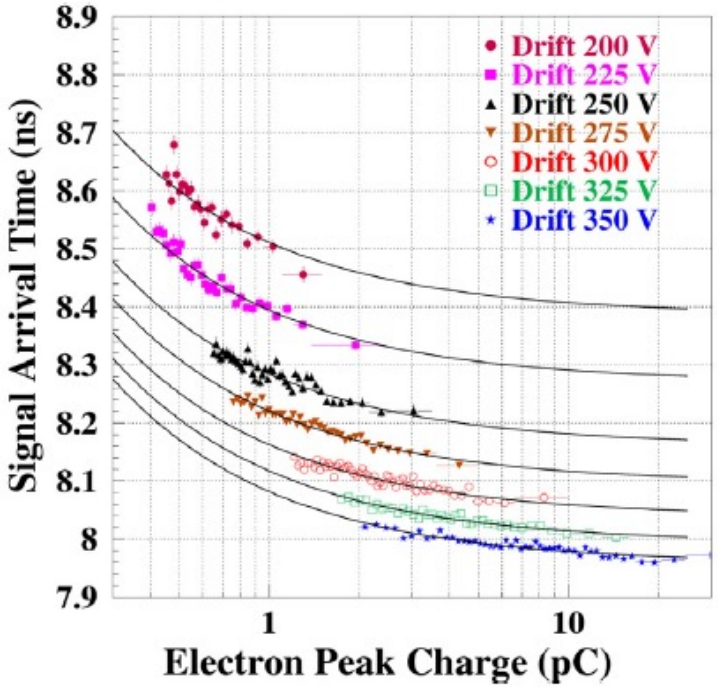

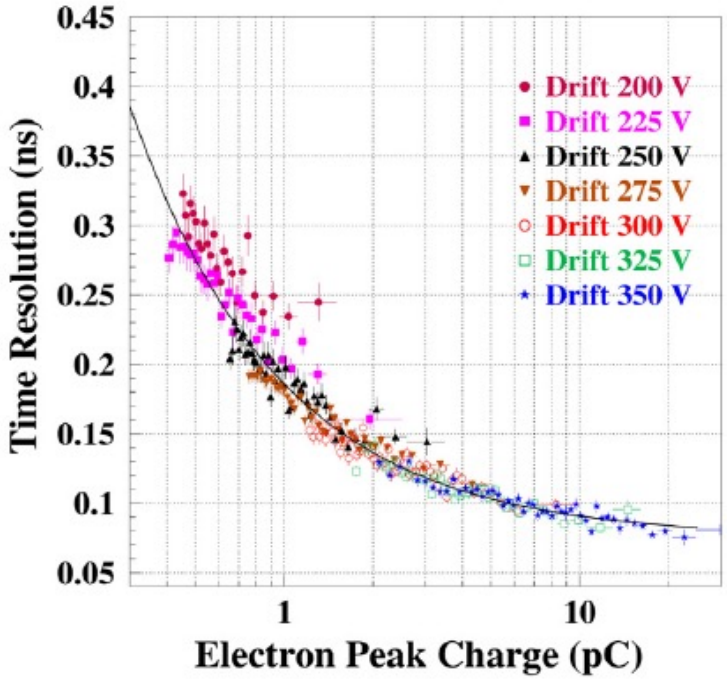

The Signal Arrival Time (SAT) depends non- trivially on the e-peak charge:
- bigger pulses → smaller SAT
- higher drift field → smaller SAT

* Pulse shape identical in all cases → timing with CFD method does not introduce dependence on pulse size
* Responsible for "time-walk" of SAT: **detector physics**

CERN-RD51 PICOSEC Micromegas

Timing MIP with 24 ps precision

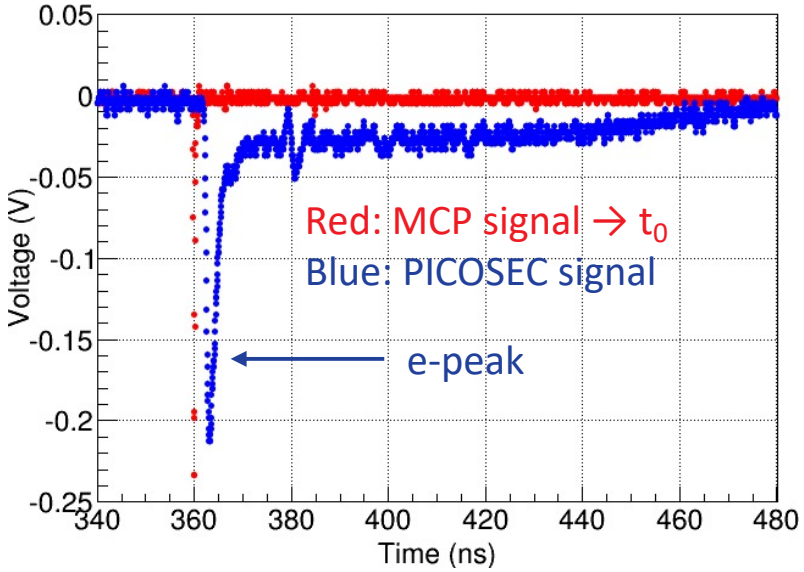

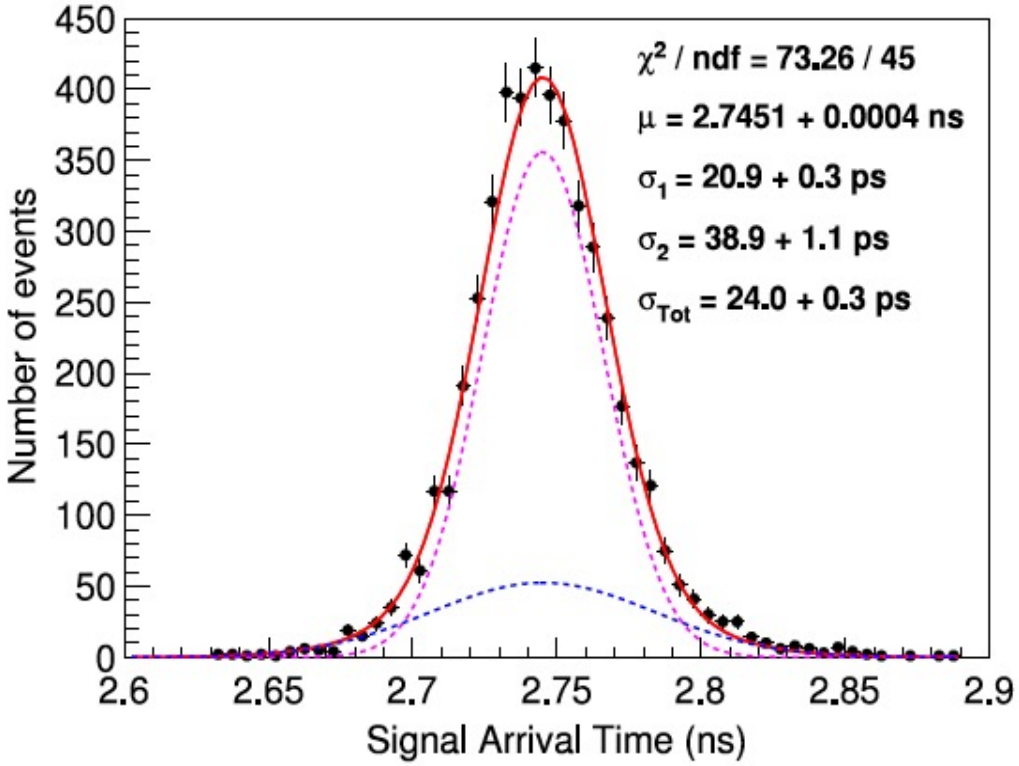

- Same detector as for Laser tests (MgF_2 radiator, CsI photocathode, Bulk MicroMegas, COMPASS gas)
- **Best time resolution: 24.0±0.3 ps**
- **@ Drift/Anode: -475V/+275V**

- J. Bortfeldt et. al. (RD51-PICOSEC collaboration), Nuclear. Inst. & Methods A 903 (2018) 317-325
- I. Manthos et al. (RD51-PICOSEC collaboration) AIP Conference Proceedings 2075, 080009 (2019)

CERN-RD51 PICOSEC Micromegas

Detailed Simulation studies

Use **Garfield++** to simulate PICOSEC for single photoelectrons, **ANSYS** for the electric field

Anode voltage does not affect much the timing properties of the signal. So, we split the simulation in three stages:

Anode: 450 V , E = 35 kV/cm

Cathode: 300-425 V ,
E =[15, 21] kV/cm

1) Drift region: simulation till the mesh.

2)Simulation in the amplification region

3) Electronics

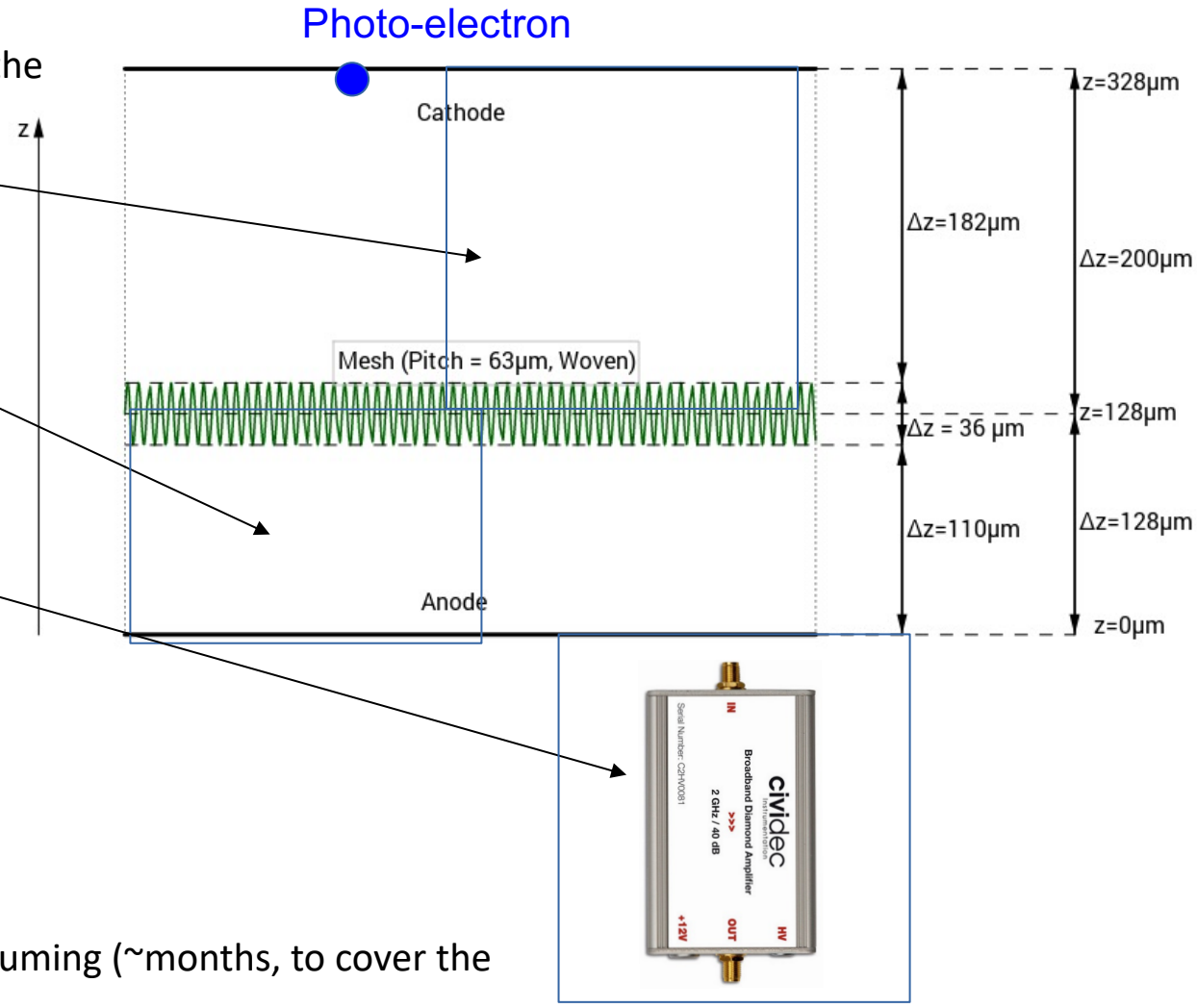

Each photoelectron produces $10^5 - 10^6$ other electrons:
A simulation of the amplification region as well would be very time-consuming (~months, to cover the various voltage etc settings tried).

CERN-RD51 PICOSEC Micromegas

Simulation studies

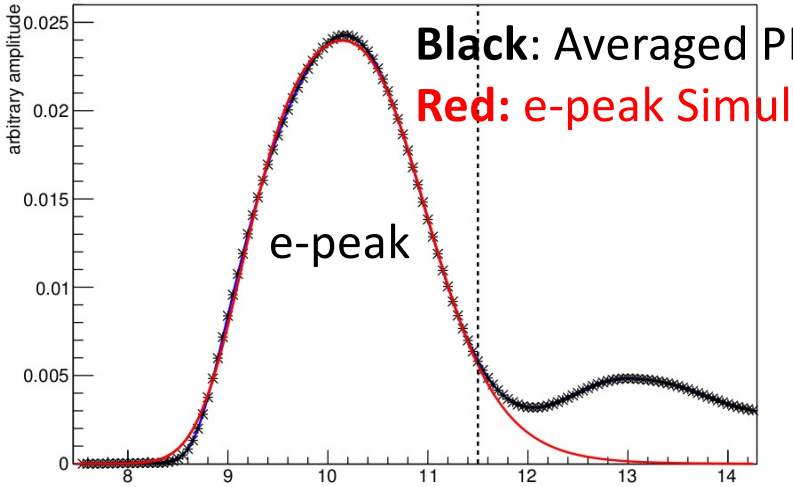

Black: Averaged PICOSEC waveforms in a certain e-peak charge region

Red: e-peak Simulation Prediction (Garfield++ and Electronics Response)

J. Bortfeldt et. al. (RD51-PICOSEC collaboration), Nuclear. Inst. & Methods A 993 (2021) 165049

All behaviors seen in single p.e. laser data are also seen in these detailed Garfield++ simulations!!!

The Signal Arrival Time (SAT) depends non-trivially on the e-peak size:

* bigger pulses
  → smaller SAT
* higher drift field
  → smaller SAT

* Time resolution depends mostly on e-peak charge

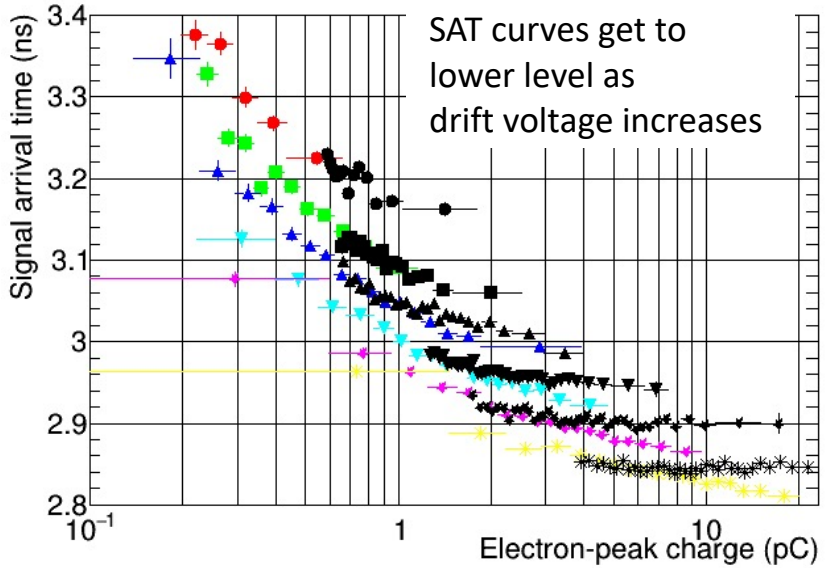

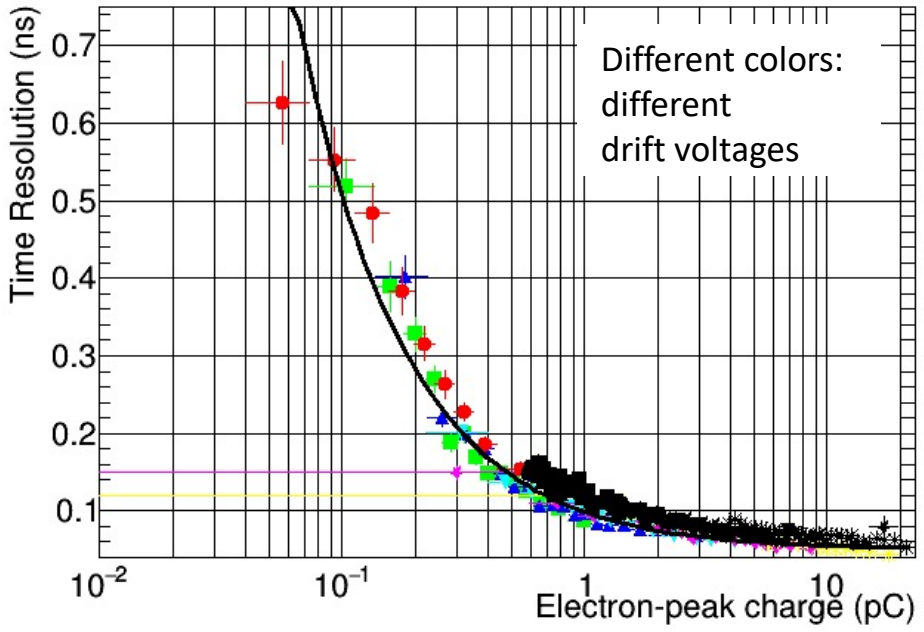

Color: Simulation – Black: Data

CERN-RD51 PICOSEC Micromegas

Simulation studies: Under the hood

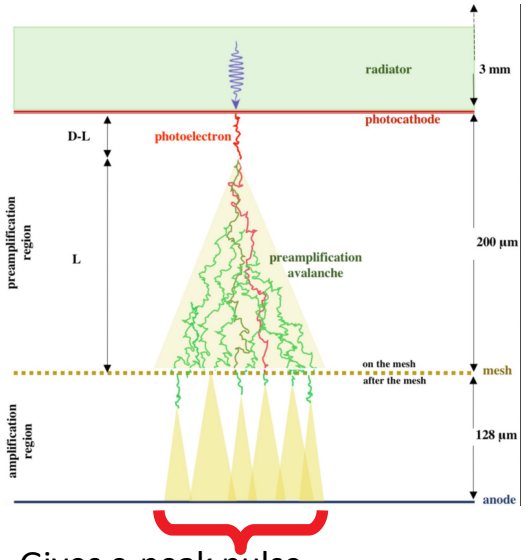

Gives e-peak pulse

Microscopic equivalent to e-peak's SAT = Mean Time (T) of all electron arrival times on the mesh

* **<SAT> linear with <T>**
* **RMS(SAT) linear with RMS(T)**

Correspondence of experimental Observables to Relevant Microscopic Variables

Sets of avalanches of a certain e-peak charge

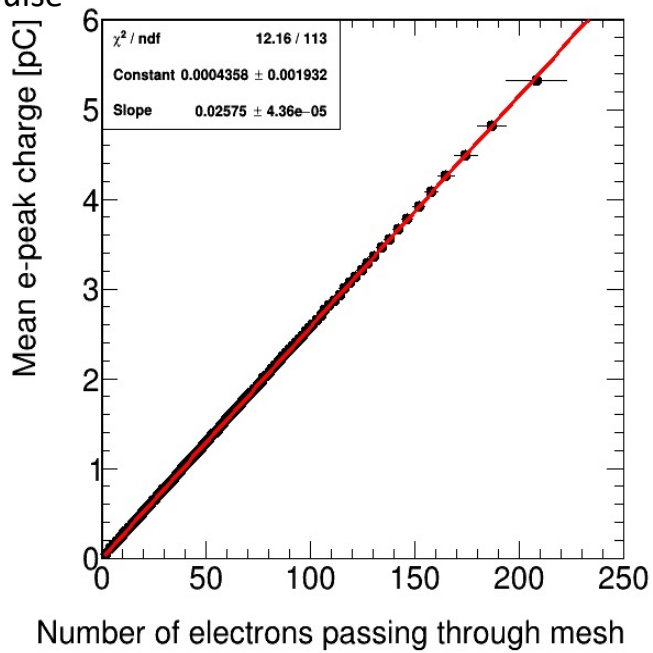

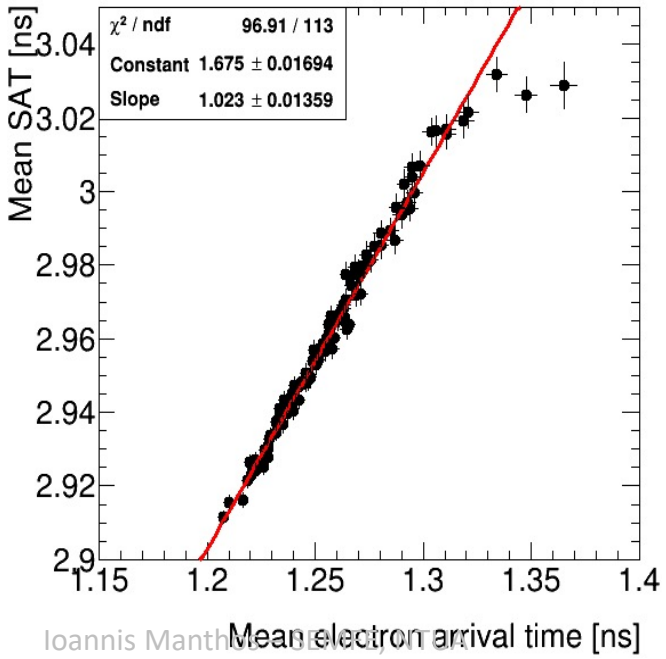

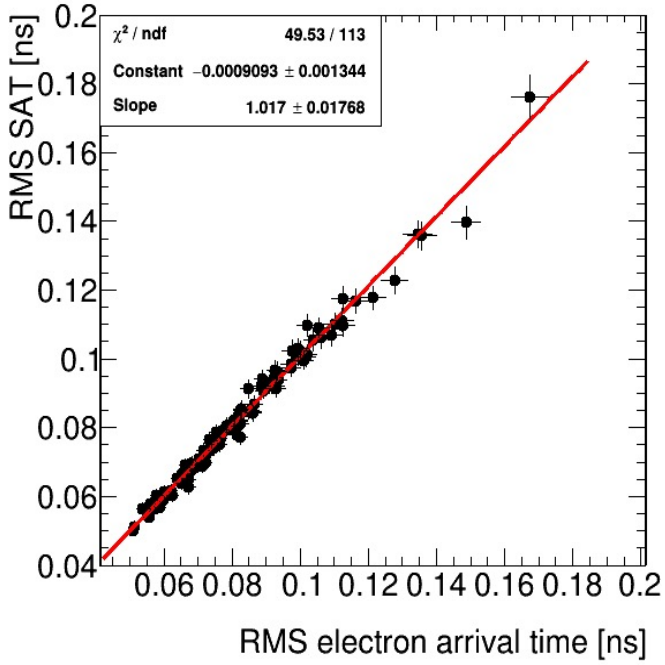

CERN-RD51 PICOSEC Micromegas

Simulation studies: Under the hood

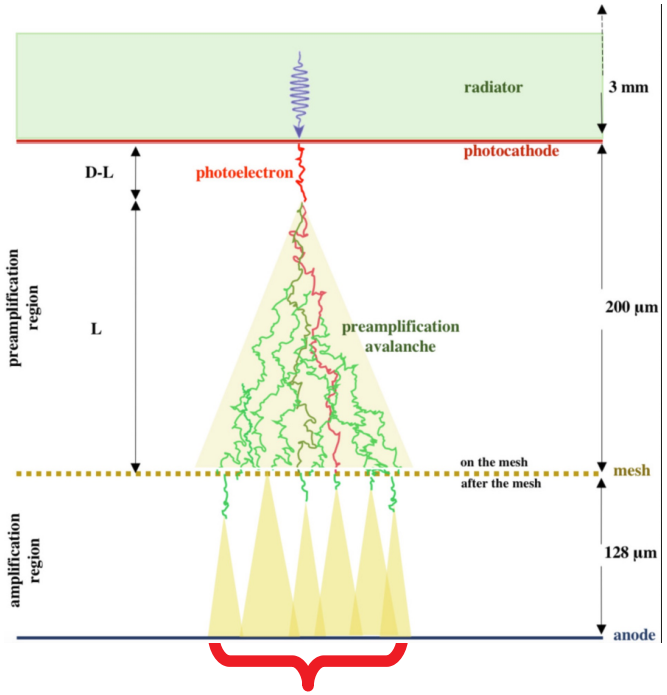

Gives e-peak pulse

Total arrival time reduces with avalanche length

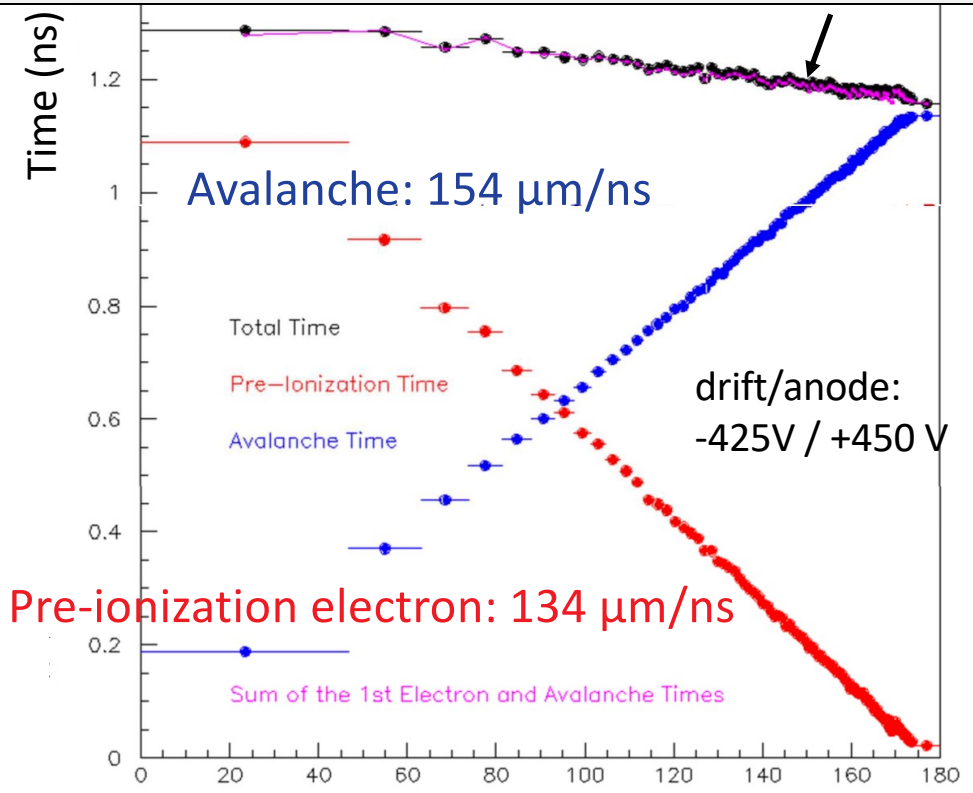

Avalanche runs with higher drift velocity than **pre-ionization electron**

So, SAT "time-walk" seen in single p.e data is explained:

SAT reduces with avalanche length

Long avalanches → big e-peak charge

} **SAT reduces with e-peak charge**

CERN-RD51 PICOSEC Micromegas

Phenomenological model: A deeper sight under the hood

- An ionizing electron in the avalanche, every time it ionizes, will gain a time **ξ** relative to an electron that undergoes elastic scatterings only.
- A newly produced electron by ionization starts with low energy, suffers less delay due to elastic backscattering compared to its parent. Relative to its parent it will have a time-gain **ρ**
- Parameters **ξ** and **ρ** should follow a joint probability distribution determined by the physical process of ionization and the respective properties of interacting molecules

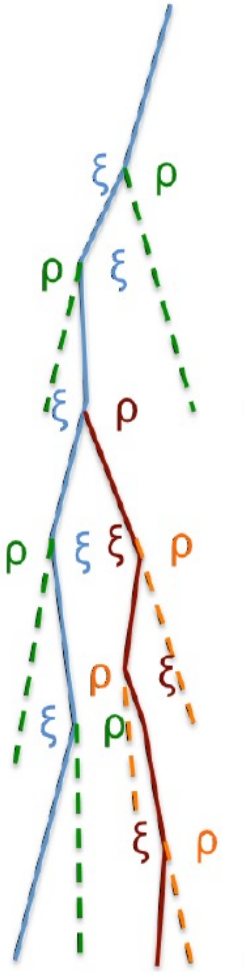

J. Bortfeldt et. al. (RD51-PICOSEC collaboration), Nuclear. Inst. & Methods A 993 (2021) 165049

CERN-RD51 PICOSEC Micromegas

Phenomenological model: A deeper sight under the hood

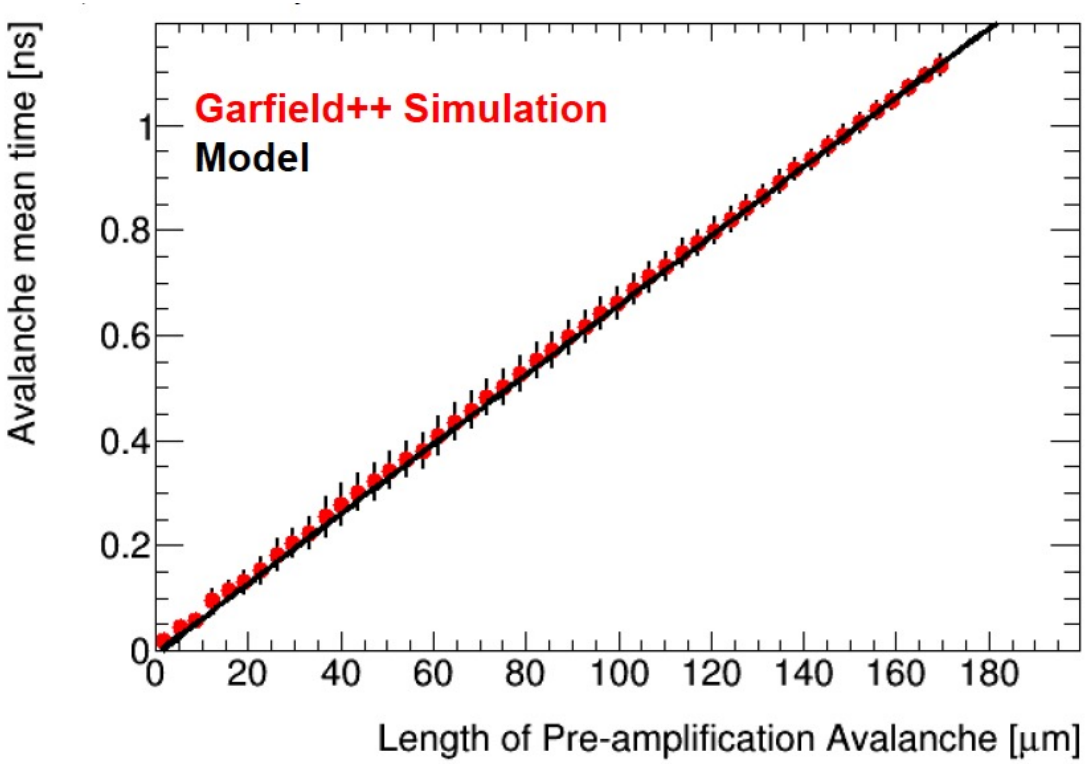

We can predict the effective drift velocity of the avalanche

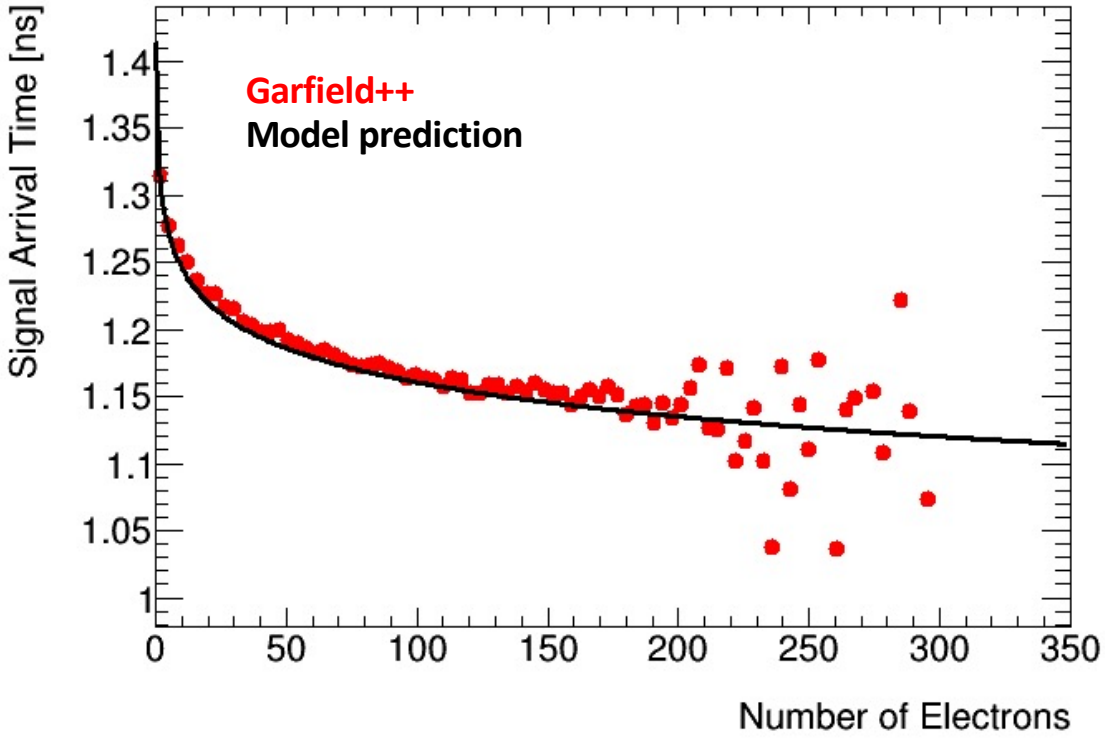

We can describe and explain the SAT dependence on the number of avalanche's electrons (i.e. on the e-peak size)

- The other parameters of the model are: the drift velocity of the photoelectron and the first Townsend coefficient.
- The model treats the number of electrons in an avalanche as continue variable.

CERN-RD51 PICOSEC Micromegas

Phenomenological model: A deeper sight under the hood

We can describe and explain the Resolution dependence on the length of the avalanche and on the number of avalanche's electrons (i.e. on the e-peak size)

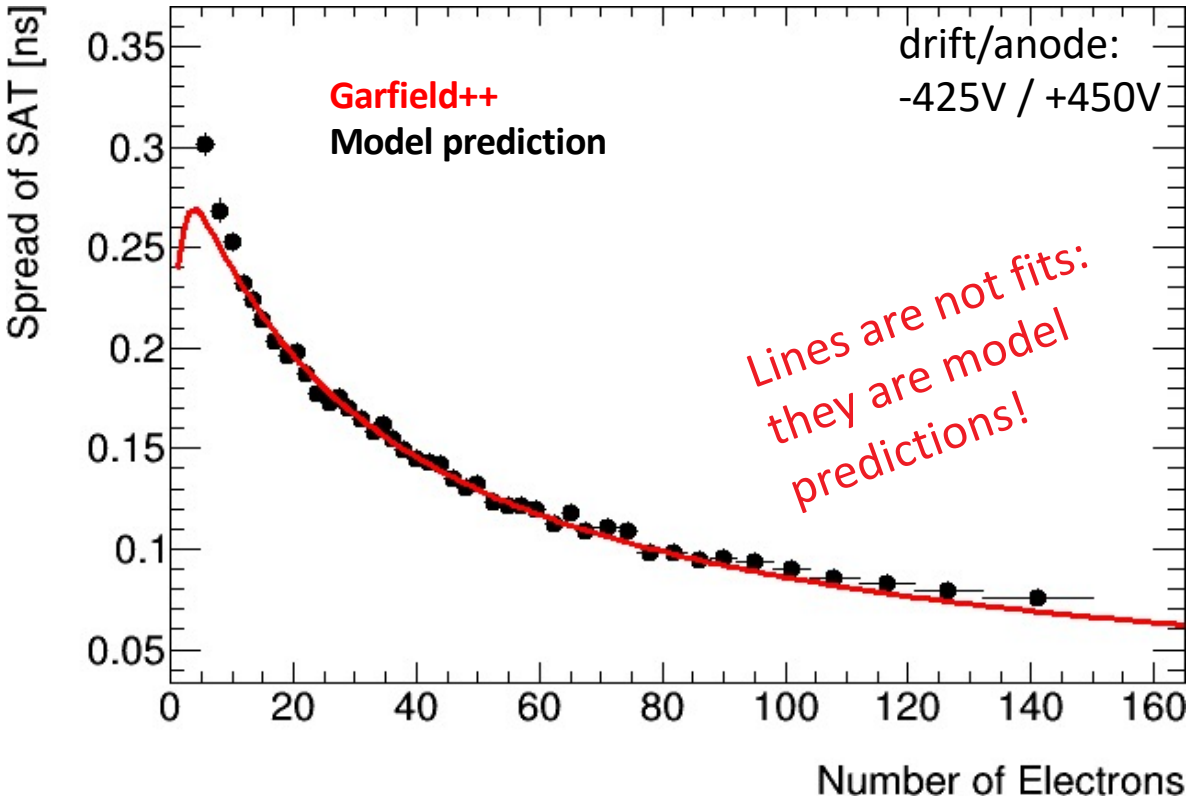

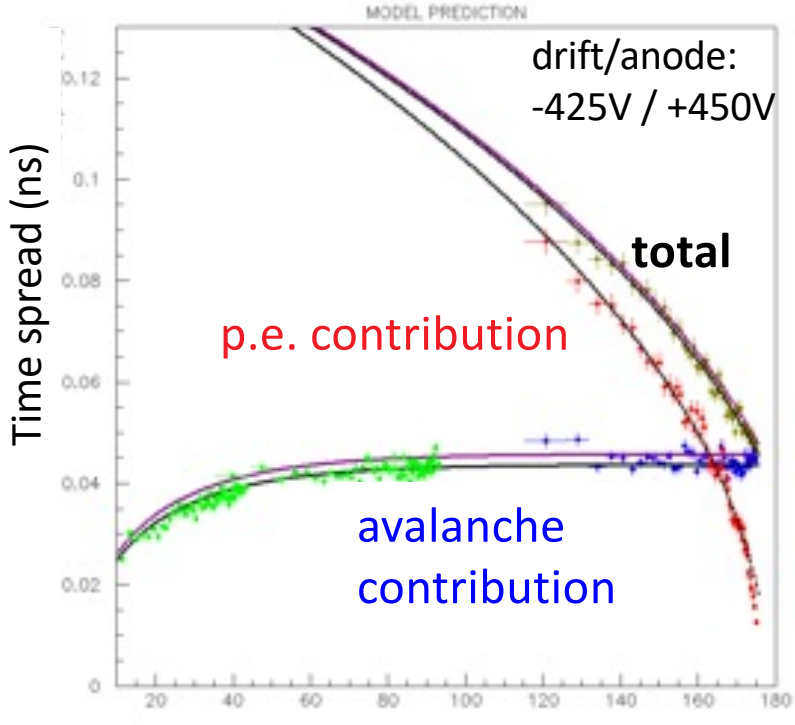

The model describes SAT and Resolution

a) vs. avalanche length &

b) vs. number of electrons in avalanche

(i.e, vs. e-peak charge)

→ Before and after the mesh

Full distributions vs. values of operational parameters obtained (e.g. drift voltage)

CERN-RD51 PICOSEC Micromegas

Estimation of the photocathode yield on MIP

Precise alignment based on the charge-weighted beam profile

Consistent and unbiased method to evaluate photocathodes performance

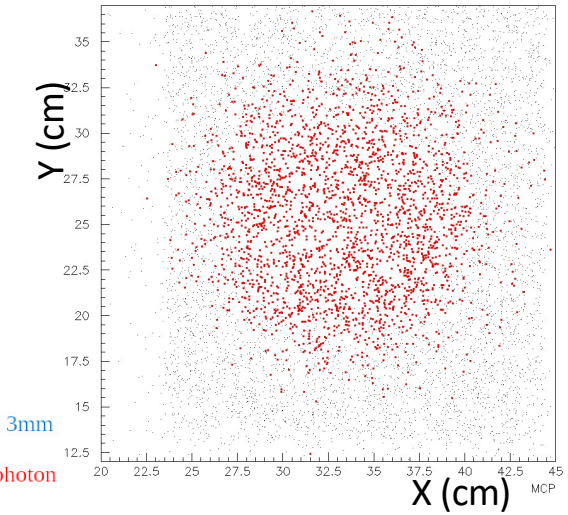

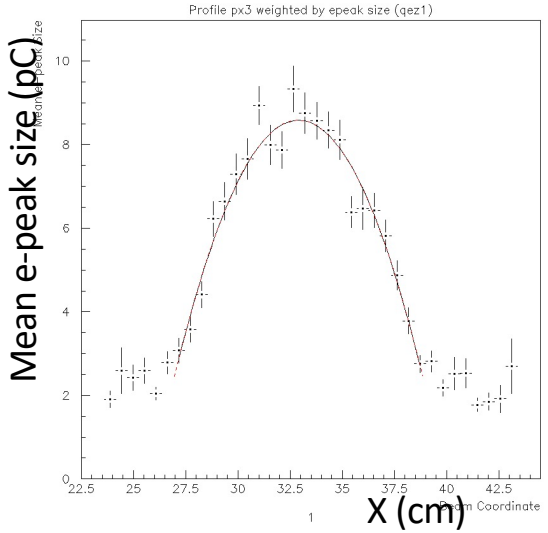

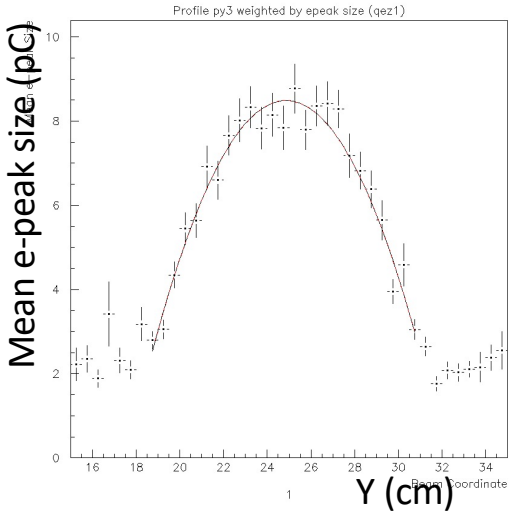

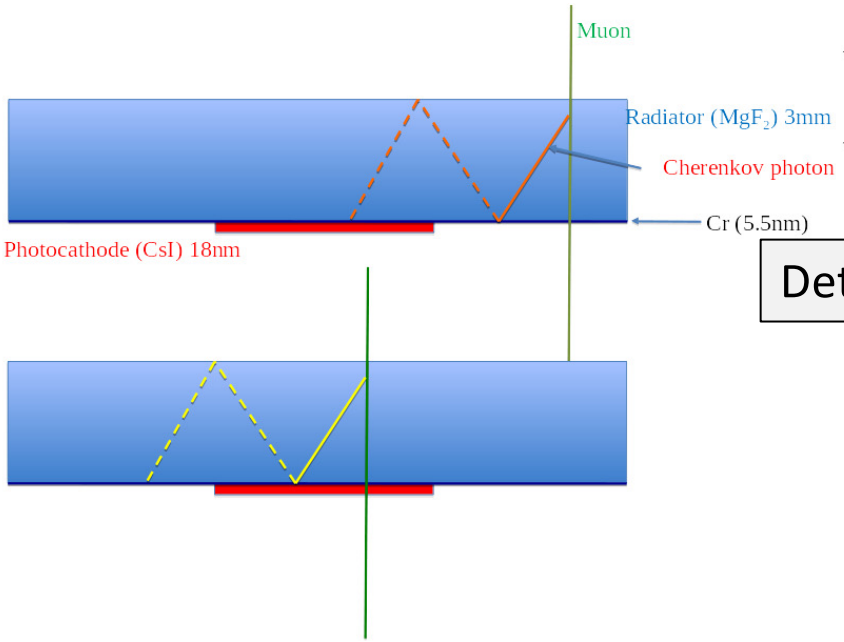

Determination of the anode geometrical acceptance taking into account reflections

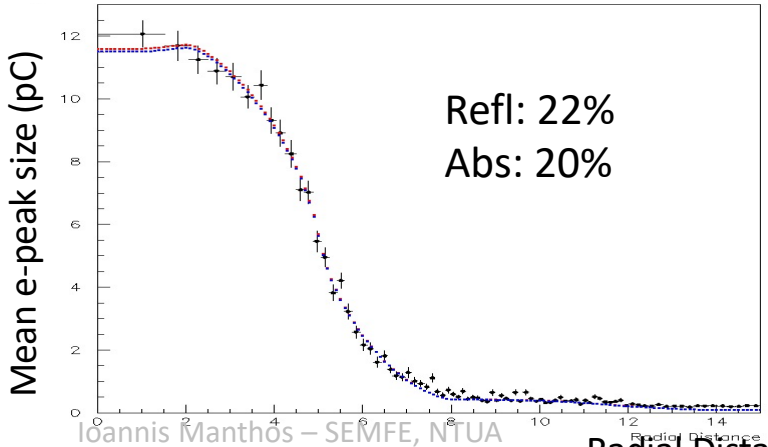

Mean charge per track (pC) vs the track radial distance (mm)

CERN-RD51 PICOSEC Micromegas

Estimation of the photocathode yield on MIP

Determination of charge distribution parameters when **PICOSEC MM responds to a single-pe** using UV calibration data

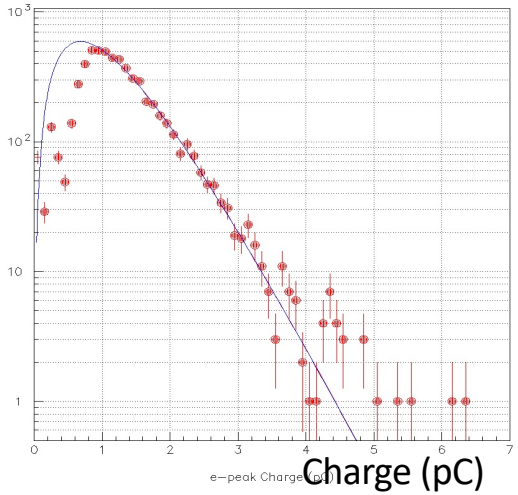

Polya fit to the single-p.e. charge distribution

$$P_{spe}\left(Q;a=b=\theta+1,\bar{Q}_e\right)dQ=\frac{1}{Q_e}\frac{(\theta+1)^{(\theta+1)}\left(Q/\bar{Q}_e\right)^{\theta}}{\Gamma(\theta+1)}e^{-(\theta+1)Q/\bar{Q}_e}dQ$$

$$E\left[Q_{spe}\right]=\bar{Q}_e=\langle Q_e\rangle$$

$$V\left[Q_{spe}\right]=\frac{1}{\theta+1}\langle Q_e\rangle^2=RMS^2$$

Fit the charge distribution of the PICOSEC **response to muons**

If N is the mean number of pes produced per muon track, then a muon passing through the radiator at distance R from the anode center will result to a PICOSEC signal with charge Q.
Q follows a p.d.f. F(Q,R;N) which can be expressed using the geometrical acceptance A(R), as a convolution of a Poissonian distribution with mean N·A(R)

$$\Pi(N_{pe};N,A(R))=\frac{[N\cdot A(R)]^{N_{pe}}}{N_{pe}!}\cdot\exp[-N\cdot A(R)]$$

and the multi-Polya distribution

$$P(Q;N_{pe},\theta,\overline{Q_e})=\underbrace{P_{spe}\otimes P_{spe}\cdots\otimes P_{spe}}_{N_{pe}\ times}=\frac{1}{\overline{Q_e}}\frac{(\theta+1)^{N_{pe}(\theta+1)}(Q/\overline{Q_e})^{N_{pe}(\theta+1)-1}}{\Gamma(N_{pe}(\theta+1))}\cdot\exp[-(\theta+1)\cdot Q/\overline{Q_e}]$$

as

$$F(Q,R;N)=\sum_{N_{pe}=0}^{\infty}\Pi(N_{pe};N,A(R))\cdot P(Q;N_{pe},\theta,\overline{Q_e})$$

CERN-RD51 PICOSEC Micromegas

Estimation of the photocathode yield on MIP

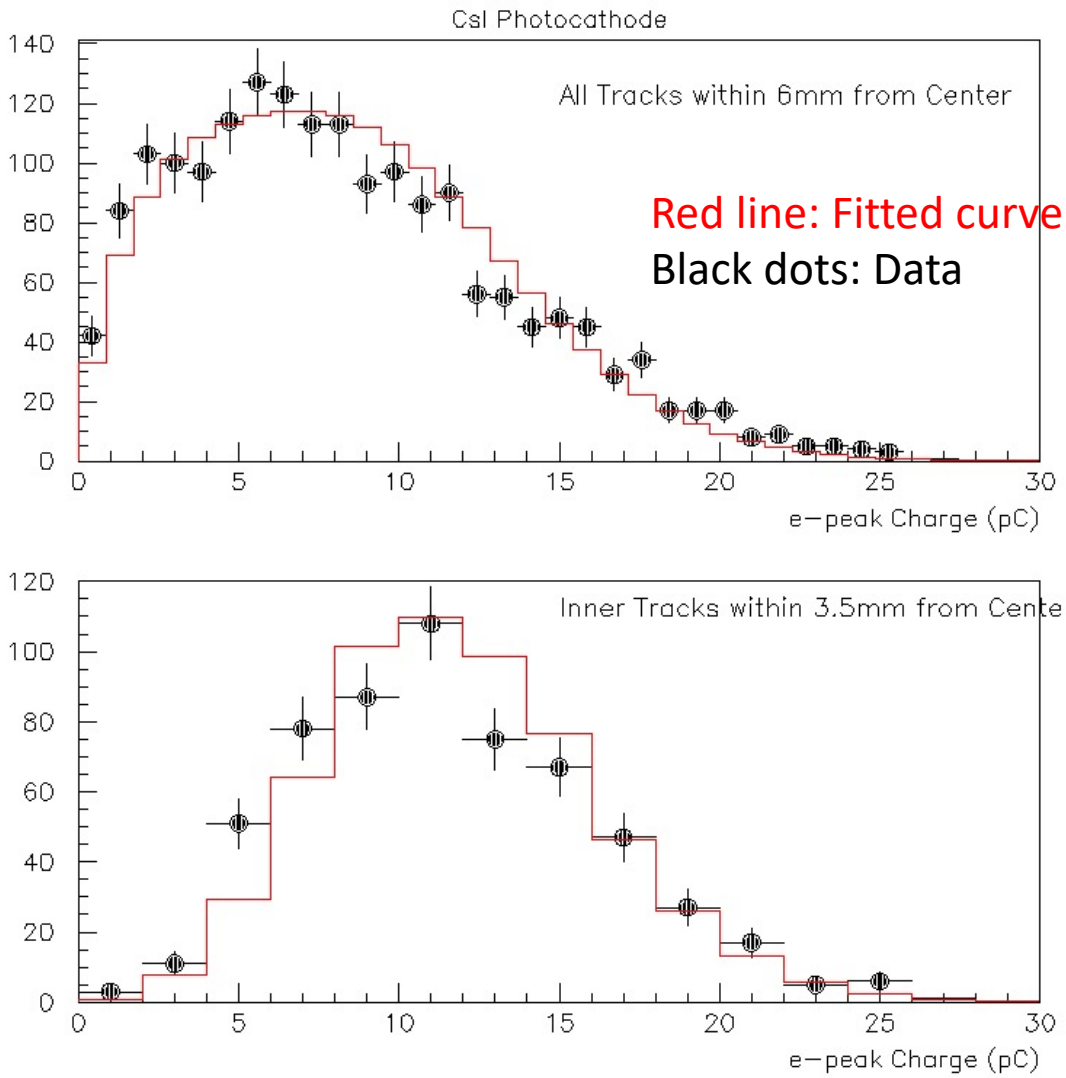

11.5 ±0.4(stat)±0.5(syst) photoelectrons per muon track

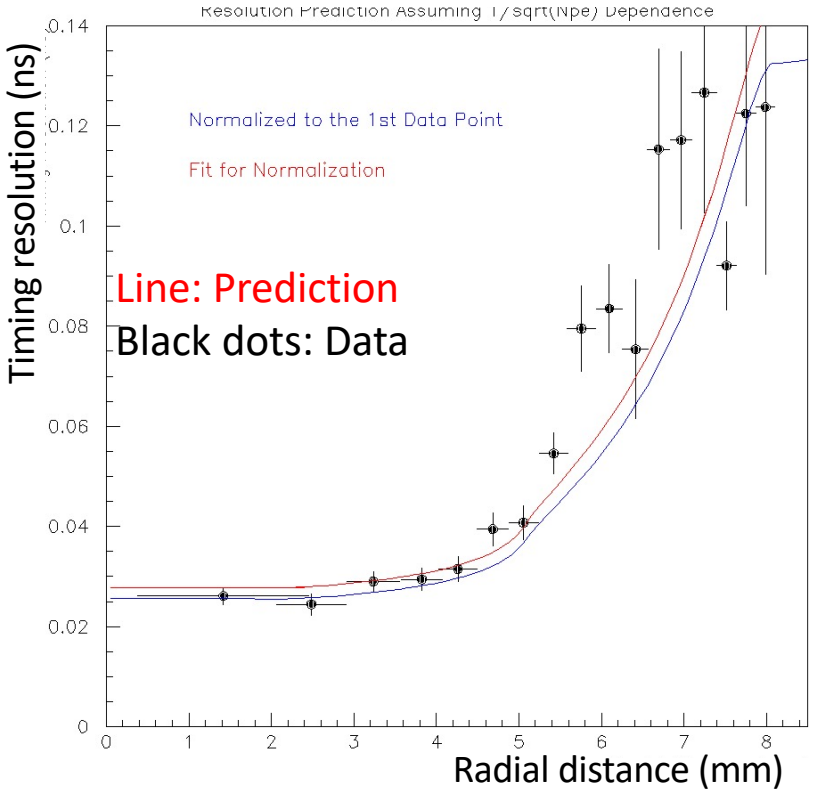

Resolution prediction vs distance from the anode center, assuming **1/sqrt(Npe)** dependence

I Manthos et al 2020 J. Phys.: Conf. Ser.1498 012014

CERN-RD51 PICOSEC Micromegas

Large area coverage – Multipad PICOSEC

- Like the single-pad (MgF2/CsI/bulkMM/COMPASS gas) PICOSEC which achieved 24ps per MIP
- Hexagonal pads 5mm side
- Readout 4 pads → 2 oscilloscopes

Non perfect planarity

Peripheral pads presented worse timing resolution than central one

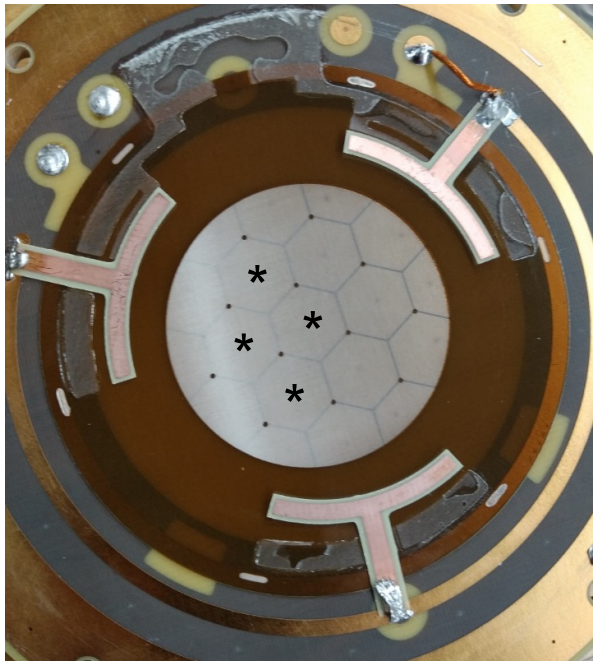

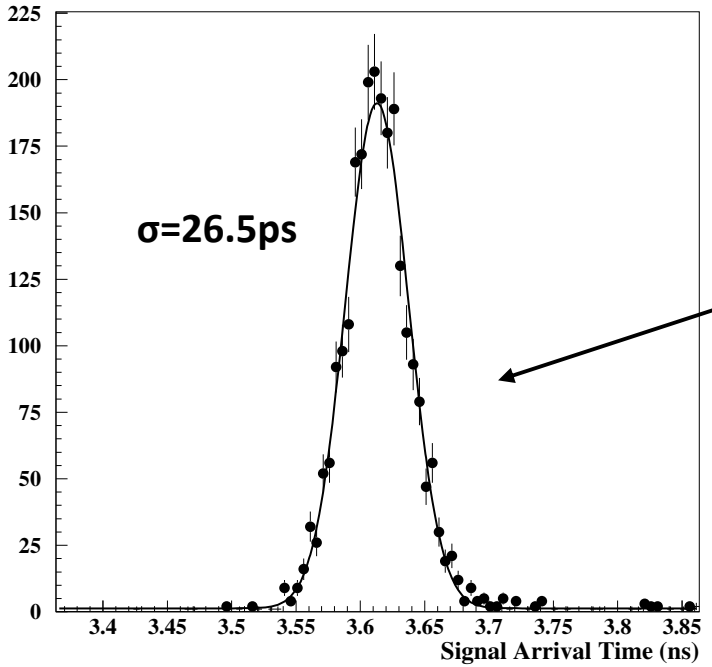

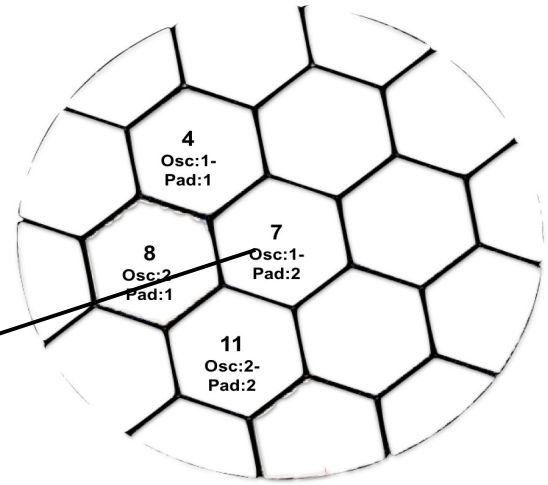

CERN-RD51 PICOSEC Micromegas

Large area coverage – Individual pad response

Multi-pad: Same resolution as single-pad

After applying flatness correction:

Timing resolution of **25ps for all pads**

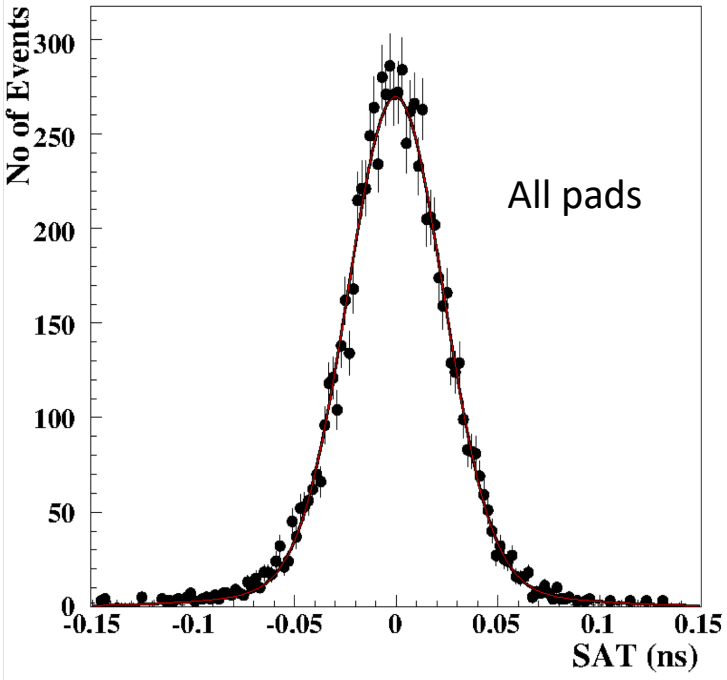

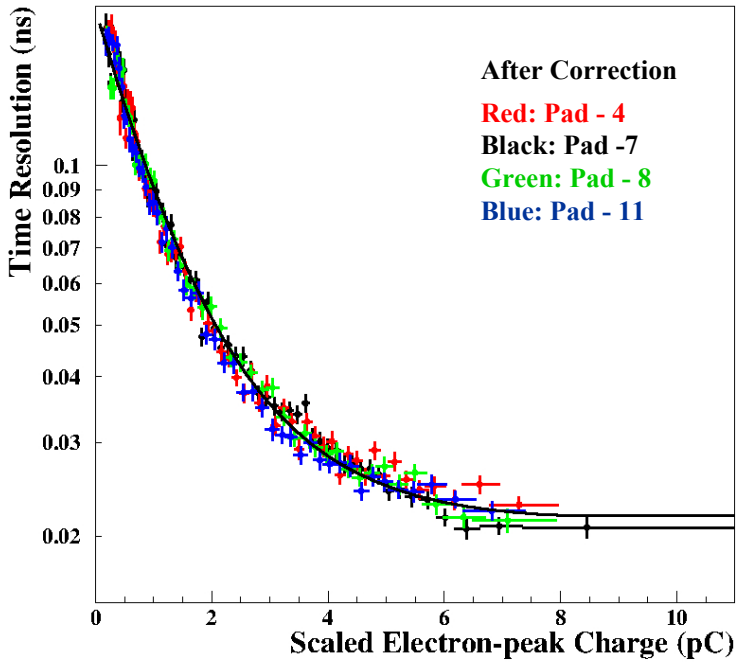

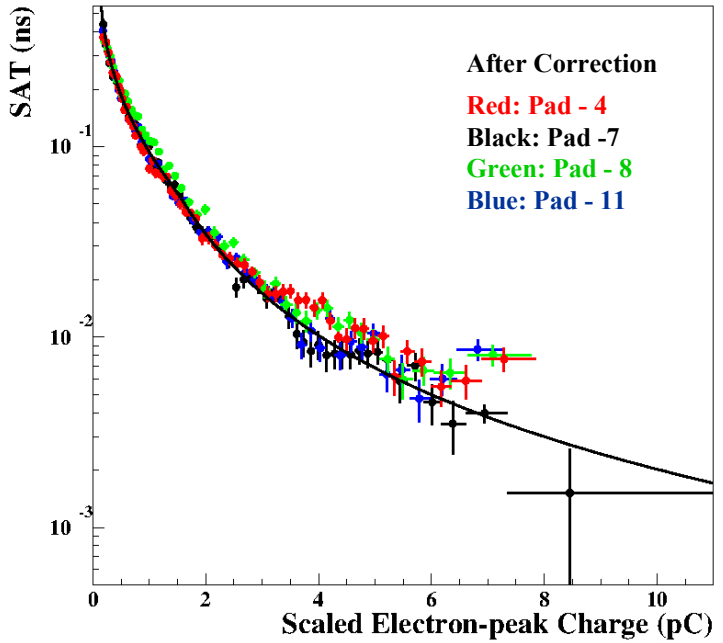

S. Aune et al. for the PICOSEC Collaboration, NIM-A, Vol. 993, (2021), 165076 - arXiv:2012.00545v2

CERN-RD51 PICOSEC Micromegas

Large area coverage – the "3 pads" area

Not the easiest regions

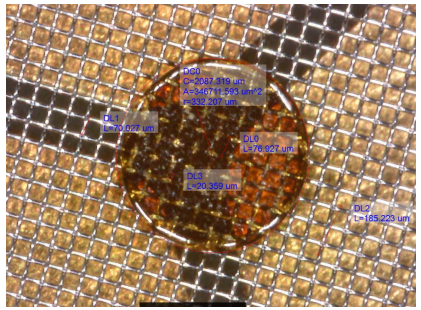

Pillars of ~650μm diameter

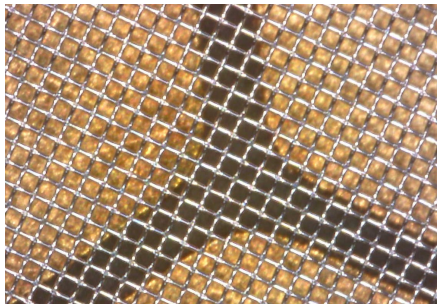

200μm inter-pad space

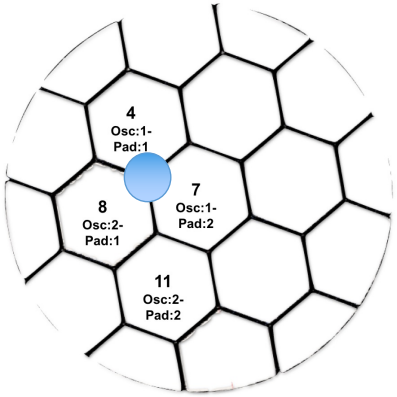

Possible non-uniformities on the field to be studied

Individual pad responses

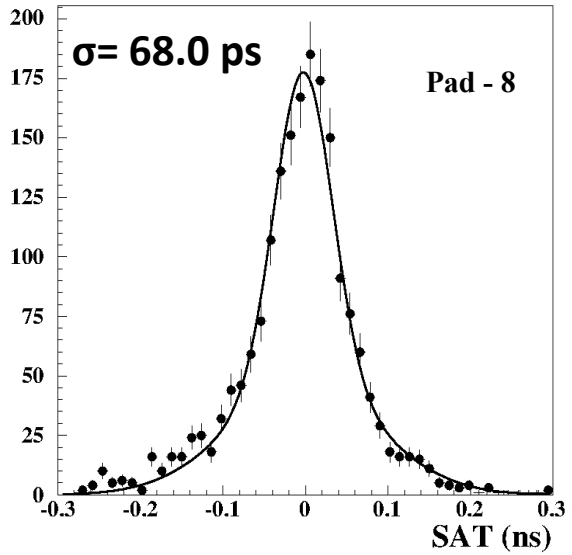

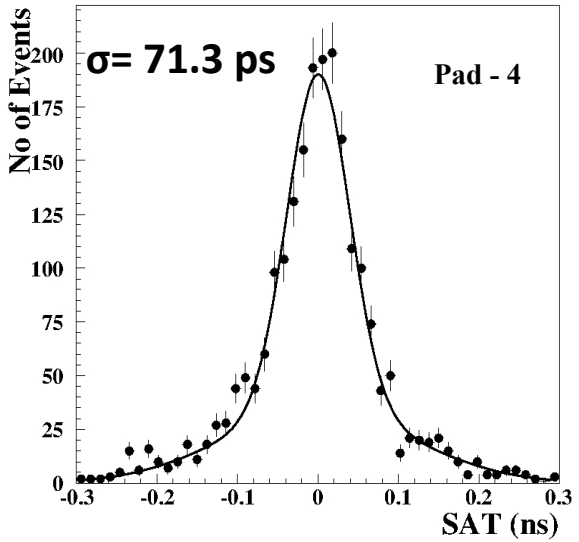

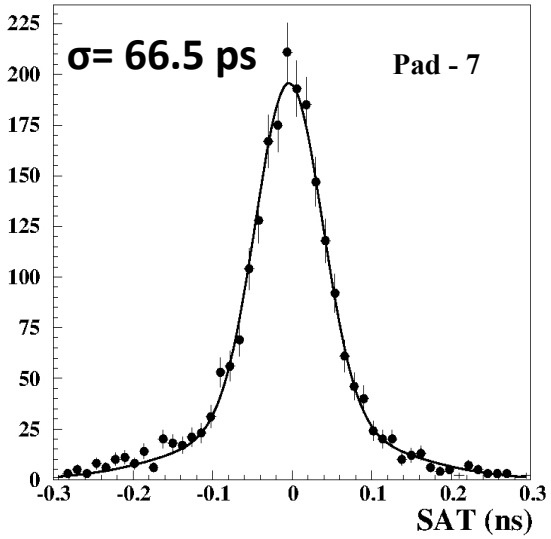

SAT: Signal Arrival Time

Naive estimation: <σ>/sqrt(3)≈**40 ps**

CERN-RD51 PICOSEC Micromegas

Large area coverage – the "3 pads" area

combined pad response

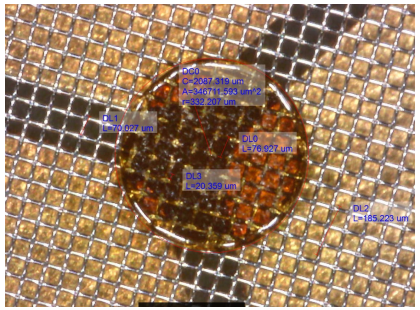

Pillars of ~650μm diameter

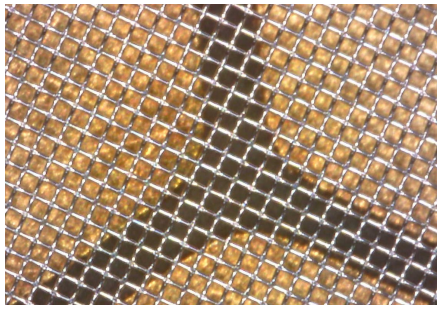

200μm inter-pad space

$$\chi^2 = \sum_{m=1,M} \frac{\left(T_{comb.} - \left[T^m_{f-corr.} - \tau\left(Q^m_e\right)\right]\right)^2}{\sigma^2\left(Q^m_e\right)}$$

$$\hat{T}_{comb.} = \frac{\sum_{m=1,M} \frac{\left(T^m_{f-corr.} - \tau\left(Q^m_e\right)\right)^2}{\sigma^2\left(Q^m_e\right)}}{\sum_{m=1,M} \frac{1}{\sigma^2\left(Q^m_e\right)}}$$

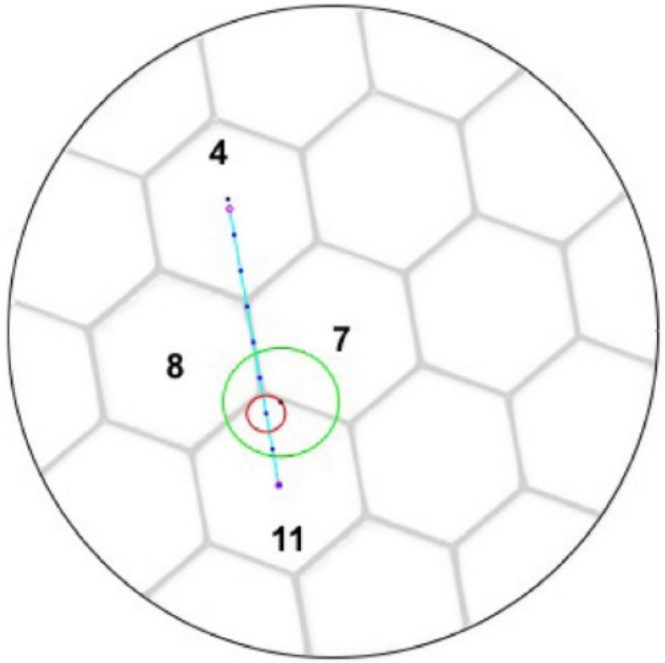

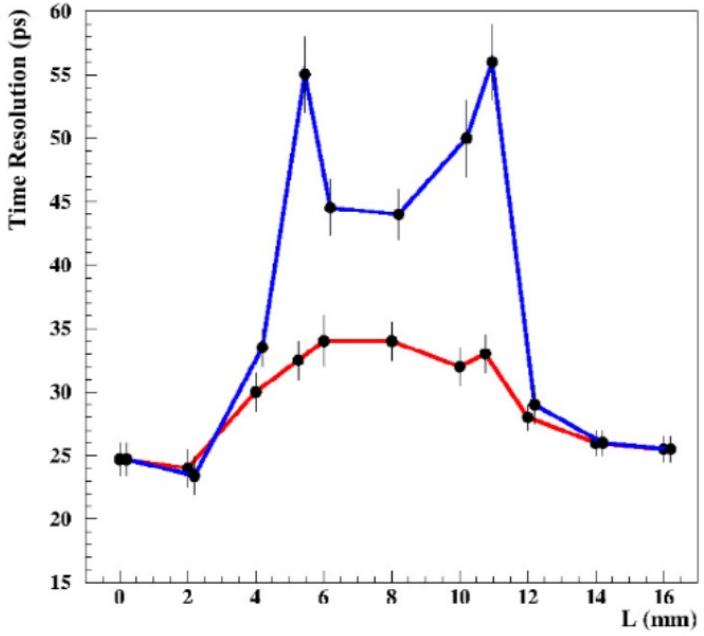

S. Aune et al. for the PICOSEC Collaboration, NIM-A, Vol. 993, (2021), 165076 - arXiv:2012.00545v2

CERN-RD51 PICOSEC Micromegas

Reducing drift gap to 119 μm

Laser test beam: LYDIL laser laboratory of CEA-IRAMIS (France)

1 photoelectron (pe)

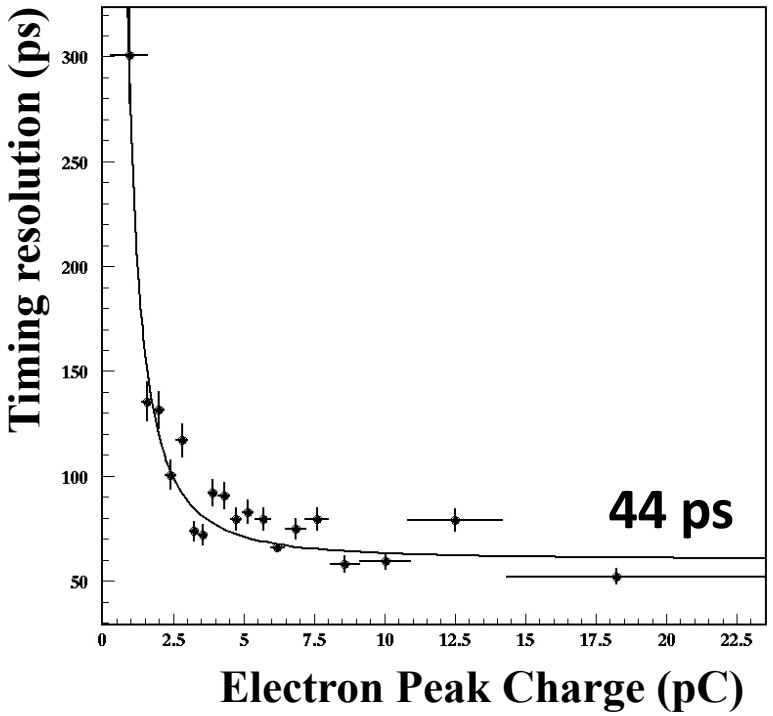

7.8 pes

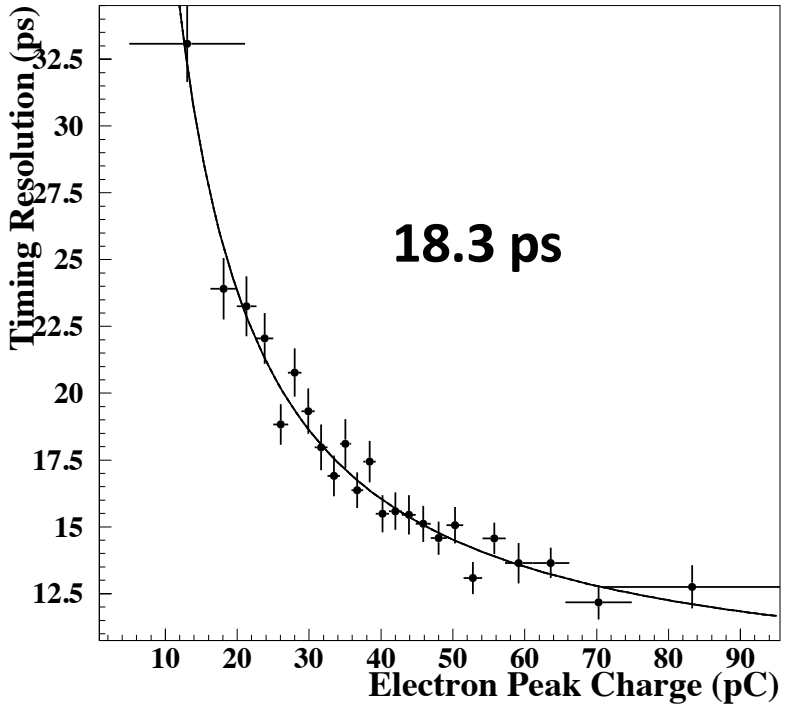

70 pes

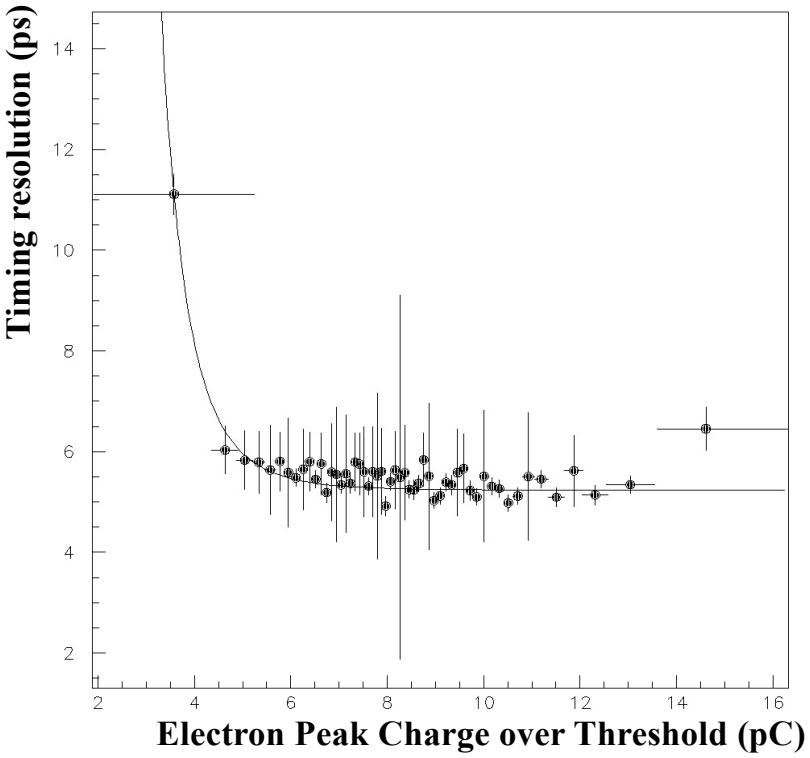

CERN-RD51 PICOSEC Micromegas

Alternative timing methods

- Using single threshold electronics (e.g. NINO chip)

Red: Standard offline analysis (CFD@20%)
Black: Single threshold 100 mV, correcting time-walk with the highest available Charge over Threshold (100, 200, 400, 600 mV) – SAT parameterization

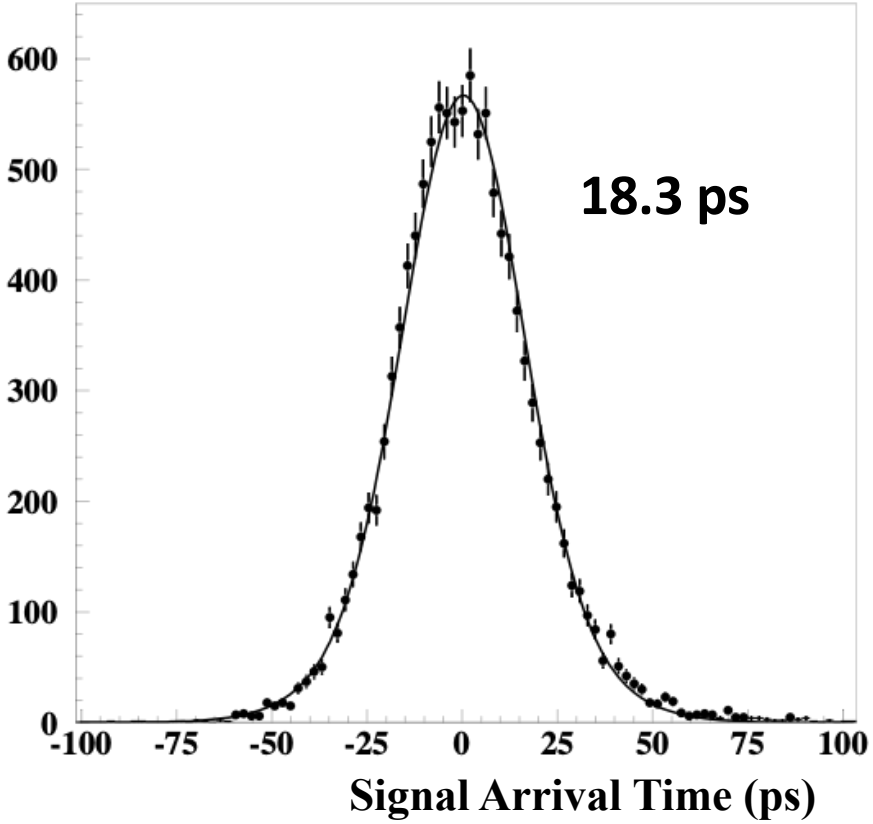

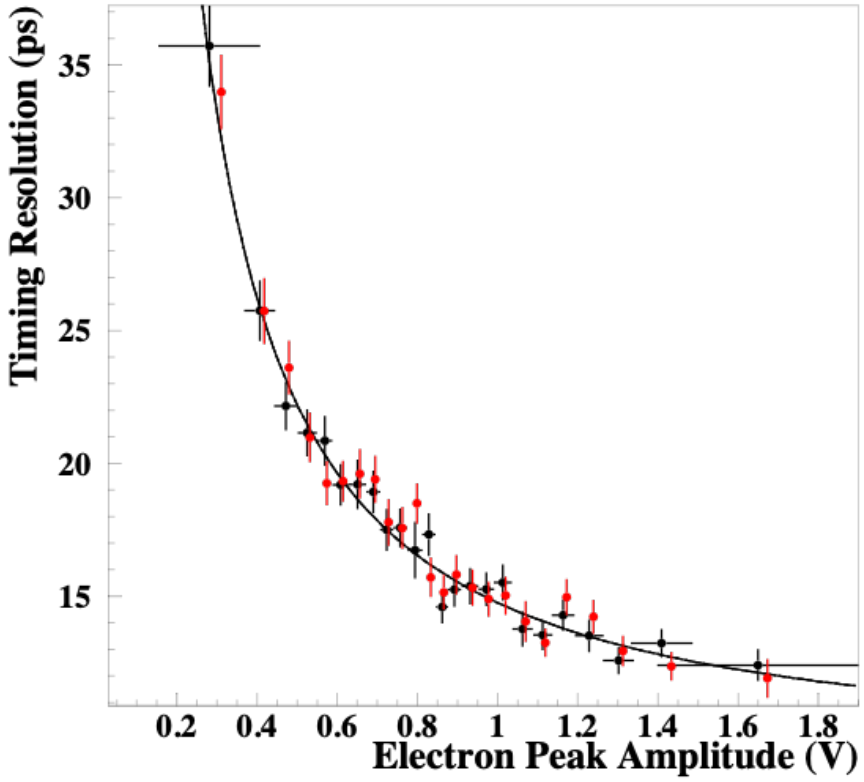

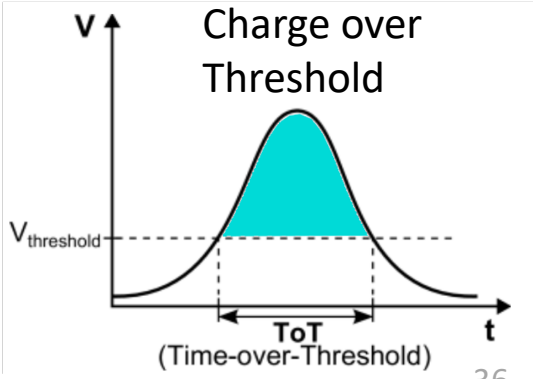

CERN-RD51 PICOSEC Micromegas

Alternative timing methods

- Digitize only the Leading edge and using artificial Neural Networks (SAMPIC electronics)

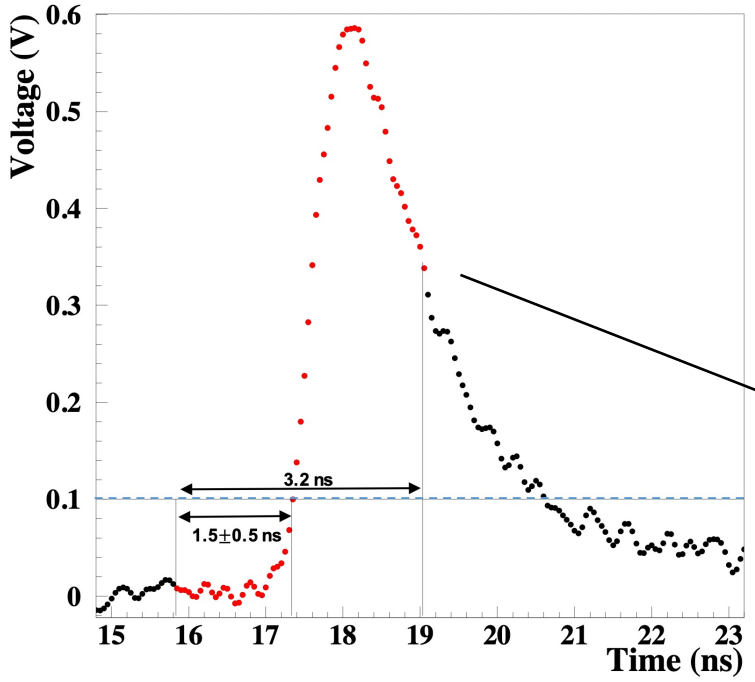

Network input: 64 bits (red)

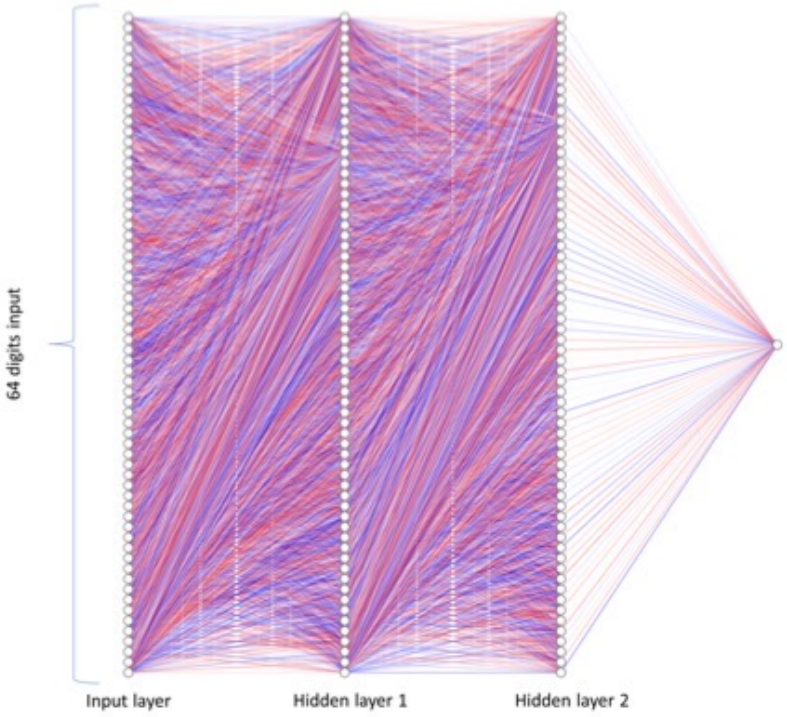

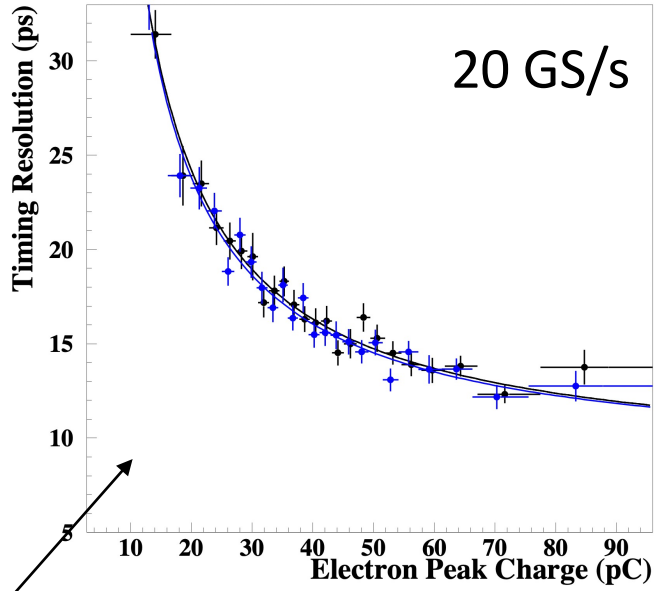

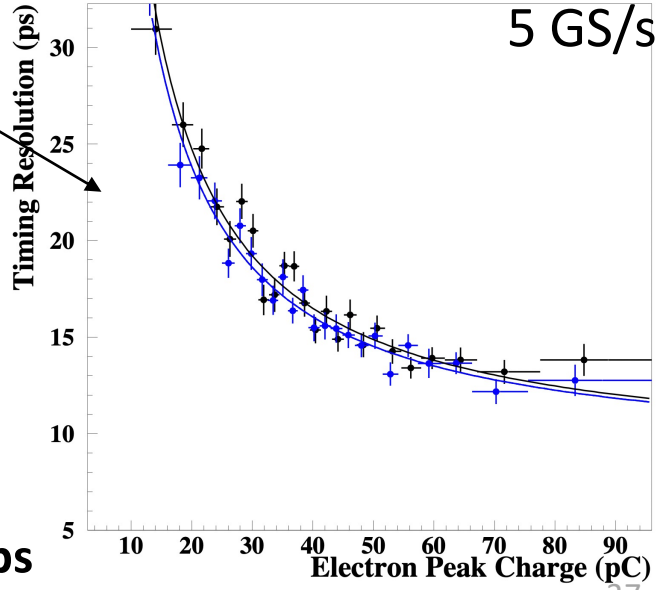

Presented at PSD12 conference – proceedings under preparation
Publication under preparation

Blue: Offline analysis **18.3ps**
Black: Neural Network **18.3ps** (20GS/s) – **19.2ps** (5Gs/s)

Career path

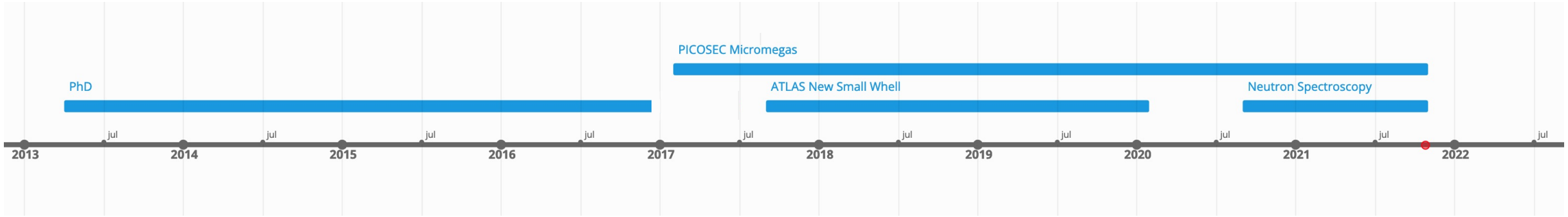

- **Apr. 2013 – Nov. 2016:** Ph.D. - Detection and study of extensive air showers using innovative detectors and algorithms *(University of the Aegean – Hellenic Open University)*
- **Sep. 2017 – Jan. 2020:** ATLAS New Small Wheel, LM2 drift panels construction and QA/QC *(Aristotle University of Thessaloniki)*
- **Feb. 2017 – today:** PICOSEC Micromegas R&D *(Aristotle University of Thessaloniki)*
- **Sep. 2020 – today:** Fast Neutron Spectroscopy with the Spherical Proportional Counter *(University of Birmingham)*

Fast neutron spectroscopy with the Spherical Proportional Counter

UNIVERSITY OF BIRMINGHAM

Dark matter underground experiments

- MeV neutrons produce signals in the region of interest for WIMP detection

  - ➢ Sources: Radioactivity of cavern, muon induced hadronic and electromagnetic showers (cosmic rays)
  - ➢ Elastic scattering with target nuclei of gas, interaction with detector material

- Neutron background can not be discriminated using event properties
- Neutron rejection: shielding and use of high-purity materials.
- Data analysis require an estimation of the neutron background expected in order to compare with the observed number of events.

e.g. cavern background at SNOLAB *(from A. Brossard Ph.D thesis)*

	Source	Contamination / flux	Unit	Events rate <1 keV [dru]	Events rate in [1;5] keV [dru]	Total rate [mHz]
Cavern	Gamma	4.87×10^{-8}	$\gamma/cm^2/s$	0.0084	0.0095	0.00464
	Neutron	4000	$neutron/m^2/day$	0.0044	0.0004	3.54×10^{-11}
	Muon	0.27	$muon/m^2/day$	0.00062	0.00044	5.04×10^{-8}

Current neutron detector status

^{3}He proportional counters

$n + {}^3He \rightarrow {}^3H + p + 765\ keV$

✓ Efficient for thermal and fast neutrons, low efficiency in γ-rays

✗ Wall effect → high pressure (impractical)
^{3}He extremely expensive

This research has been funded by the European Union's Horizon 2020 Research and Innovation Programme under the Marie Sklodowska-Curie Grant Agreement No 845168 (neutronSphere)

Neutron detection with the Spherical Proportional Counter

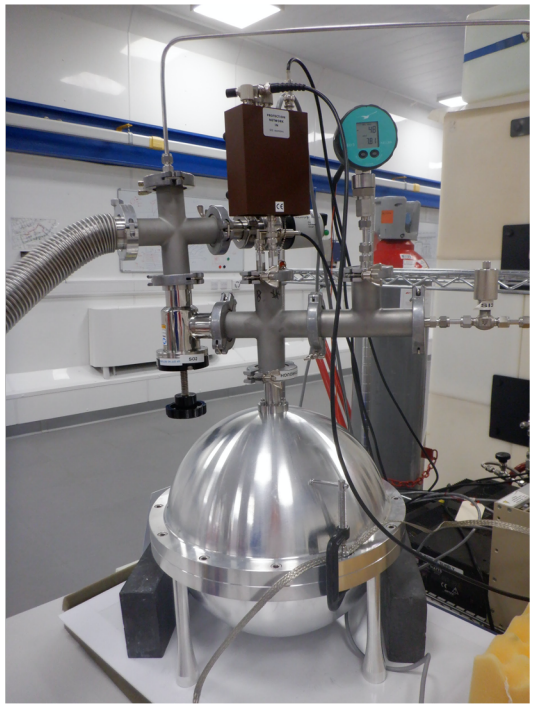

+

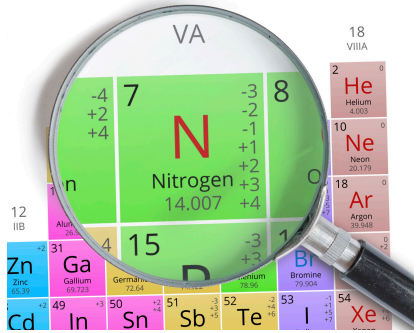

- ✓ Non-toxic
- ✓ Non-flammable
- ✓ Simple and robust setup
- ✓ Easy deployment and operation
- ✓ Cost efficient

- ✓ Wall effect suppressed due to higher atomic number of N_2 relative to ^3He → lower pressure
- ✓ Good efficiency in detecting thermal and fast neutrons in large volumes
- ✓ Low γ-ray efficiency
- ✓ Spectroscopic measurement of neutrons

Nitrogen as target

$^{14}N + n \rightarrow {}^{14}C + p + 625$ keV, $\sigma_{th} = 1.83$ b

$^{14}N + n \rightarrow {}^{11}B + \alpha - 159$ keV, thres=1.7 MeV

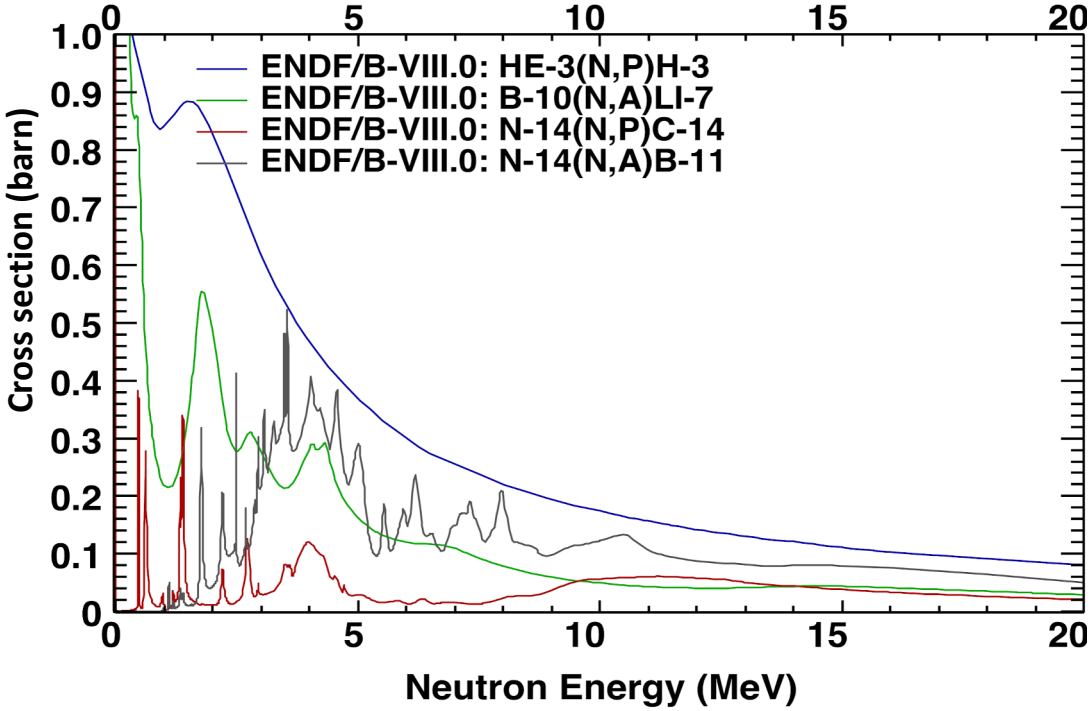

The Spherical Proportional Counter

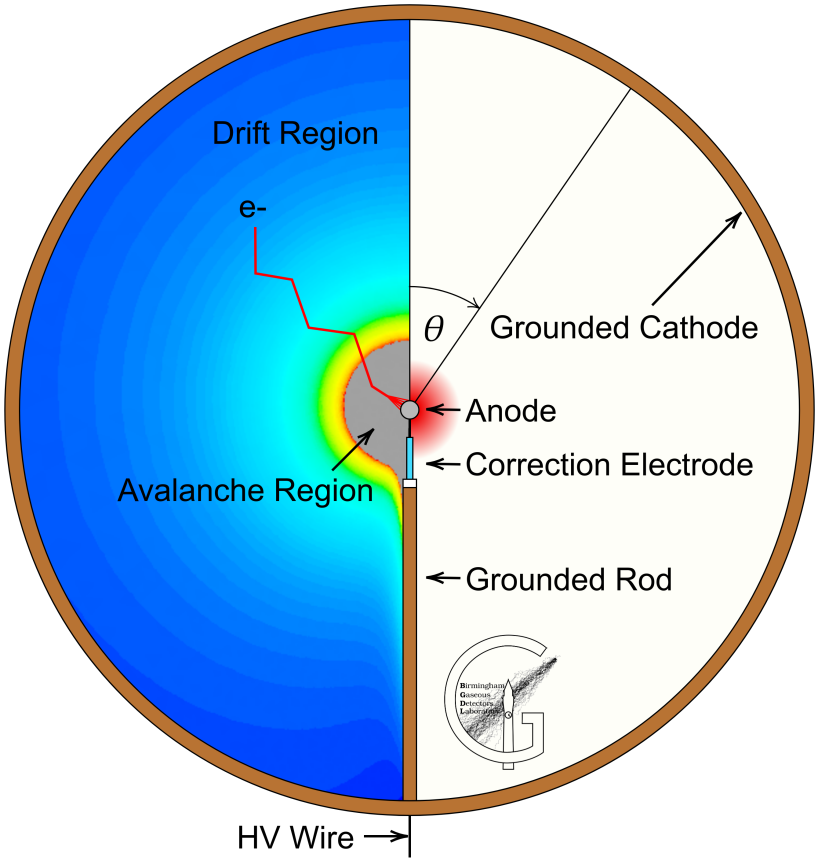

Electric field scales as $1/r^2$

- Divided into "drift" and "amplification" regions

$$\vec{E} = \frac{V_1}{r^2}\frac{r_c r_a}{r_c - r_a}\hat{r} \approx \frac{V_1}{r^2} r_a$$

Capacitance independent of detector size

- Low electronic noise

$$C = 4\pi\varepsilon_0 \frac{r_c r_a}{r_c - r_a} \approx 4\pi\varepsilon_0 r_a \sim 1\text{pF}$$

- Large gain - Single e^- threshold
- Maximum volume-to-surface ratio
- High pressure operation
- Simple, robust design with a flexibility in target gas
- Applications in n-spectroscopy to DM!

Rise time selections to:

- Distinguish point-like versus extended ionisations
- Fiducialise detector

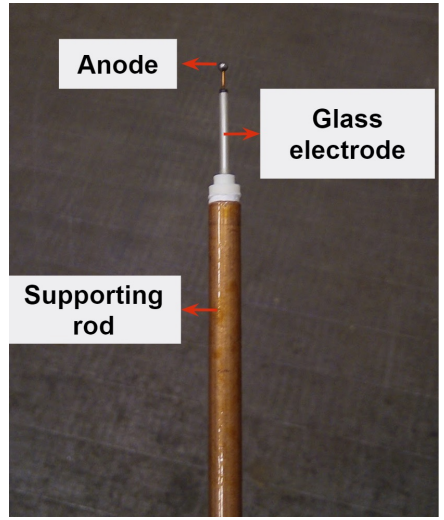

r_c = cathode radius
r_a = anode radius

UNIVERSITY OF BIRMINGHAM

I.Giomataris et al, JINST, 2008, P09007

Neutron detection with the Spherical Proportional Counter
Proof of principle and state-of-the-art advancements

- ^{252}Cf, $^{241}Am^{9}Be$ and ambient fast neutrons
- Thermal neutrons
- N_2 at 0.1-0.5 bar
- HV ~ 6 kV

Bougamont, E et al (2017). NIM A, 847, 10–1

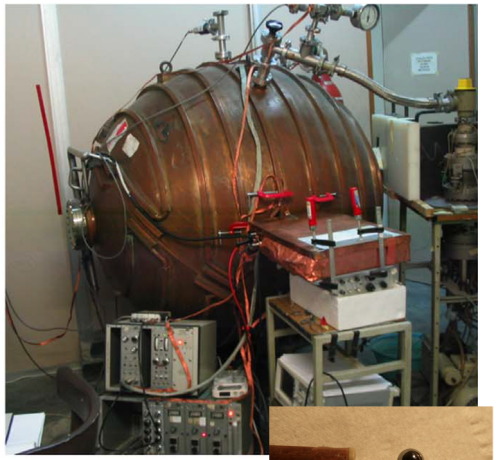

SPC 140 cm Ø
Anode 8 mm Ø

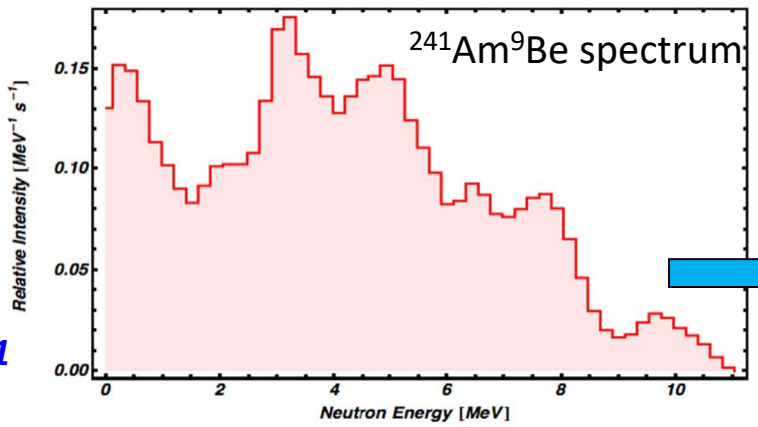

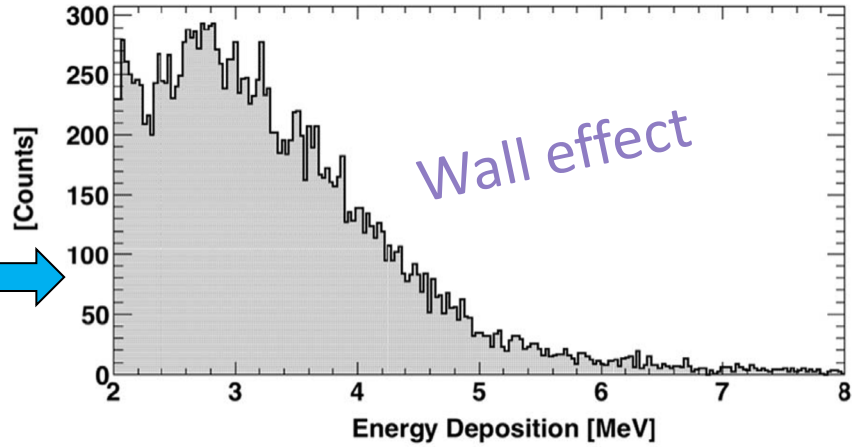

UNIVERSITY OF BIRMINGHAM

Neutron detection with the Spherical Proportional Counter
Proof of principle and state-of-the-art advancements

- ^{252}Cf, ^{241}Am^{9}Be and ambient fast neutrons
- Thermal neutrons
- N_2 at 0.1-0.5 bar
- HV ~ 6 kV

Bougamont, E et al (2017). NIM A, 847, 10–1

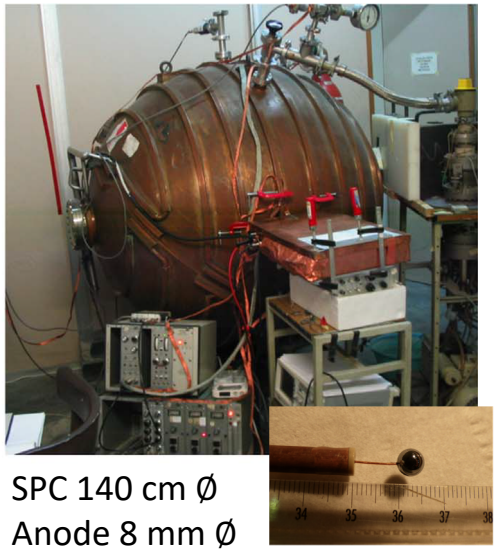

SPC 140 cm Ø
Anode 8 mm Ø

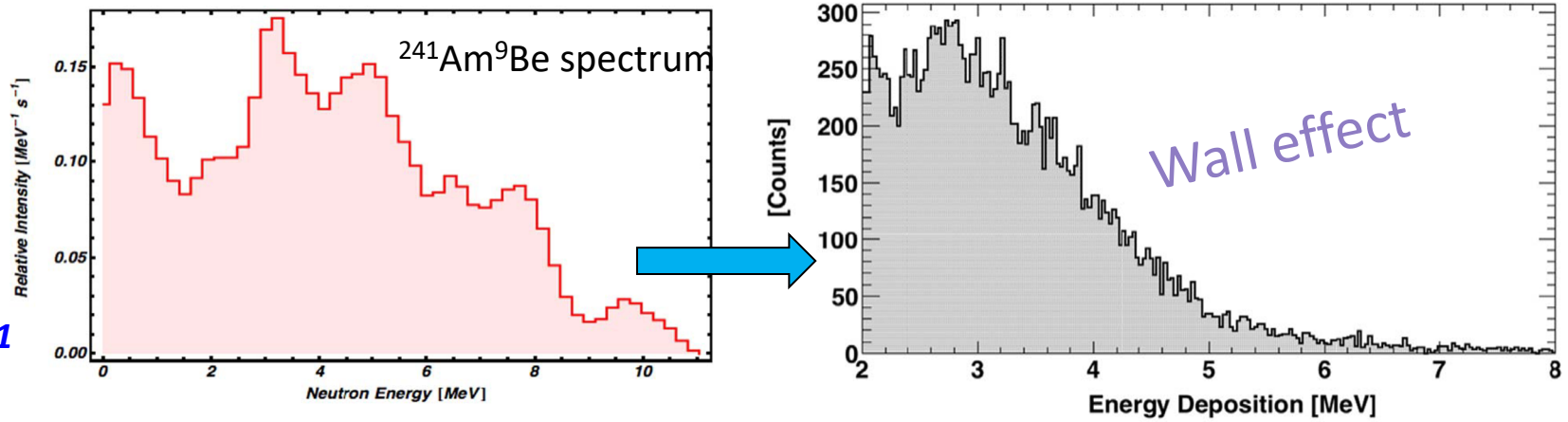

Resistive Multi-anode sensor (achinos)

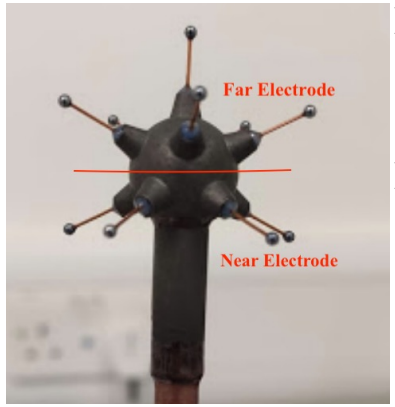

- Decouples drift and amplification fields
  - Small anode size → high gain
  - More anodes → Efficient charge collection
- Allows for increased target mass
  - Larger volume
  - Higher pressure

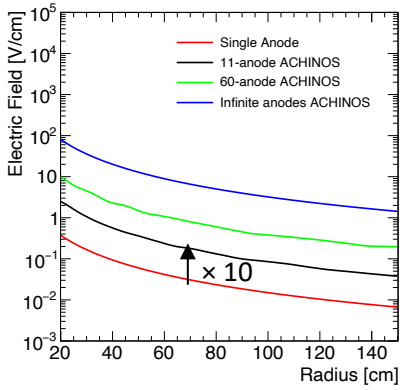

Gas purification techniques

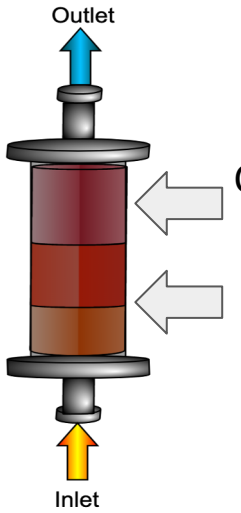

Copper Oxide H_2O removal

Molecular sieves for O_2 removal

UNIVERSITY OF BIRMINGHAM

The Graphite stack @ University of Birmingham

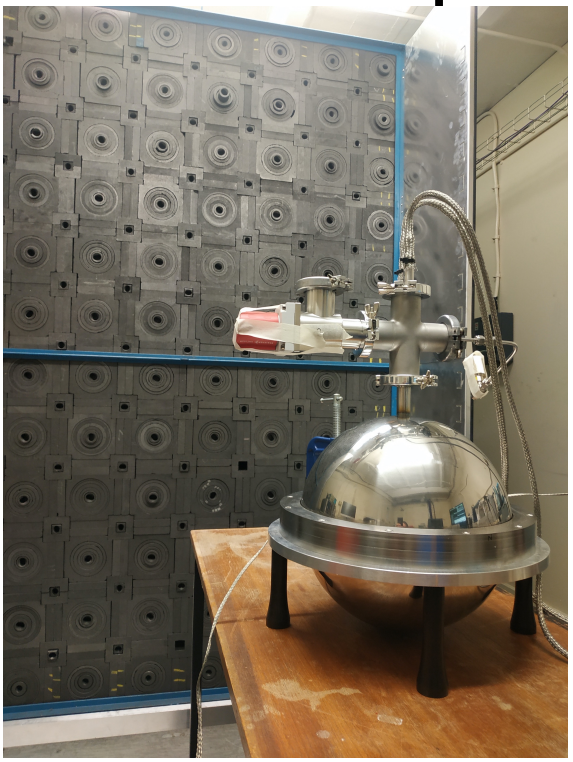

Investigate the capability of the SPC to detect fast neutrons and neutrons thermalized by the graphite.

<u>Spherical Proportional Counter</u>

- 30 cm Ø
- N_2 gas filling

<u>Multi-anode sensor</u>

- 11 anodes
- 1mm Ø
- Reading in 2 channels (near – far)

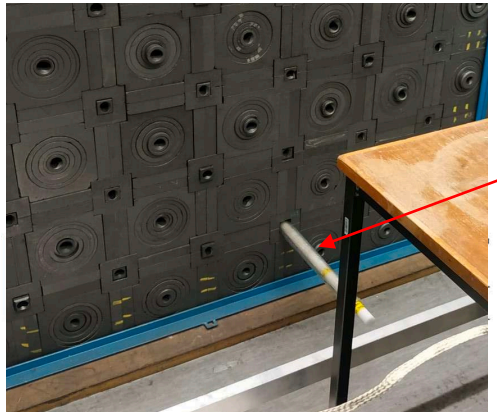

$^{241}Am^{9}Be$ neutron source
A = 2.6 x 10^6 Bq

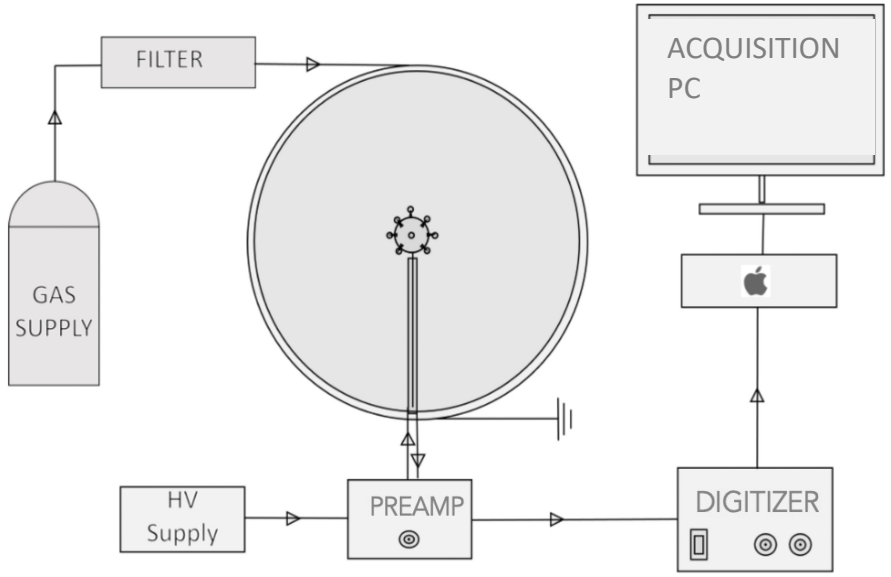

- Calibration measurements
- Thermal and fast neutrons at 1 bar and [3.6, 4.2] kV bias
- Thermal and fast neutrons at 1.5 bar and 4.5 kV bias
- Thermal neutrons at 2 bar and 5 kV bias

Neutron measurements with the Spherical Proportional Counter
Calibration of the detector

- Gain curve
  ^{210}Po source (alpha 5.3 MeV)
  1 bar N_2 filling

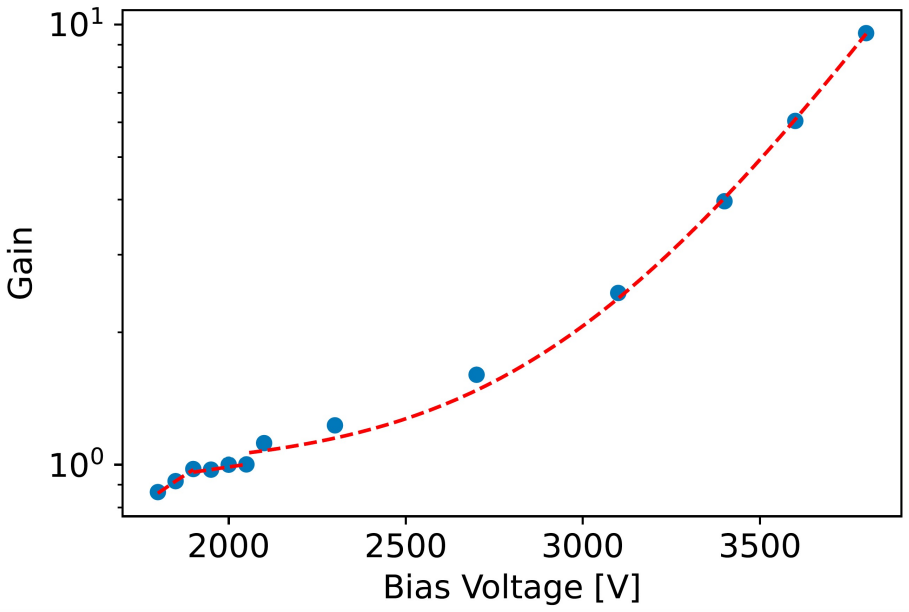

- Getter filter emits ^{222}Rn, Radon decay chain used for calibration

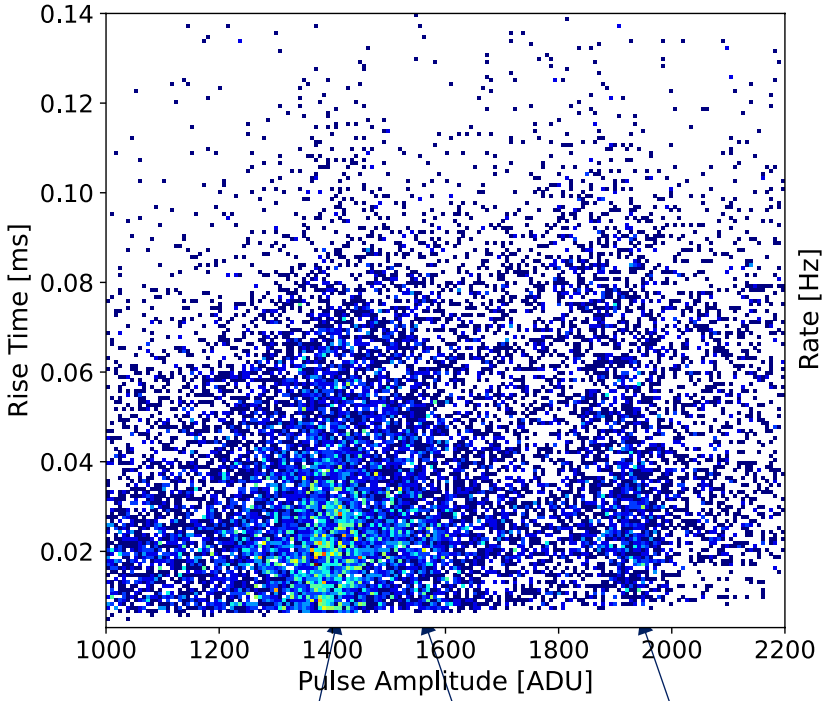

- Confirm Radon decay rate with 3% accuracy (half-life ~3.8 days)

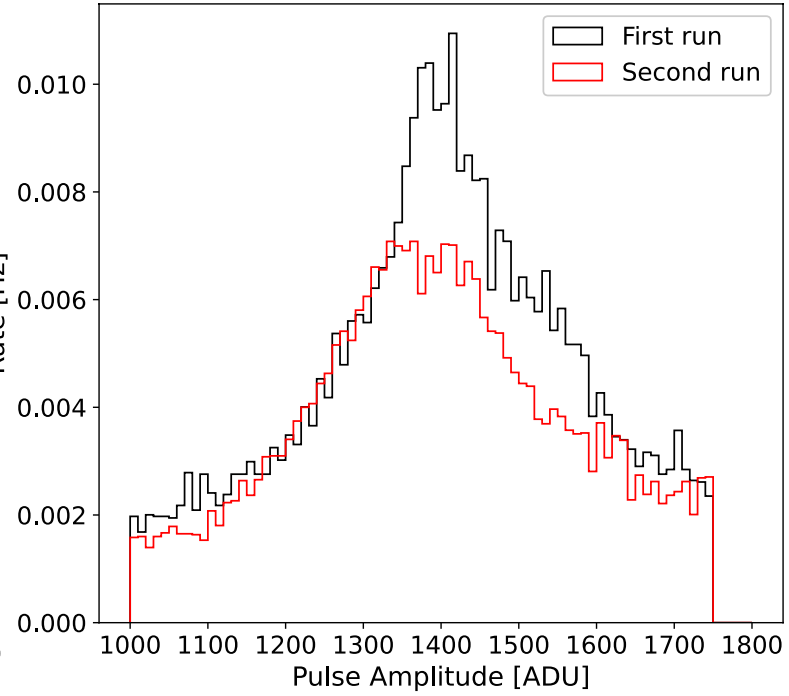

Neutron measurements with the Spherical Proportional Counter

$^{241}Am^{9}Be$ neutron source

1 bar N_2, 3.6 kV

Response of near channel to thermal neutrons

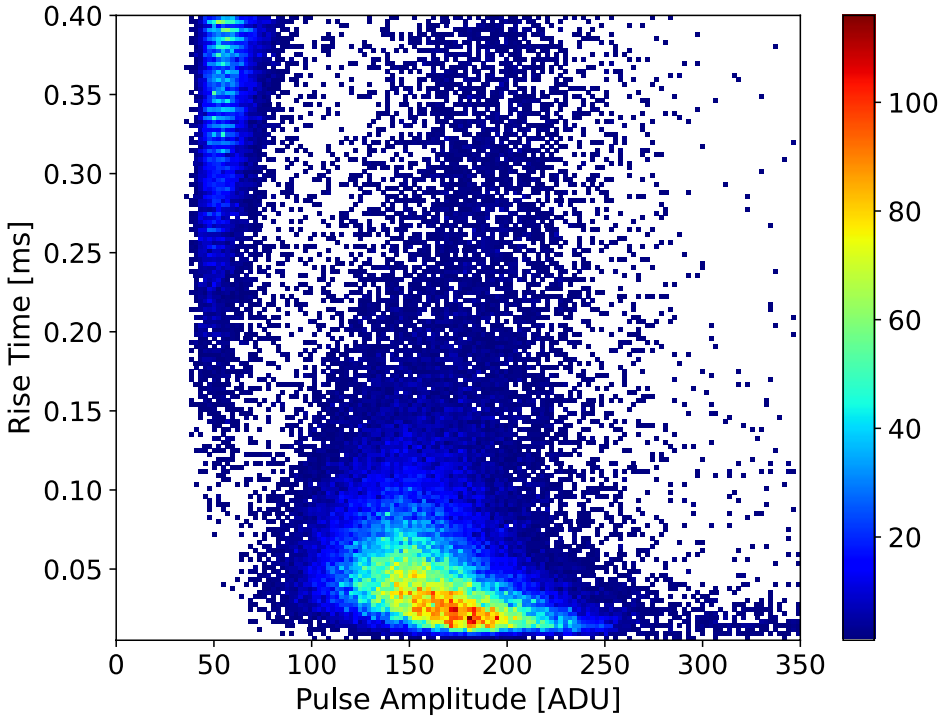

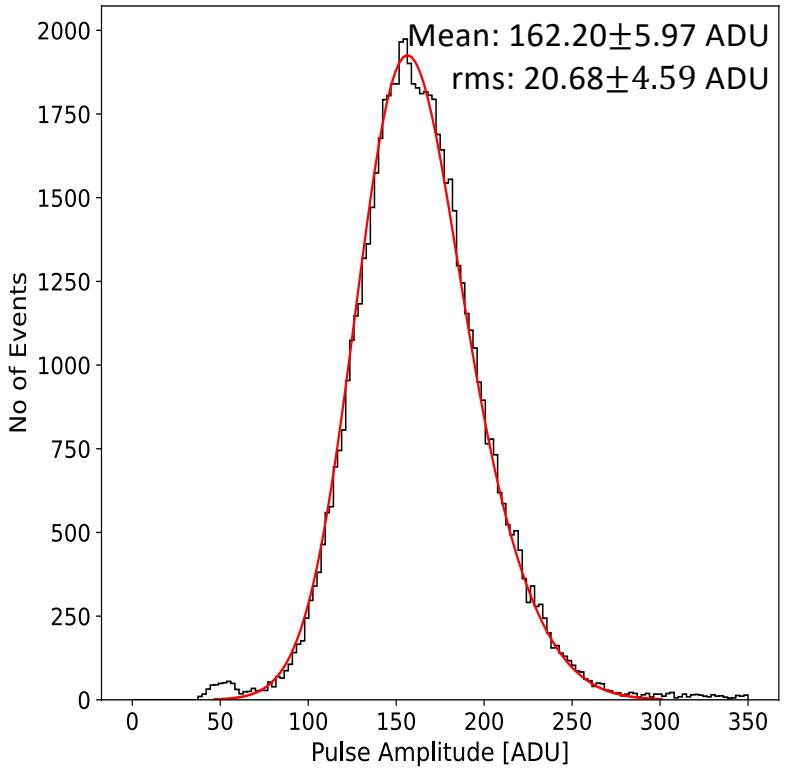

Rn peak at 1295 ADU (5.59 MeV) confirms thermal peak (625 keV)

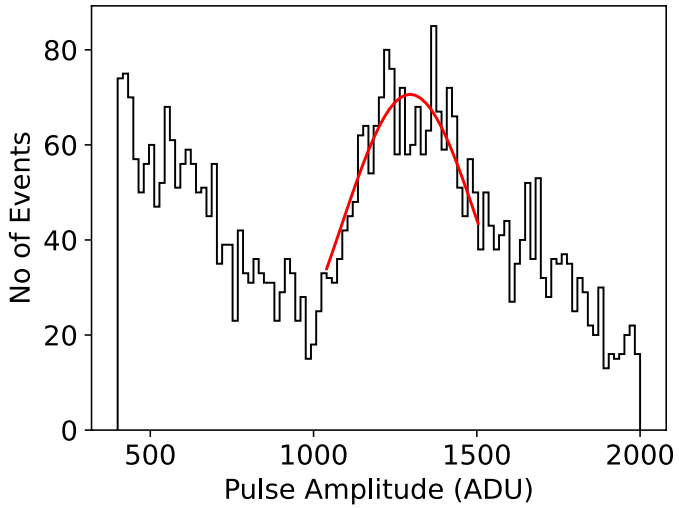

Thermal peak correspond to 625keV recoil energy ($^{14}N + n \rightarrow {}^{14}C + p + 625$ keV)

Neutron measurements with the Spherical Proportional Counter

$^{241}Am^{9}Be$ neutron source

1.5 bar N_2, 4.5 kV

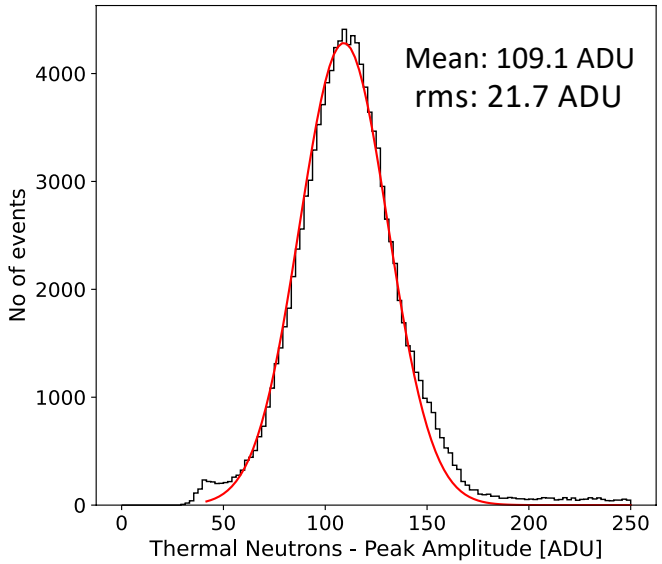

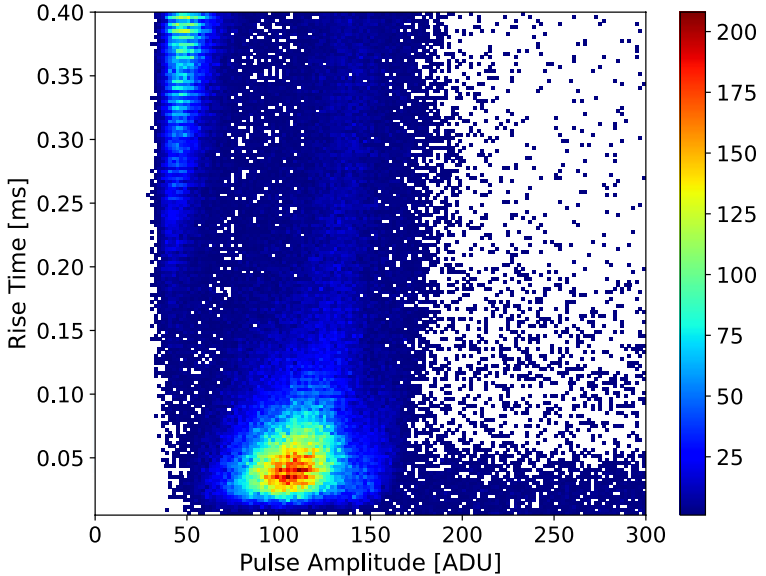

Confirmation of thermal neutrons peak from Rn peak

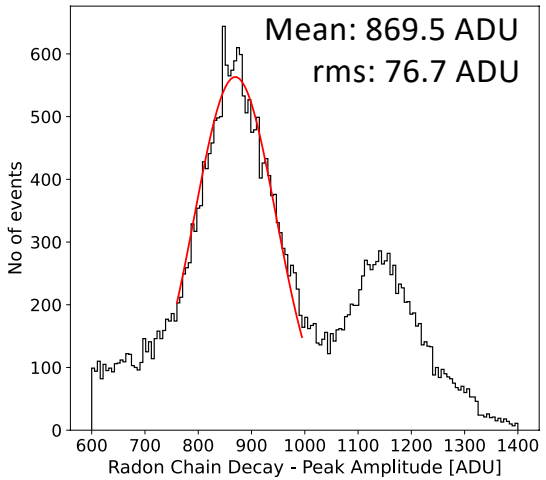

Thermal neutrons detected also with N_2 at 2 bar pressure

- Detection of thermal and fast neutrons

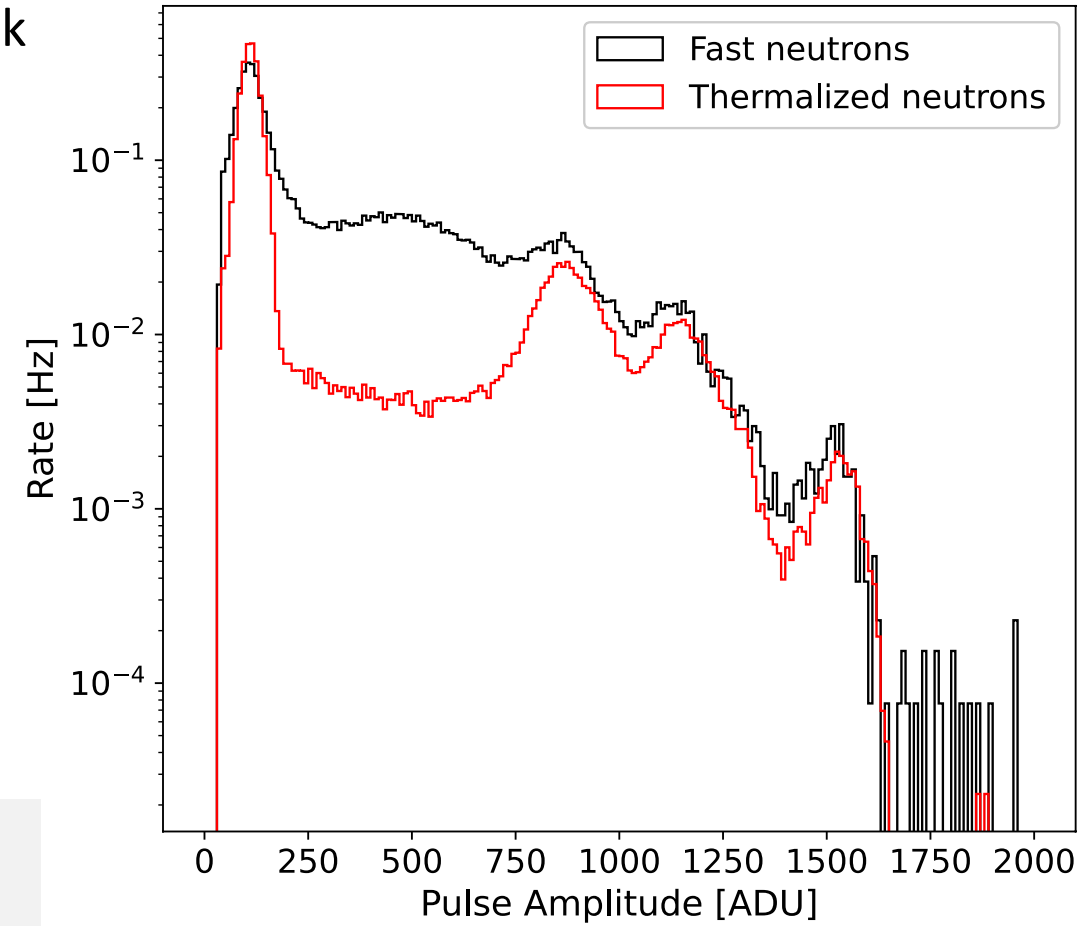

Gas purification studies with the Spherical Proportional Counter

- **Effect on gain, contaminating three times with 67.5 ppm O_2**
  ^{210}Po source (alpha 5.3 MeV)

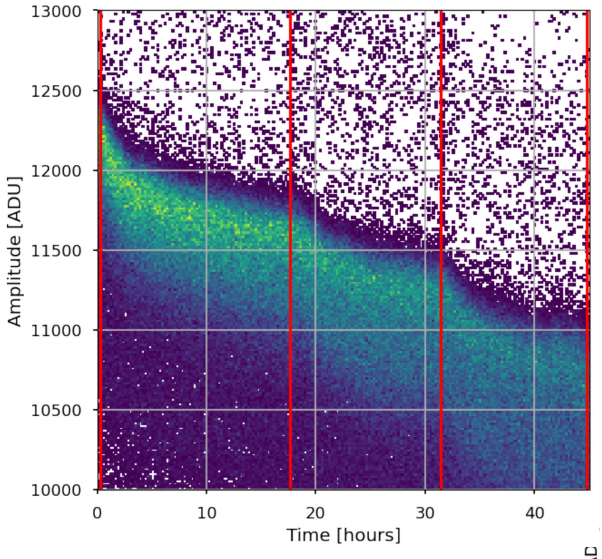

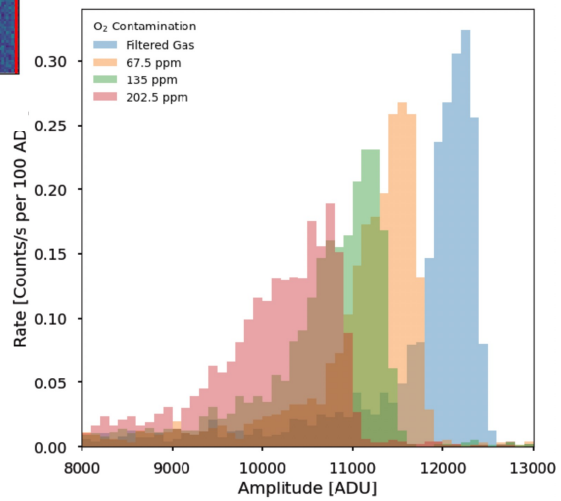

- **Rn emission with different filters**

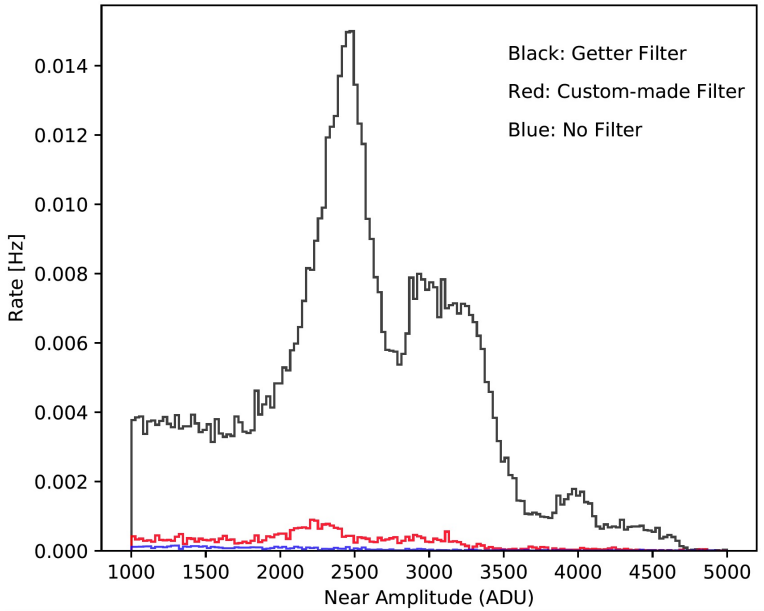

<u>Rn emission rates:</u>
Getter Filter: 0.563 Hz
Custom-made filter: 0.029 Hz
No Filter: 0.004 Hz

Neutron measurements at the Boulby Underground Laboratory

- Underground facility 1100 m under surface, North Yorkshire (UK)
- Instrumentation R&D and neutron measurements at controlled environment.
- 30cm Ø Spherical Proportional Counter installed and operating
- ^{252}Cf neutron source available
- Data acquisition ongoing

Science and Technology Facilities Council

Boulby Underground Laboratory

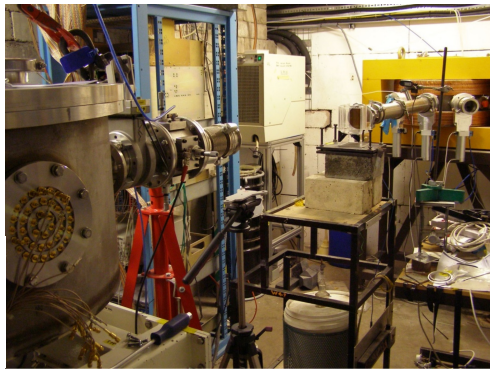

UNIVERSITY OF BIRMINGHAM | CYCLOTRON FACILITY

Near – future plans:

- Mono-energetic neutron measurement (possibly @ Demokritos, Greece)
- Medical application - Measurement of energy spectra of the neutron-induced dose to patients during proton therapy treatment sessions @ MC40 cyclotron facility (UoB)

<u>Since Sept. 2020:</u>

2 posters (IoP2021, TIPP21) – 2 oral presentation(HEP21,IEEE21)
1 conference proceeding submitted (TIPP21)
2 NEWS-G collaboration meeting talks
Paper under preparation

MARIE CURIE ACTIONS

Thank you for your attention!

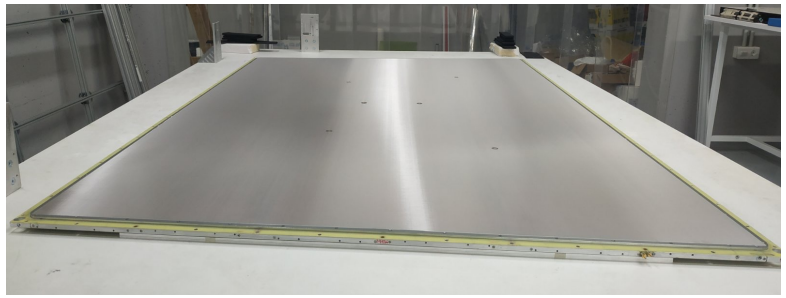

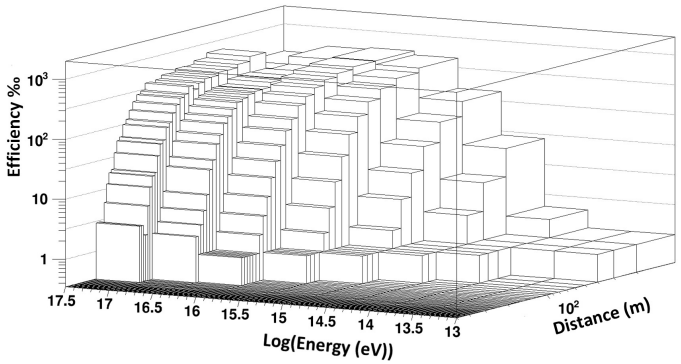

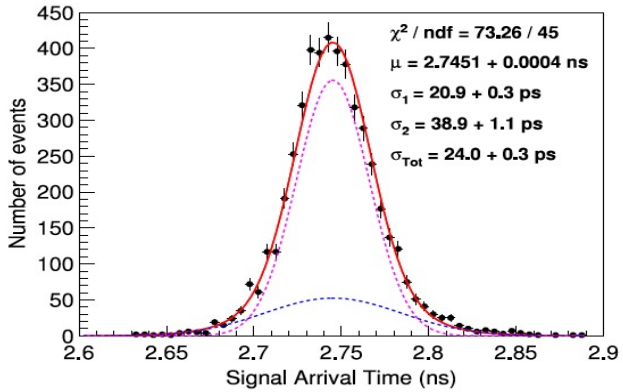

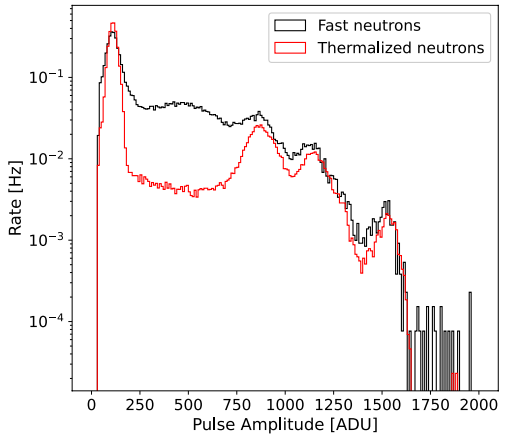

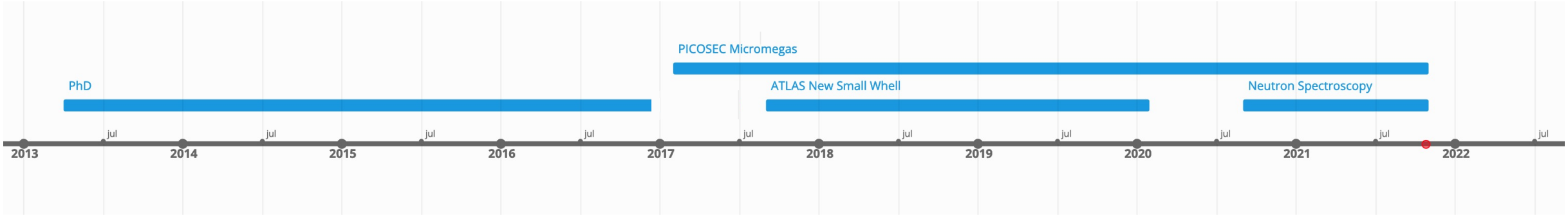

Back up slides

Astroneu array
Telescope description

3 detection stations at Hellenic Open University campus (Patra, GR)

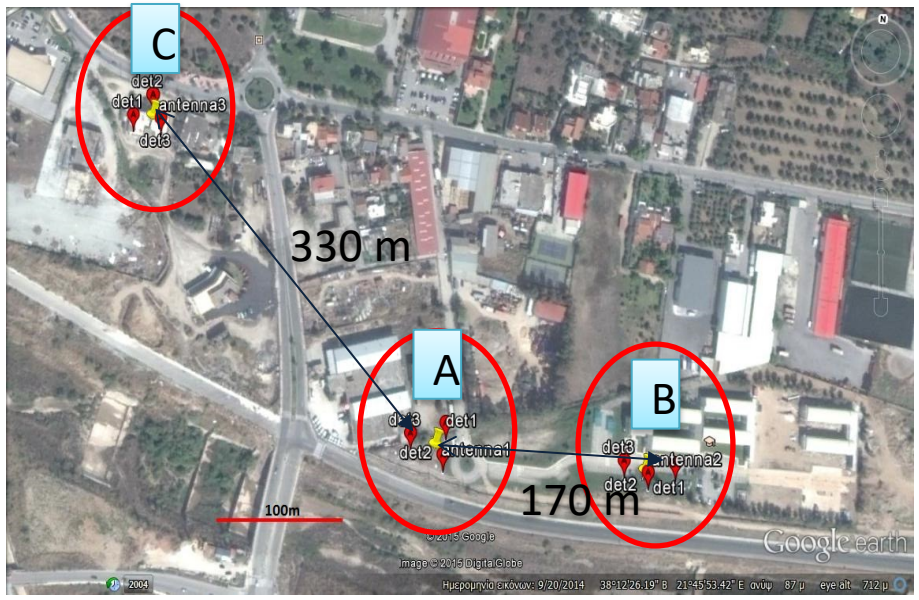

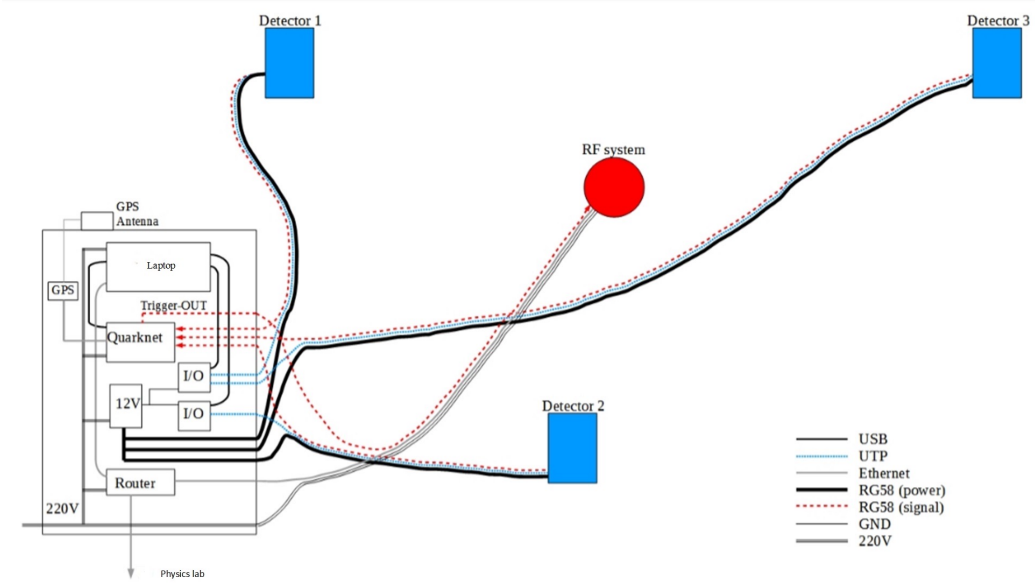

Each station comprises:

- 3 plastic scintillators (in a distance ~30m)
- 1 RF antenna (at station centre)
- Power supply , control and supervision unit
- DAQ providing trigger to RF antenna from scintillator coincidence

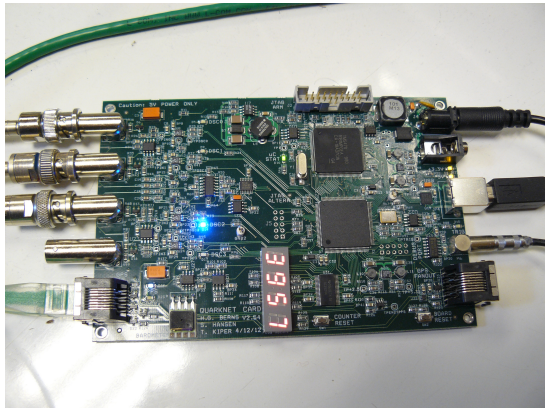

Quarknet Data acquisition at scintillators
(Leading edge with Time-over-Threshold timing)

Astroneu array

RF signal detection

Criteria for EAS signal:

- Triger from Scintillators
- Signal to Noise Ratio
- Rise time (10-70%) of cumulative signal 128 ns around peak <28ns.
- Polarization (NS vs EW)

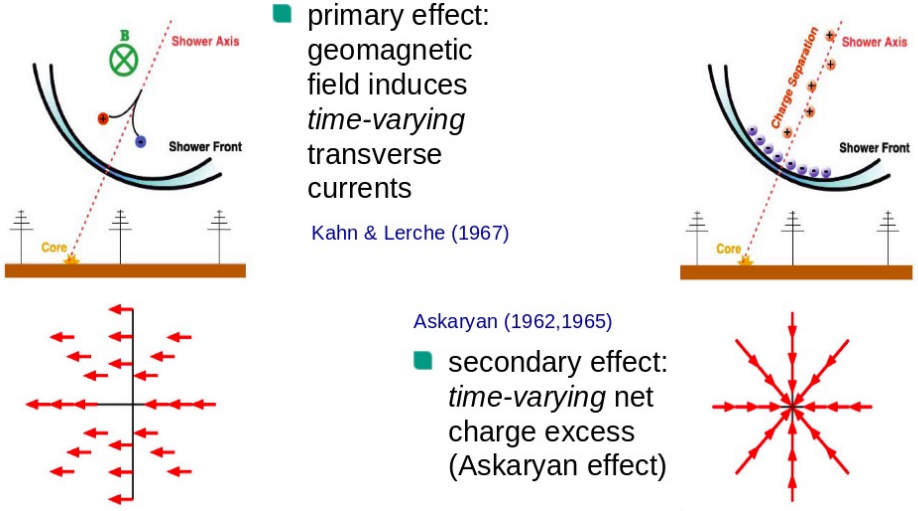

- primary effect: geomagnetic field induces *time-varying* transverse currents

Kahn & Lerche (1967)

Askaryan (1962,1965)

- secondary effect: *time-varying* net charge excess (Askaryan effect)

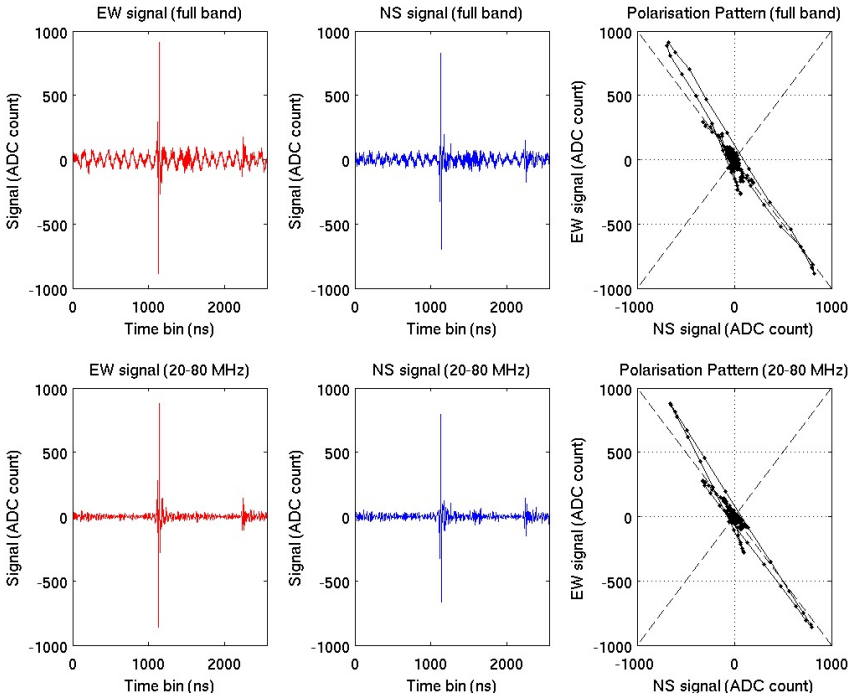

Example of cosmic event

- Detected signal amplified by a Low Noise Amplifier
- Detected waveform corresponds to electric field using antenna's response function $V_a = S'_{21}\vec{\mathcal{H}}_r\vec{\mathcal{E}}$
- Supress outlier with Tukey filter
- Fourier transform, keeping only 20-80MHz
- Inverse Fourier transform
- Stronger signal at EW, due to Geomagnetic field

CERN-RD51 PICOSEC Micromegas

Simulation studies: Drift region

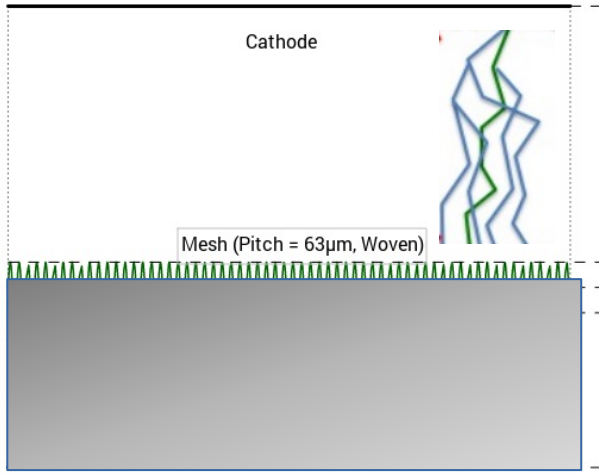

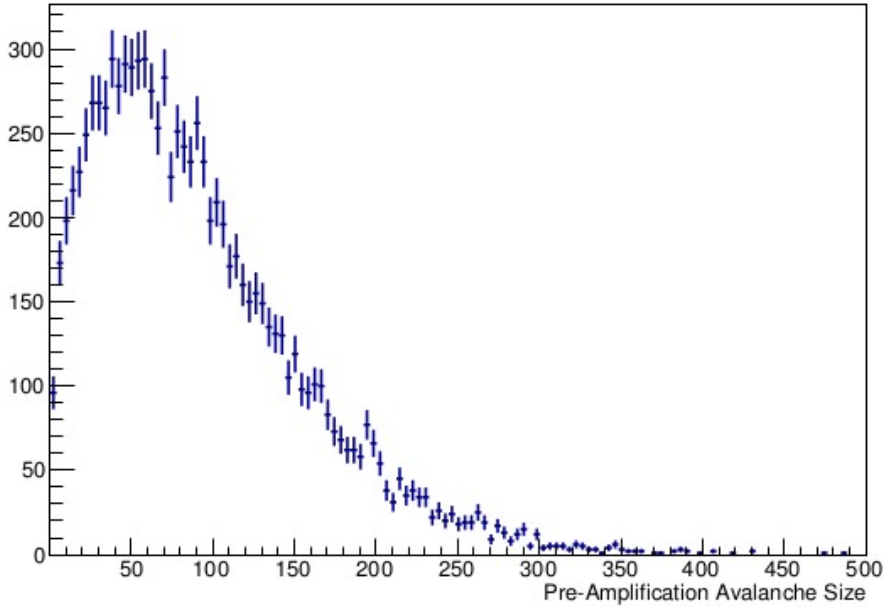

We start with one photoelectron,
and we follow the avalanche it creates
till the mesh.

We then count:
- **how many** electrons pass the mesh and **when**

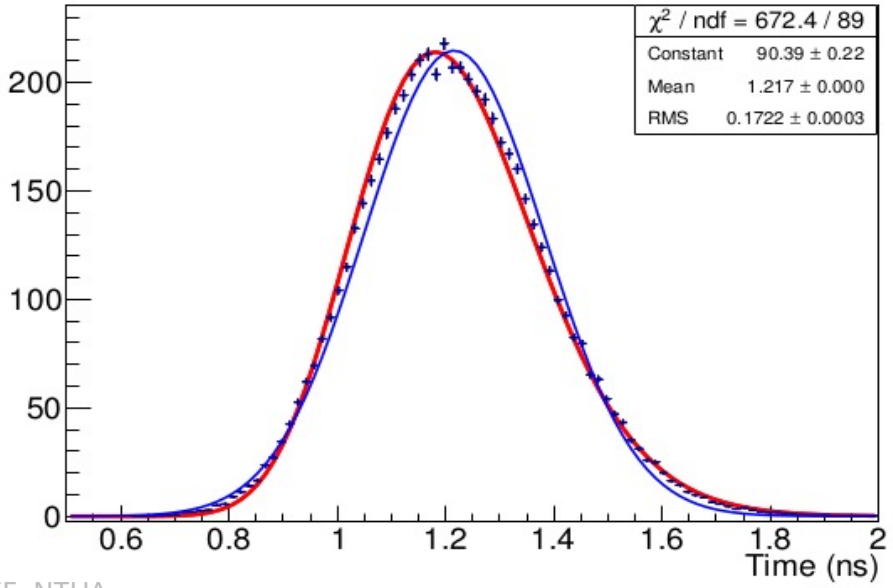

CERN-RD51 PICOSEC Micromegas

Simulation studies: Amplification region

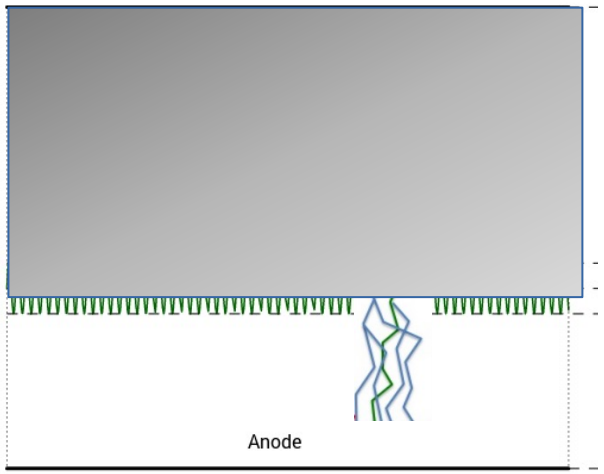

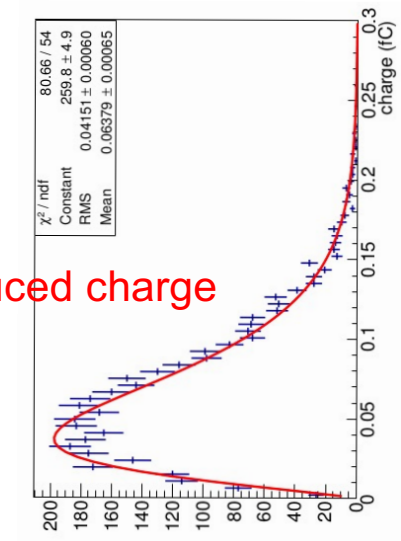

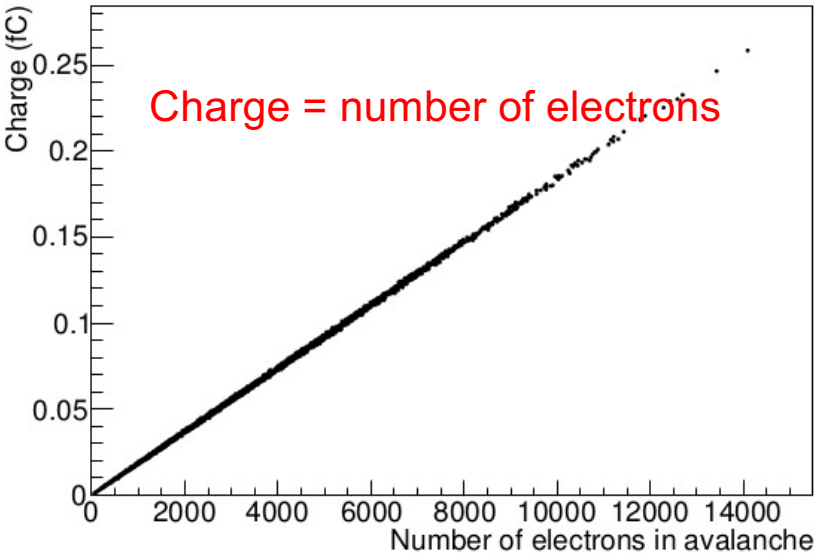

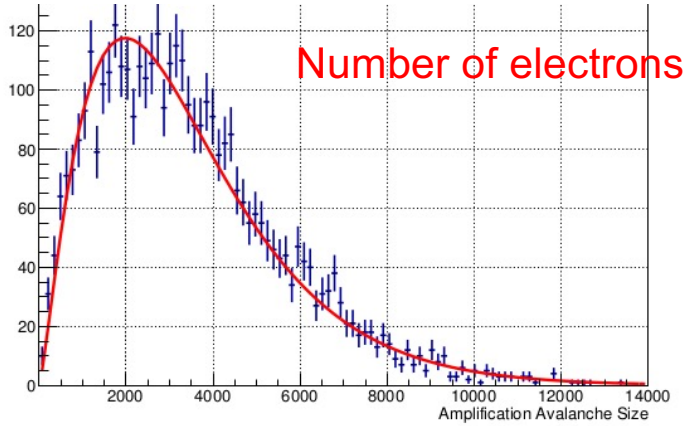

For each electron passed through the mesh:

- Follow the avalanche it produces in the amplification region
- Count **how many electrons** arrive on the anode and the **induced charge**: **one-to-one correspondence**

The distribution fit nicely with a Polya (red)

→ for each electron passing the mesh, we get a representative number of electrons on the anode, by picking randomly from this Polya.

CERN-RD51 PICOSEC Micromegas

Simulation studies: Response of electronics

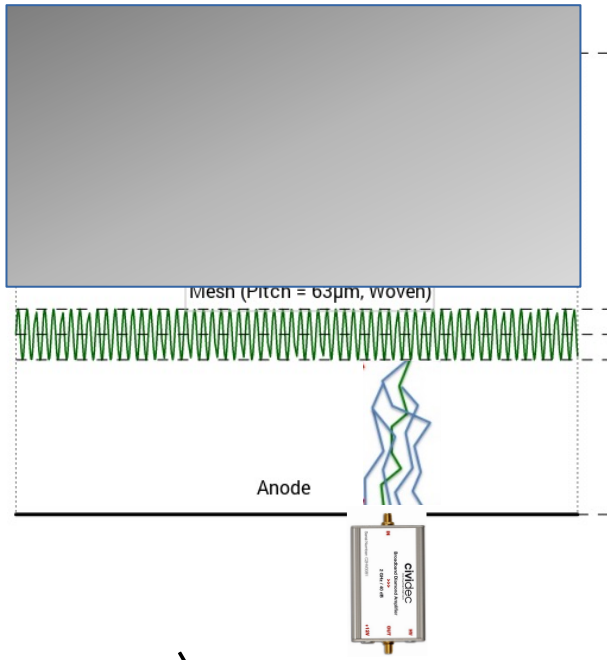

- Assume simulated pulse is described with the difference of two logistics

- Find the parameters by using experimental data, in a statistically coherent way:

a) Describe the pulse shape produced from one electron passing the mesh and entering the amplification region. Take distributions of “mean arrival times” for the electrons reaching the anode (from Garfield++) and convolute them with the shape of the electronic response

b) Compare the result with the average waveform observed in the experimental data.

$$\frac{\langle S(t)\rangle_{Q_{tot}=Q}}{Q} = \int_0^\infty f(t-\tau)\,\langle \Phi(\tau)\rangle_{Q_{tot}=Q}\,d\tau$$

Normalized waveform

Average waveform / its total charge (experimental data) $=$ Response function of the electronics with all gains=1 (convolution) $*$ Distribution of Mean Arrival times (simulation)

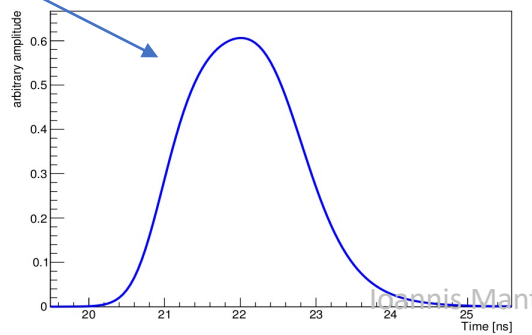

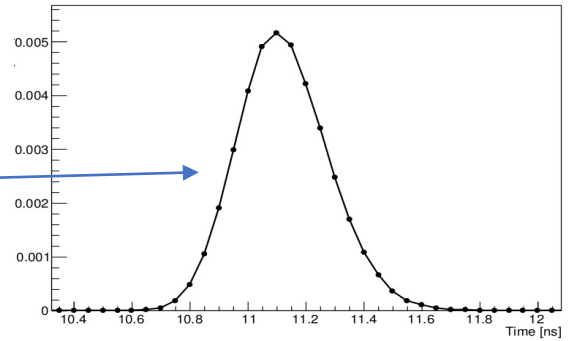

CERN-RD51 PICOSEC Micromegas

Simulation studies: Electronic gain

Pulse generation in Garfield++ –no extra electronic gain

$$S(t) = \sum_{i=1}^{N} q_i \cdot f(t - \tau_i)$$

N electrons pass through the mesh at times $\tau_1, \tau_2, \ldots, \tau_N$

Each one of these N electrons contributes a pulse **f(t)** (previous slide)**, displaced by the respective time $\tau_1, \tau_2, \ldots, \tau_N$**

we need the Gain, G, of the electronics in order to construct **G*S(t)**

Pulse generation in Garfield++ – including electronic gain

G should be a constant.

But…

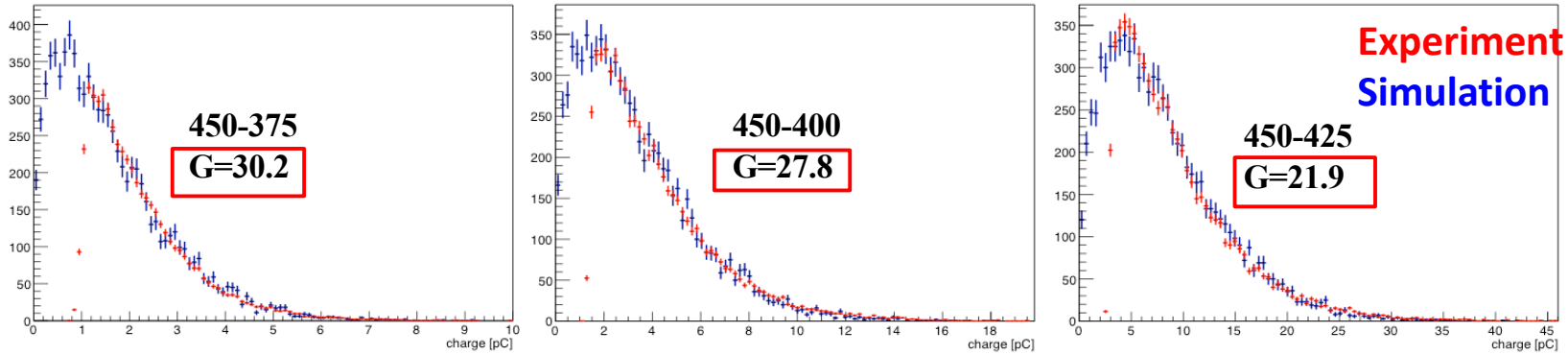

r=50% for the **"Penning Transfer Rate"** allows to use a constant electronic gain G, independent of the voltage in the drift region.

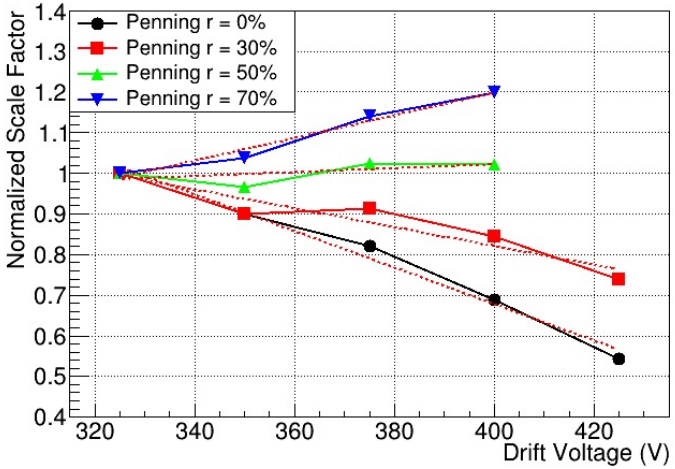

CERN-RD51 PICOSEC Micromegas

Alternative timing methods

Goal of this study: Test the capability of timing methods (alternative to CFD) on ps order.

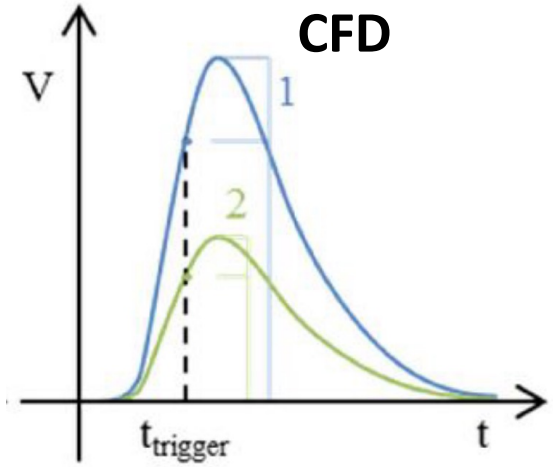

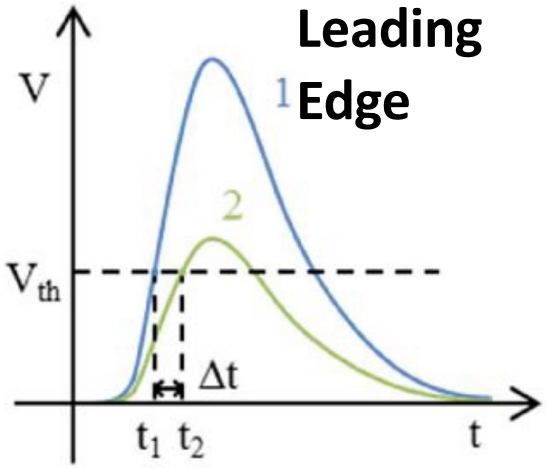

Constant Fraction Discrimination (CFD)

✔ No time-walk effect

✘ Requires full waveform

Leading edge – Time over Threshold (ToT)

✔ Provides timestamp (minimum information required)

✘ Time-walk effect (correction required, using the time that the pulse remains above the threshold)

- CFD method: preferable during R&D
- Leading edge-ToT: practical for applications - experiments

CERN-RD51 PICOSEC Micromegas

Alternative timing methods

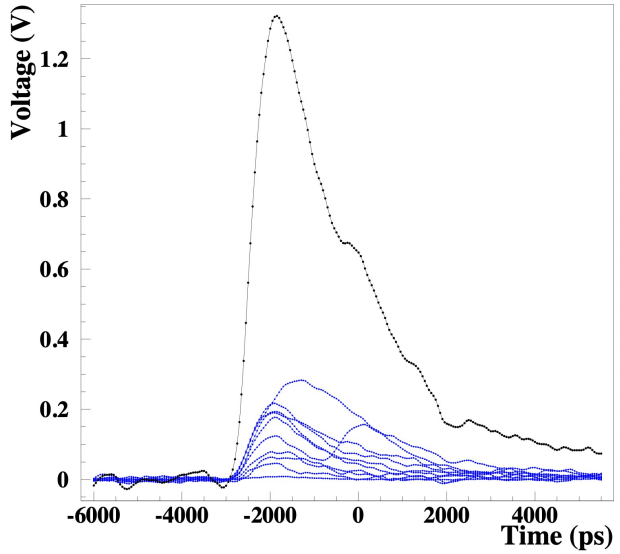

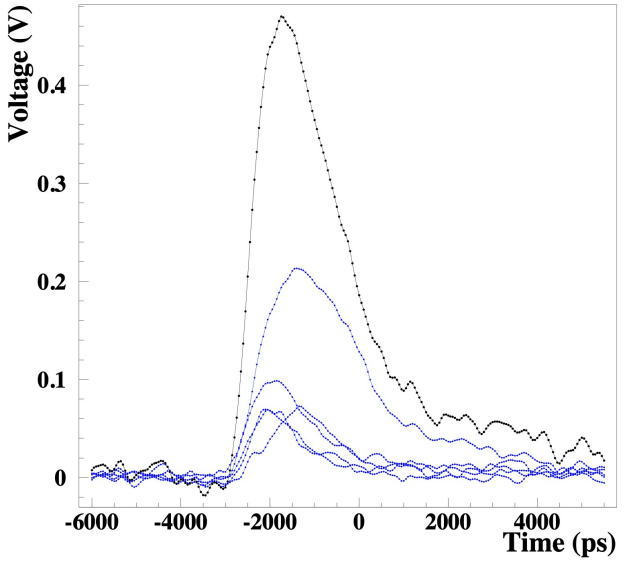

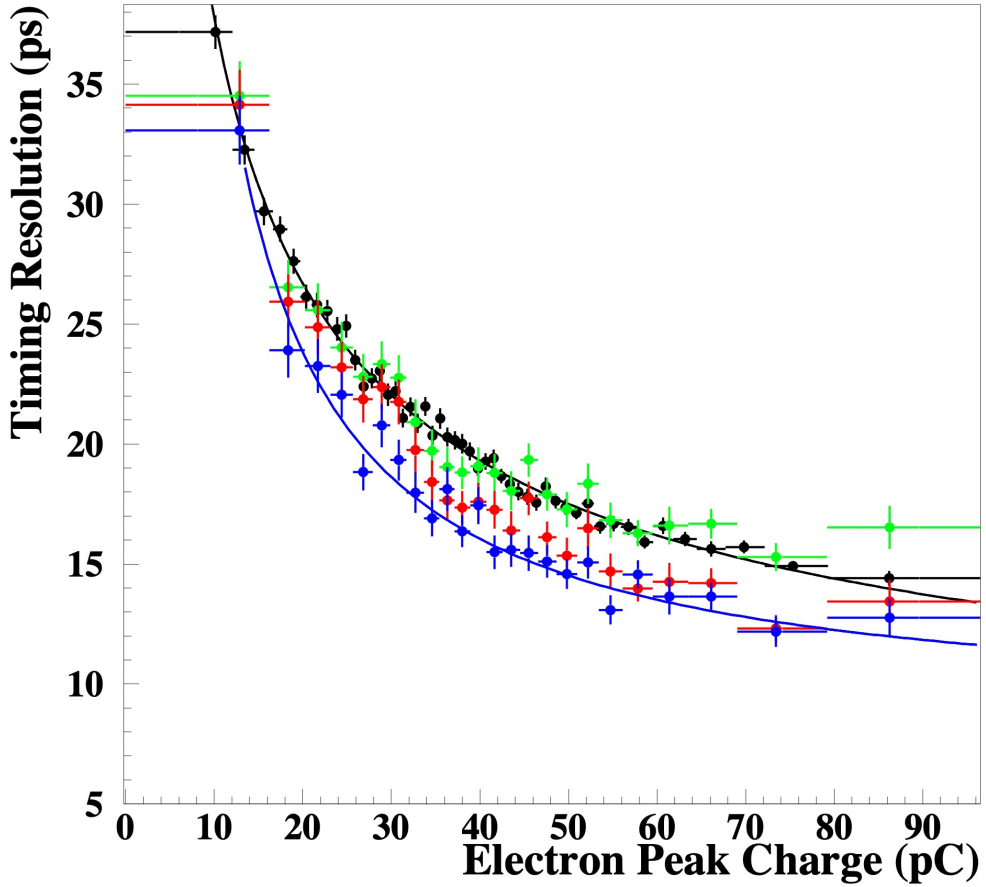

Neutron measurements with the Spherical Proportional Counter

$^{241}Am^{9}Be$ neutron source

- Thermal neutrons peak follows exponential form for various biases

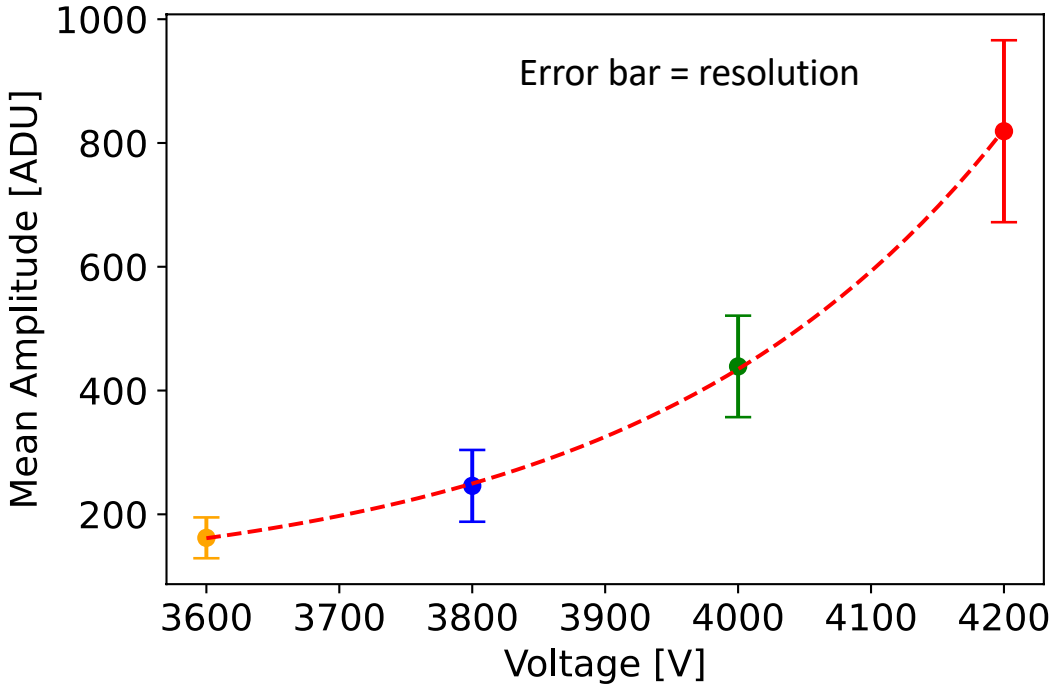

- Simulation study: Probability of each neutron to reach detector volume after thermalized in graphite stack (~$5x10^{-3}$)

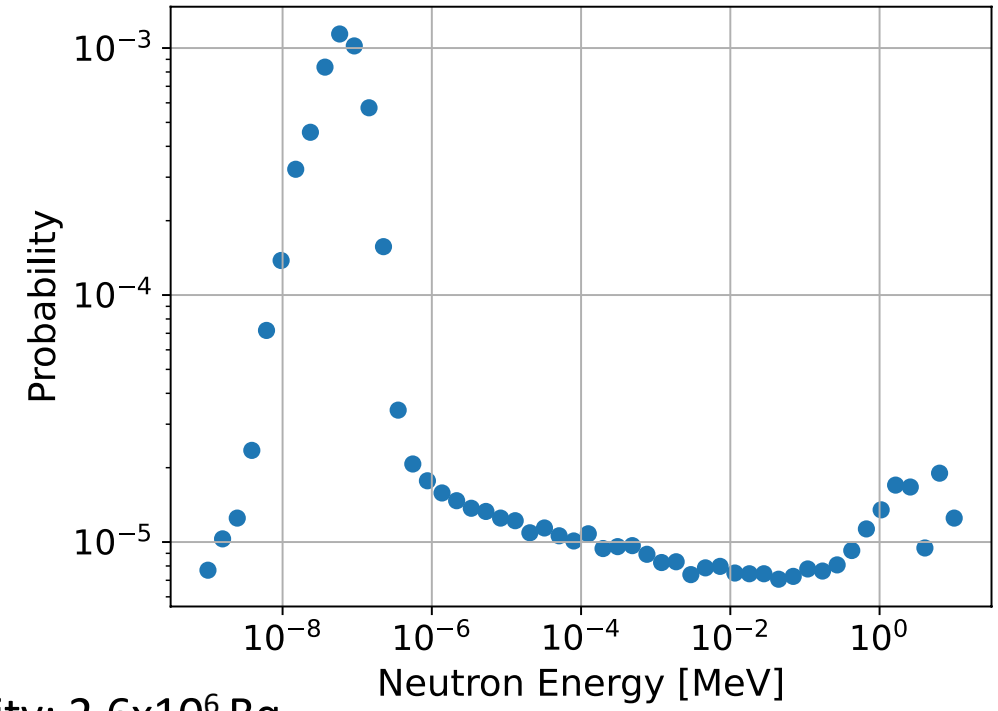

Source activity: $2.6x10^{6}$ Bq
Detection rate:~5Hz
→ Efficiency: ~$3.7x10^{-4}$

Simulation preliminary results → Efficiency: ~$2.2x10^{-4}$

Neutron measurements with the Spherical Proportional Counter

$^{241}Am^{9}Be$ neutron source

1 bar N_2, 3.8 kV

Detection of fast neutrons

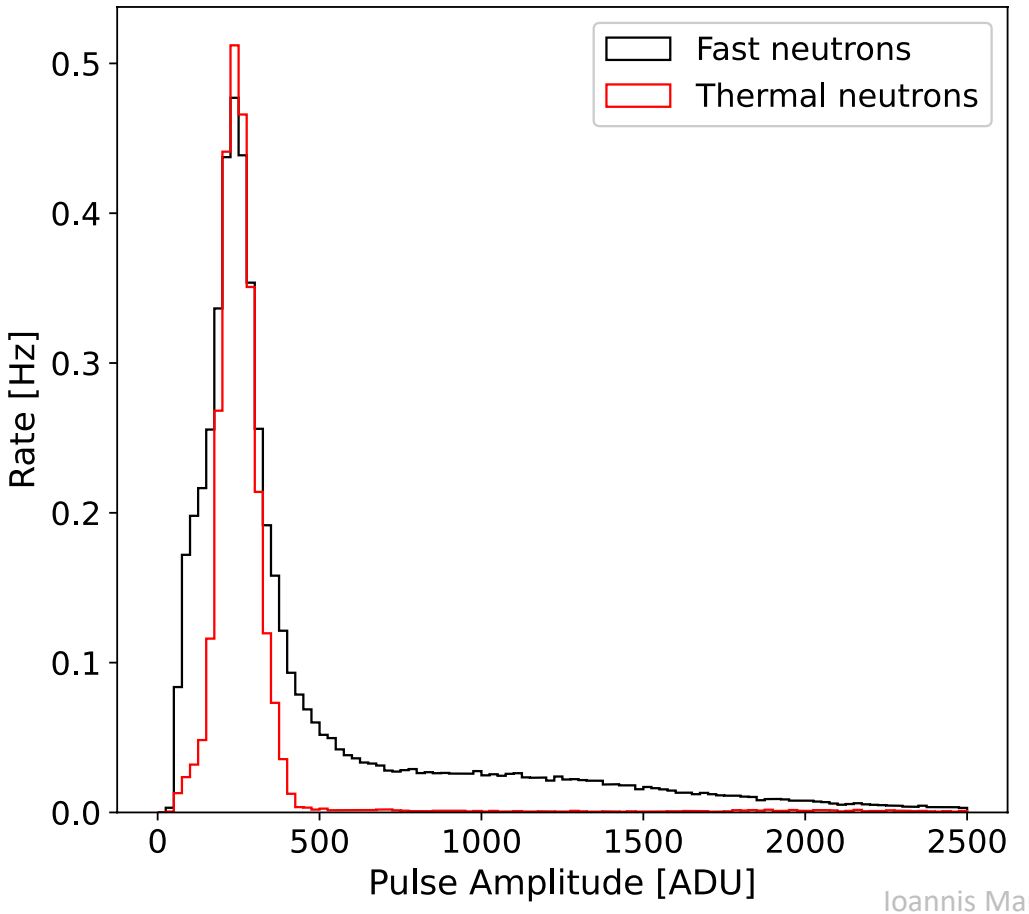

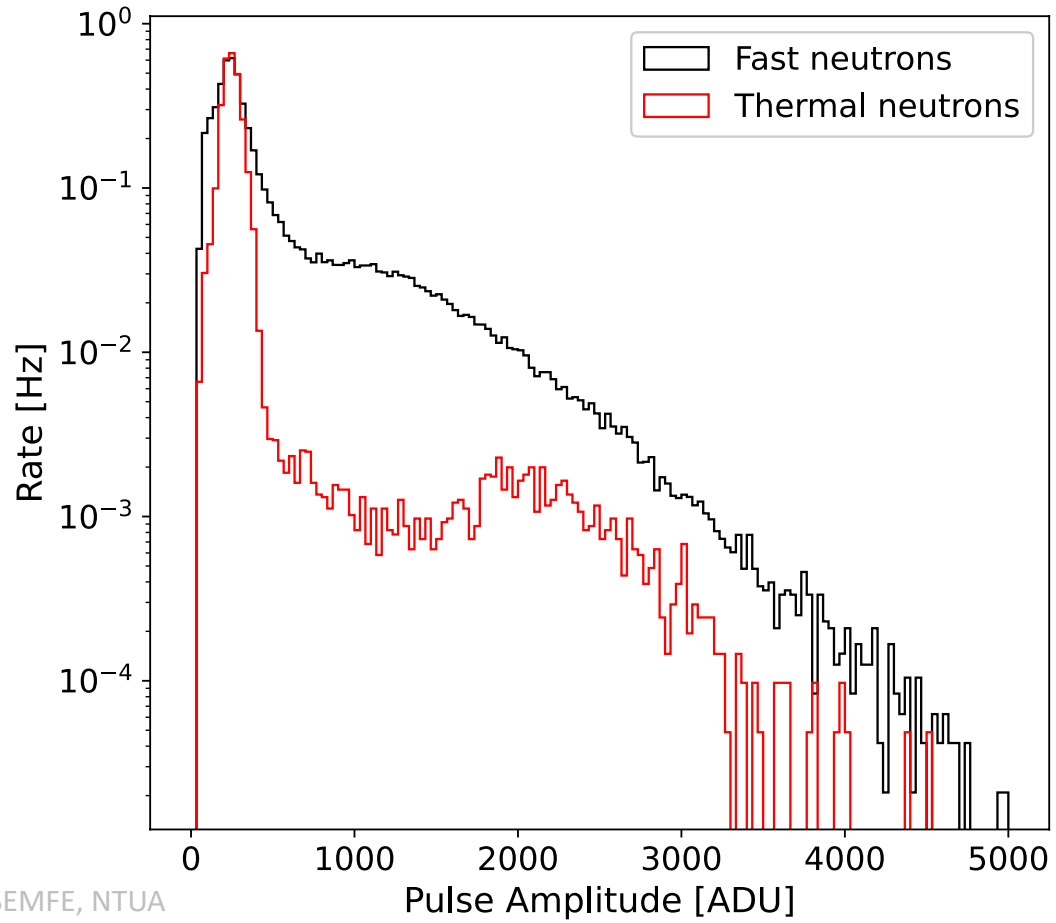

Neutron measurements with the Spherical Proportional Counter

$^{241}Am^{9}Be$ neutron source

2 bar N_2, 5 kV

Thermal neutrons detection